JOURNAL OF THE AERONAUTICAL SCIENCES

VOLUME 13 AUGUST, 1946 NUMBER 8

Symposium on Notch Effects in High-Strength Aluminum Alloys*

Part I. Notch Sensitivity in High-Strength Aluminum Alloys—Theoretical Aspects

L. SCHAPIRO AND H. E. NORTH

Douglas Aircraft Company, Inc.

ABSTRACT

A study has been made of the effect of various types of notches and notched depths on static ultimate tensile strength of 14ST, 75ST, and 24ST aluminum alloys. An ideal, stress notch insensitive material is defined in terms of a logarithmic relationship between notched ultimate stress and notch depth. Test data indicate that the logarithmic relationship is a good first approximation and that a scale of stress notch sensitivity may be established. Alloy 75ST is shown to be more stress notch sensitive than 14ST, and alloy 24ST more sensitive than either. Caution in the commercial application of this conclusion is urged as well as need for differentiating between stress notch sensitivity and strain notch sensitivity.

INTRODUCTION

THE ADVENT OF NEW, higher strength aluminum alloys has been welcomed by the aircraft industry, both the airplane manufacturer and the airplane user, as making possible larger airplanes with greater load-carrying capacities and speeds. In the substitution of a new alloy for an old, the air-frame manufacturer faces the problem of accumulating new material properties and allowable design data. Where consistent methods of comparing properties of the new with the old material can be basically established, the accumulation of all necessary material properties may be short-circuited and considerable time saved in the application of the new material.

In aircraft design, where weight is of primary importance, the breaking strength of a structure or member is often the design condition with the working stress some percentage of this design allowable. It is recognized that dynamic loading is often the major criterion of structural design. As an initial step in the evaluation of parameters suitable for design use, however, the authors first studied the high-strength aluminum alloys under static loading and sought to compare the effects of section discontinuities (notches) on ultimate strength of new and old alloys.

It has been customary to characterize a material by its mechanical properties, yield strength, ultimate strength, and 2-in. elongation, as though these properties were material constants. These same parameters have served the stress analyst and machine designer and have formed the bases for design allowables on all types of structures. In recent years new parameters have been recognized and it has become customary to refer to the conventional yield and ultimate strength as "mean apparent yield stress" and "mean apparent ultimate stress." This refinement in definition of what has been considered conventional terminology is based on the realization that the results of conventional tests are the mean stresses across the section tested and are based on the original area before testing rather than on the final (reduced) area. The necessity for new parameters has arisen as a result of a demand for refinements in methods of analysis to keep pace with design improvements, and particularly in the aircraft industry's lighter weight structures. The analysis of members containing discontinuities affecting the stress distribu-

* Received February 6, 1946.

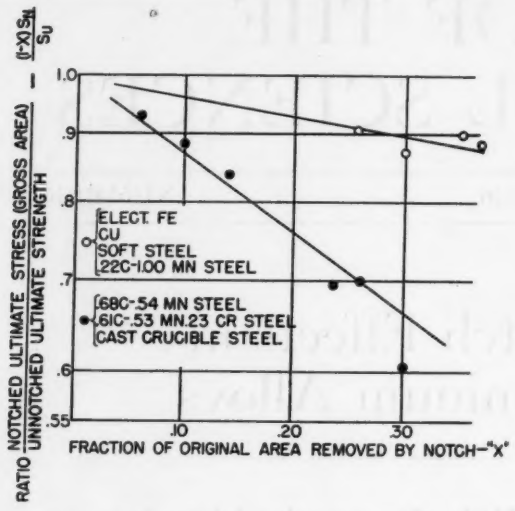

FIG. 1. Sachs and Lubahn's data[1] replotted on coordinates of Eq. (3). Stress notch sensitivity index of 0.16 for ductile materials, electrolytic iron, copper, low-carbon steel, compares with index of 0.62 for more brittle materials, high carbon steels and cast steel.

tion has been handled in other industries by adherence to conventional photoelastic analysis. This has been practical because stresses were held at all times below the proportional limit and high margins of safety were normally allowed.

Photoelastic studies have established the existence of local stress concentrations, and from such studies stress concentration factors have been set up which relate the local concentration to the uniform stress in the same plane. This system of evaluating the effect of discontinuities on stress concentration is independent of the material being studied, and applies within the elastic range only. In this investigation results were obtained that demonstrate the fallacy of applying these arbitrary factors in predicting the breaking strength of a section.

The work described in this paper and carried forward by the authors' company into large-size structural members was aimed at obtaining parameters usable in design that would recognize the occurrence of some plastic flow in specimens with section discontinuities, and allow predictions of breaking strength to be made for a given material and "notch" configuration.

THEORETICAL CONSIDERATION

A notched member, stressed in the elastic range, develops stress concentrations at the base of the notch which are functions purely of notch geometry and not of the material involved—as expressed by the classical stress concentration factors. In the plastic range, however, these stress concentrations become redistributed across the notched plane. The amount of redistribution of stress is a function of the material and proceeds by local straining and strain hardening. A notch sensitive material will undergo a small degree of stress redistribution and will rupture at the point of maximum stress concentration. The mean stress in the plane of rupture can be less than the mean apparent ultimate strength of the material. An ideal notch insensitive material will undergo the maximum amount of stress redistribution and strain hardening and will rupture across the entire plane of the notch. The ideal notch insensitive material may be defined as one which undergoes such a degree of stress redistribution and strain hardening that the fracture load in terms of the gross area will correspond to the mean apparent ultimate strength regardless of notch depth. This definition of an ideal material may be expressed mathematically by Eq. (1).

$$(1 - x)S_N = S_U, \; 0 < x < 1 \tag{1}$$

in which

S_N = notched ultimate stress, failure load ÷ original area below notch
S_U = ultimate strength (unnotched)
x = fraction of original area removed by notch

Eq. (1) may be put in the form of Eq. (2)

$$\text{Log} \frac{(1 - x)S_N}{S_U} = 0 \tag{2}$$

and this has been done because the latter plots a straight line on semilog paper and lends itself to extrapolation from few test points. The ideal material will thus plot as a horizontal straight line on a semilog chart with the left-hand term of Eq. (2) as ordinate and x as abscissa. Eq. (2) may therefore be written as given in Eq. (3)

$$\text{Log} \frac{(1 - x)S_N}{S_U} = -Nx \tag{3}$$

in which the value of N is zero. If N is termed the index of stress notch sensitivity, an ideal notch insensitive material would have an index value of zero and the more notch sensitive a material the larger its index value would be. The tests herein described were small in number but were selected to check the validity of Eq. (3) or to determine usable modifications thereof.

Sachs and Lubahn[1] have assembled notched ultimate stress data for several steels, electrolytic iron, copper, and aluminum. Plotting these data with the coordinates of Eq. (3) indicates the aluminum to be close to an ideal notch insensitive material with index approximately zero. The other materials are as shown in Fig. 1, with the conventionally considered more ductile materials having a lower index of stress notch sensitivity than the more brittle materials.

TEST PROCEDURE

Several types of notched specimens were studied. These may be classified as internal and external notches. For the former, a drilled hole on the central axis of flat

TABLE 1
Description of Notch Types Studied, Notched Depths, and Materials

Notch Designation	Notch Type	Notch Dimension	Notch Depths % Removed Area	Specimen Cross Section	Material 14ST	Material 75ST	Material 24ST
1	External, sym., sharp	60° V, 0.002-in. Root radius	4–7.8–15.3	0.505 in. diam.	Rolled	Extruded	Rolled
2	External, sym., dull	60° V, 0.02-in. Root radius	4–7.8–15.3	0.505 in. diam.	Rolled	Extruded	Rolled
3	External, pseudosym., sharp	60° V, 0.002-in. Root radius	4–8	0.500 in. by 0.150 in.	Rolled	Extruded	Extruded
4	Internal, axial	Drilled hole	4–8	0.500 in. by 0.150 in.	Rolled	Extruded	Extruded
5	External asym., sharp	60° V, 0.002-in. Root radius	4–8	0.500 in. by 0.150 in.	Rolled	Extruded	Extruded

TABLE 2
Indexes of Stress Notch Sensitivity and Factors Relating Notches and Materials

Notch Designation	Stress Notch Sensitivity Index 14ST	75ST	24ST	Relative Index Factor Compared with Notch No. 1 14ST	75ST	24ST	Average per Notch Type	Relative Index Factor Compared with 14ST 14ST	75ST	24ST
1	0.22	0.28	0.46	1.0	1.0	1.0	1.0	1.0	1.27	2.09
2	0.28	0.30	0.68	1.27	1.07	1.48	1.27	1.0	1.07	2.43
3	0.37	0.45	0.73	1.68	1.61	1.59	1.63	1.0	1.22	1.97
4	0.50	0.70	1.26	2.27	2.50	2.74	2.50	1.0	1.40	2.52
5	0.66	0.84	1.40	3.00	3.00	3.04	3.01	1.0	1.27	2.12
							Average per grade	1.0	1.25	2.22

specimens was used. For the latter, 60° V notches were made in three types: the symmetrical notch was put on round specimens; the pseudo symmetrical notch was put on opposite surfaces of a flat specimen, the notches on the two surfaces being directly opposite each other; the asymmetrical notch was put on one surface only of a flat specimen. Root radius of the 60° V notch was 0.02 in. in some tests and 0.002 in. in others. Two or more notch depths were used for each type of notch. Tests were initially conducted in a series of ten identical specimens for each notch type and notch depth. As notched ultimate stress results per series indicated uniformity of the order of 3.1 per cent maximum deviation from the mean for any single test, the test series were reduced to five and, finally, to two identical specimens per series.

The tests described above were conducted on three grades of aluminum alloys, namely: 75ST, 14ST, and 24ST. Test specimens were prepared from extruded stock and from rolled stock. A detailed list of each notched specimen type and the nature of stock from which it was prepared is presented in Table 1. Unnotched specimens representing each type of stock were tested to establish control values (0 per cent notch).

Specimens were tension loaded to failure in a Baldwin-Southwark testing machine in accordance with standard procedure.[2] Load at failure was converted to notched ultimate stress, using the net area below the notch prior to test.

RESULTS

Test results are plotted in Figs. 2, 3, and 4, for 14ST, 75ST, and 24ST materials, respectively. Agreement of test results with the logarithmic expression of Eq. (3) is of a fairly good order. Index values for each material and each type of notch have been calculated from the lines as drawn and the index values are listed in each figure for each material. These values cannot be accepted as fully substantiated in view of the small number of test points. The comparison of the indices does, however, indicate relationships that can be useful.

As assembled in Table 2 (left-hand section), it can be seen that index values are of the same order of magnitude for the five notches in each material; i.e., notch No. 2 gives each of the three materials a larger index than notch No. 1, etc. Since notch No. 1 gives each material the lowest index value of its series, the index values for the other notches are compared with the notch No. 1 value. These comparisons, presented in the center section of Table 2, indicate that each type of notch has the same order of effect on all materials; i.e., notch No.

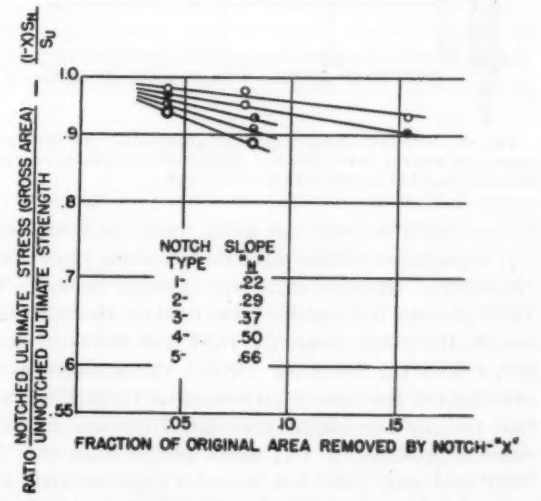

FIG. 2. Notched strength of 14ST aluminum with five notch types and several notch depths. Slopes of logarithmic relationships increase in the order of the notch types.

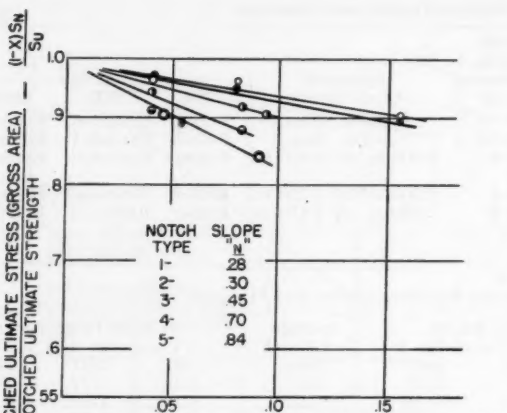

FIG. 3. Notched strength of 75ST aluminum with five notch types and several notch depths. Slopes of logarithmic relationships increase in the order of the notch types.

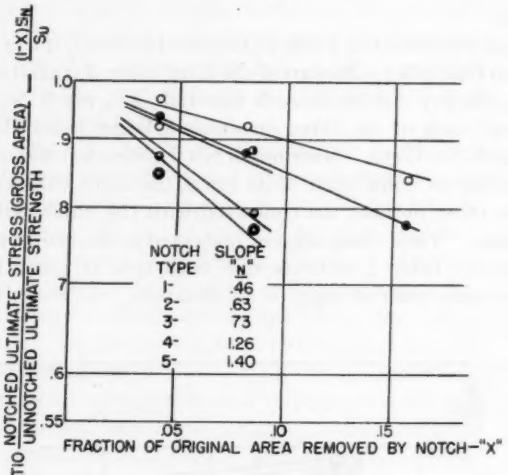

FIG. 4. Notched strength of 24ST aluminum with five notch types and several notch depths. Slopes of logarithmic relationships increase in the order of the notch types.

2 gives each material an index value approximately $1^1/_4$ times greater than the index resulting from notch No. 1, etc. Since for each type of notch the index for 14ST material is a smaller value than for the other materials, the index values for 75ST and 24ST are compared with the index for 14ST. These comparisons, presented in the right-hand section of Table 2, indicate that for any one notch type alloy 75ST has an index value approximately $1^1/_4$ times greater than that for 14ST and alloy 24ST has an index approximately $2^1/_4$ times greater than that for 14ST. The latter statement constitutes the major conclusion disclosed by the tests herein reported and may be restated in the following terms: *Aluminum alloy 75ST is more stress notch sensitive than 14ST and alloy 24ST is more stress notch sensitive than 75ST.*

DISCUSSION

It is recognized that the stress notch sensitivity indices presented herein are not to be taken as fully substantiated values. The logarithmic curves of Figs. 2, 3, and 4 are in most cases drawn through two points that are not adequate to establish the curves. Furthermore, the curves are drawn as though all pass through the origin, in accordance with Eq. (3). Later evidence collected in the authors' laboratory indicate that at least for some types of notches the relationship may be better expressed by Eq. (4).

$$\text{Log}\,\frac{(1-x)S_N}{S_U} = -a - Nx \qquad (4)$$

The striking relationships indicated by the factor numbers presented in Table 2 have been useful to the authors' company in understanding the results of static tension tests of full-scale structural members.

The reader is strongly cautioned regarding the application of the authors' major conclusion. That aluminum alloy 24ST or 75ST is more stress notch sensitive than alloy 14ST should not be construed to mean that the former alloys are less desirable for commercial applications than the latter. Rather, a recognition of this relationship permits design to compensate for a greater loss in strength at a region of section discontinuity while using an alloy for its otherwise desirable properties.

A communication from the Lockheed Aircraft Corporation[3] further indicates the effect of various notch types on ultimate stress as presented in Fig. 5.

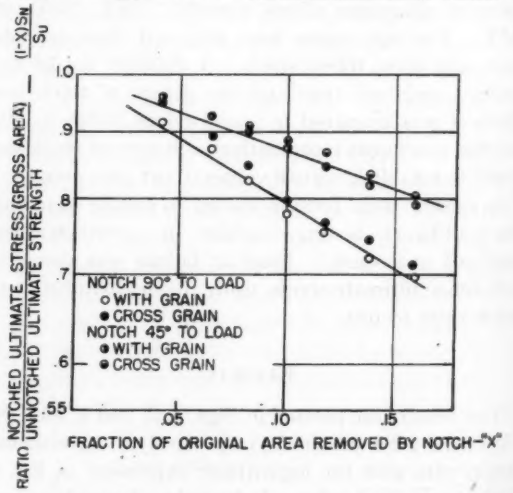

FIG. 5. Notched strength of 24STAL aluminum sheet, notched on one side for various depths through cladding. Notch at 45° to applied load results in lower index value than notch at 90° to applied load.

The Term "Notch Sensitivity"

Many workers in the field of stress studies with section discontinuities characterize notch sensitivity of a material as though this were a constant property comparable with another material. The authors have characterized their study as stress notch sensitivity to emphasize that the effect of notches (section discontinuities) in the plastic range is not necessarily similar on all mechanical properties. The study herein described with regard to ultimate stress also included measurements of 2-in. elongation of all specimens. Results of such ductility measurements are presented diagrammatically in Fig. 6 for one notch type only (Notch No. 1) to illustrate the different effect of a notch on ductility in comparison with ultimate stress. From Fig. 6 it can be seen that alloy 24ST is the least strain-notch sensitive of the alloys tested. The distinction between stress notch sensitivity and strain notch sensitivity must, therefore, be clearly made.

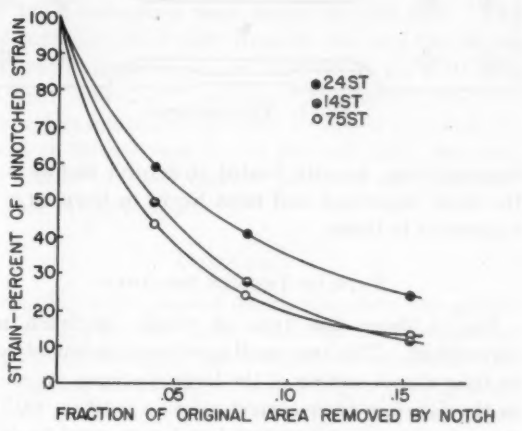

FIG. 6. Ductility of 14ST, 75ST, 24ST aluminum as affected by notch No. 1. Alloy 14ST and 75ST suffer greater ductility loss than 24ST.

References

[1] Sachs, G., and Lubahn, J., *Effect of Notching on Strained Metals*, Journal of the American Welding Society, Supplement, p. 272, June, 1944.

[2] *Standard Methods of Tension Testing of Metallic Materials*, A.S.T.M. Designation E 8-42.

[3] Kommer, F. J., *Preliminary Investigation of the Effects of Surface Scratches*, Lockheed Aircraft Company Report No. 4945.

Part II. The Effects of Open Holes on the Tensile Strength of Some Aluminum Alloys

C. H. STEVENSON

Douglas Aircraft Company, Inc.

Abstract

Experimental data are presented to show the effect of holes on the ultimate tensile strength of 14ST, 24ST, and 75ST aluminum alloys. Variations in efficiency of from 75 to 105 per cent are shown for the different alloys and products. Curves useful in design are given to show the effect of single and multiple holes of various sizes in plate, bar, and extrusion.

Introduction

A series of static test failures, both higher and lower than the calculated loads, caused an investigation to be made regarding notch sensitivity at ultimate strength in the higher strength aluminum alloys. A survey of available literature was made.[1] Large quantities of information (both theoretical and experimental) were found on notch effects in the elastic range, but no experimental data are available (and only a slight amount of theoretical investigation has been made) of notch effects in the plastic range. None of these data pertained to ultimate failures! The experimental work reported herein was undertaken in an attempt to provide designers with sufficient information to avoid failures at loads other than those desired.

Design Problem

The design problem that appears to be most pressing is the effect of holes in large structural members. This problem naturally divides itself into three classifications: first, that of a single hole; second, that of multiple holes; and third, that of a hole which is used to apply the load to the member. The most important part of the problem at the time this work was undertaken was that of tension loads. As a result, this work was confined to axially loaded tension specimens only. The materials investigated were aluminum-alloy plate, sheet, bar, and extrusions in the commercially designated 14S, 24S, and 75S alloys. A few specimens only were made in sheet, all of which were 0.102 in. in thickness. Most of the work was done on specimens $^1/_2$ in. thick

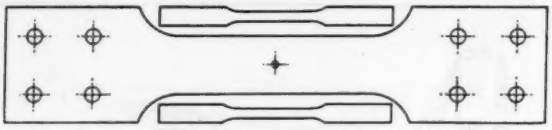

FIG. 1. Test specimens.

because large, heavily loaded structural members are the most important and most likely to have large attachments in them.

TYPE OF TENSILE SPECIMEN

Fig. 1 shows the type of tensile specimen used throughout. The two small specimens shown adjacent to the reduced section of the large specimen are shown in the figure in their correct relative position with respect to the original material and were used to determine the actual ultimate strength of the material. The two small test bars were standard A.S.T.M. sheet specimens. The large specimen is nonstandard and some discrepancies may exist because of its large size. If such discrepancies do exist they are unimportant because structural members will not conform to standard tensile coupons.

SINGLE HOLES

Single holes were drilled in the center of the large tensile specimens as shown in Fig. 1, and the ultimate strength determined with an ordinary tensile testing machine. The size of the hole was varied to change the amount of area removed for different tests. Results are shown in Fig. 2. The ordinate—per cent efficiency—is based on net area after drilling the holes. The abscissa—per cent area removed—is the ratio of the hole diameter to the width of the specimen. It will be noted that the curve for 75ST bar is somewhat erratic and does not have the characteristic shape of the other curves in this figure. This bar was an experimental piece of material and was considered to be unsatisfactory by the fabricator. With the exception of this 75ST bar, all the curves have the same general

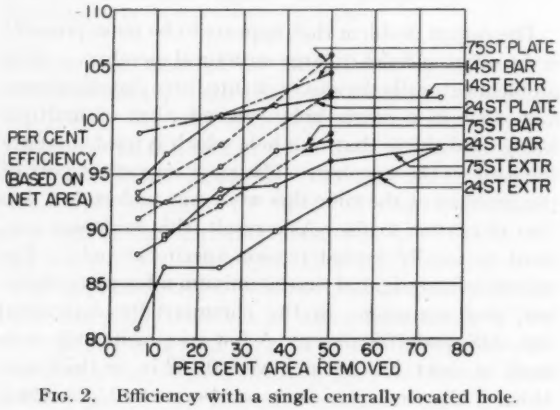

FIG. 2. Efficiency with a single centrally located hole.

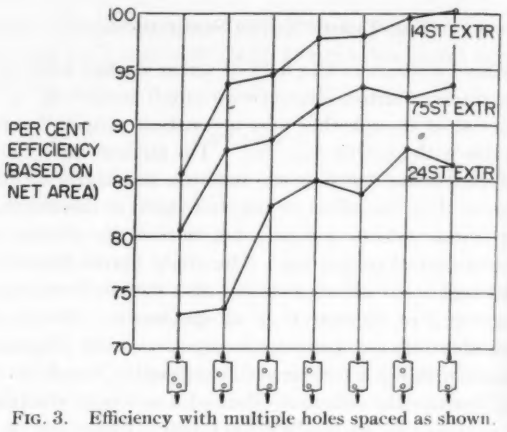

FIG. 3. Efficiency with multiple holes spaced as shown.

shape but are displaced vertically depending upon the alloy and the method of fabrication.

It is interesting to note that, when any one alloy is considered, the order from top to bottom in all cases is plate, bar, and extrusions. If any one method of fabrication is considered, the order from top to bottom is always 14ST, 75ST, and 24ST. No explanation is offered for the fact that in some cases efficiencies in excess of 100 per cent were measured. It is believed that these efficiencies can be justified on a theoretical basis but sufficient work has not been done as yet to establish a definite explanation.

MULTIPLE HOLES

Fig. 3 shows the effect of multiple holes. The ordinate in this figure is the same as that of Fig. 2. The abscissa is merely a convenient method of presenting the data. The specimens were arranged to show increasing efficiency for the sake of clarity. The amount of material removed in all cases was 25 per cent, and the hole locations are shown approximately to scale in the figure.

In order to determine whether the amount of the material removed or the radius of the hole was the controlling variable, a series of specimens was prepared with slotted holes, holding a constant radius at the ends of

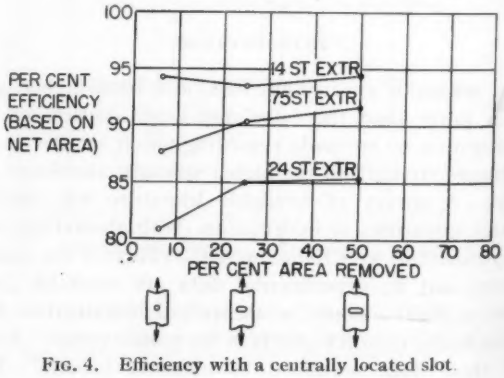

FIG. 4. Efficiency with a centrally located slot.

the slot and varying the length of the slot so as to vary the percentage area removed. These results are shown in Fig. 4. It appears from this figure that the radius has a much larger effect on the efficiency than the amount of removed area has. This information may be of some theoretical value, but it is of little practical value since most structural fastenings are circular in nature.

Pin-Loaded Members

The problem of pin-loaded members is much more complicated than that of centrally located holes because many more variables are present. It was first thought that the pin length would have considerable effect on the efficiency of the member. An attempt was made to determine the magnitude of this effect by testing a series of specimens, each of which was designed to fail at the same load based on the nominal strength of the material, but having different ratios of pin diameter to pin length. All pins were of the same diameter with the variation created by varying the thickness of the specimen and the amount of material around the hole. The series consisted of 17 specimens, some of 24ST and others of 75ST, with the pin length to diameter ratio varying from $^1/_2$ to 2. No significant variation of efficiency was noted from these tests and it was concluded that pin length was unimportant.

Next, a series of specimens was constructed with a variation in the amount of area removed from each. These specimens contained steel bushings through which the load was applied by a conventional pin. Bushing outside diameters were 1 in. installed with a light press fit of from 0.001 to 0.0025-in. interference. Only 75ST and 24ST extrusions were tested in this case. The efficiencies for 75ST vary from 88 per cent for 40 per cent area removed to 98 per cent for 75 per cent area removed. For 24ST extrusions the efficiencies vary from approximately 85 per cent for 50 per cent area removed to 90 per cent for 70 per cent area removed. The scatter in these cases is excessive and therefore the data are not reliable.

Conclusion

Figs. 2 and 3 represent information that the author believes may be used safely in design work to prevent both excessive weight and insufficient strength. The experimental work recorded here is only a start on what is hoped will be an extensive investigation of the nature of plastic failures as affected by practical design problems.

It has been standard practice throughout the industry to use substitute parts and materials on prototype airplanes to expedite their construction. The data in Fig. 2 emphasize the necessity for careful consideration of not only a change in alloy, but also a change in method of fabrication of this alloy wherever substitutions are to be made; and further emphasize the necessity for careful consideration in the design of the form in which an alloy is to be used as well as the alloy itself.

Reference

[1] Holleman, Clarence H., *Tension Joints in Aircraft Structures*, Journal of the Aeronautical Sciences, Vol. 10, No. 8, p. 295, October, 1943.

Part III. Notch Effects in High-Strength Aluminum-Alloy Spar Caps

D. L. MOSELEY

Douglas Aircraft Company, Inc.

Summary

For spar caps having an area of 4 to 6 sq.in. and with 15 to 25 per cent of this area removed by bolt holes, the average net area efficiency was 85 per cent for 14ST billets and 91 per cent for 75ST extrusions.

The general design trend in wing construction is to use large spar caps in medium and large airplanes. The Douglas Company is using only 14ST and 75ST caps in its most recent designs; the older airplanes had 24ST caps. In certain cases it may be desirable to have large bolt holes in the caps for the attachment of nacelles, flap brackets, landing gears, and similar items. In the case of the large airplanes, the problem of cap splicing is more predominant because the necessary lengths cannot be obtained in one piece. The purpose of this paper is to show the effect on the ultimate tensile strength of several arrangements of bolt holes in large spar caps of different materials.

Test Procedure

Three spar cap configurations were investigated for the effects of stress concentrations caused by large bolt holes in 14ST and 75ST spar caps. The hole patterns selected are typical for problems of this kind and the

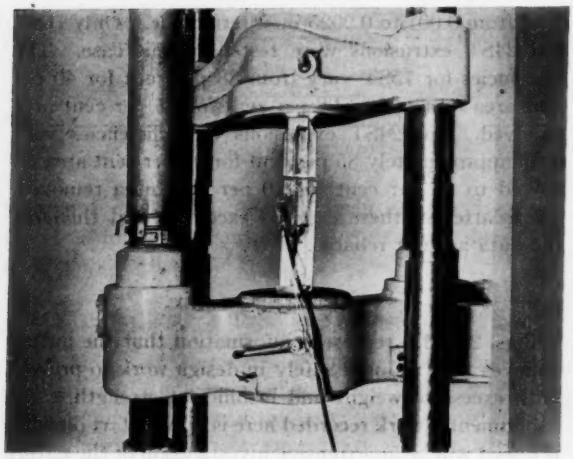

FIG. 1.

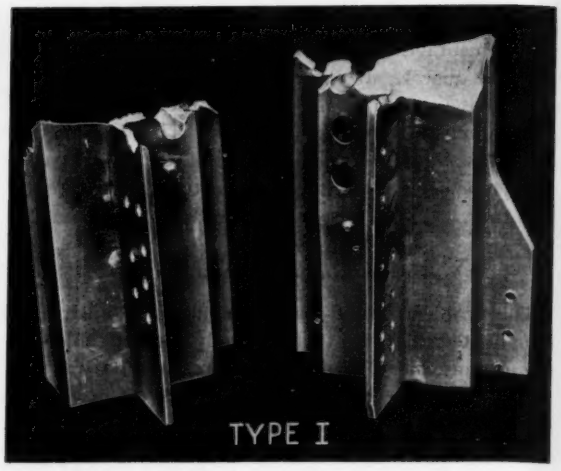

FIG. 2.

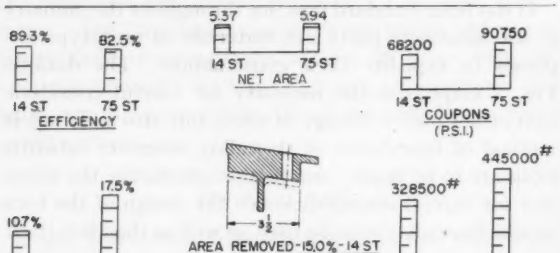

FIG. 3.

FIG. 4.

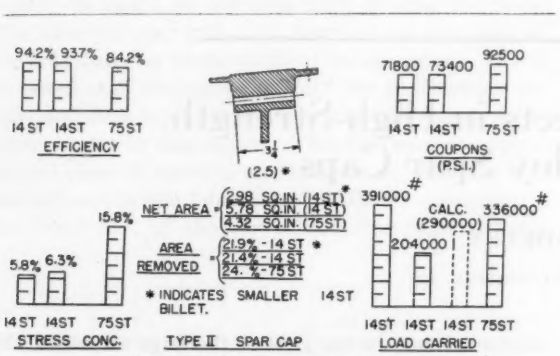

FIG. 5.

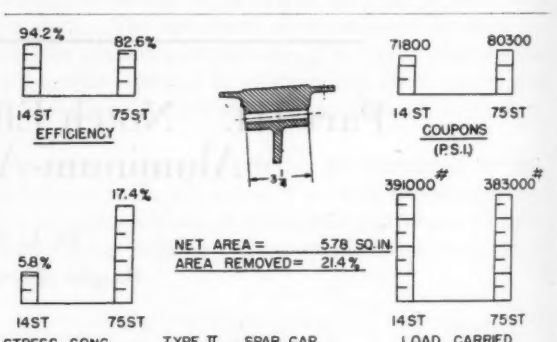

FIG. 6.

shape of the caps is common to many airplanes. The materials used were 14ST rolled billets, 75ST extrusions, and one 75ST rolled billet. The holes were not loaded in these tests.

The term "stress concentration" is used with respect to stress at ultimate failure and not to stress in the elastic range; it is used interchangeably with "stress notch sensitivity." The efficiency of the caps is based on the ratio of net area ultimate stress (S_N) of the caps to the ultimate stress (S_U) of the coupon materials.

Fig. 1 shows the test setup in the Southwark-Emery testing machine. Strain gages were used for checking the alignment of the cap specimen in the machine. Tensile coupons were taken out of several different zones in the cap cross sections in order to obtain an average that would be representative for the whole cap.

Coupons were taken as close as possible to the test specimen in order to minimize variations in properties which occur along the spars.

Fig. 2 shows a type I test specimen after failure. This cap had three large holes in a row passing vertically through one side of the cap. The net area used in subsequent computations takes the small holes in the flanges into account.

A comparison of a 14ST rolled billet with a 75ST extrusion for a type I spar cap is shown in Fig. 3. The two sections were the same size except that the body of the 75ST specimen was slightly deeper. The amount of eccentricity present is expressed as a function of the shift in neutral axis due to the hole divided by the width of the body of the cap ($3^1/_2$ in. in this case). In comparison with the 14ST cap, the 75ST cap had 10 per cent more net area, 32 per cent stronger (coupon) material, carried 35 per cent more load and had a 6.8 per cent greater stress concentration effect. The relative efficiencies of 14ST and 75ST were 89.3 and 82.5 per cent, respectively. Therefore, if the area of the 75ST cap had been increased only 7 per cent, the load carried should have decreased by 3 per cent to a new value of approximately 32 per cent and then the increase in area would have just offset the stress concentration effect of the hole.

Fig. 4 shows a type II test specimen after failure. This cap had one large horizontal hole through it, which was located below the neutral axis.

Two 14ST rolled billets are compared with a 75ST extruded specimen in Fig. 5. One 14ST cap was larger and the other was smaller than the 75ST cap. The amount of eccentricity present is expressed as a function of the shift in neutral axis caused by the hole divided by the depth of the cap body. From the data provided by the two 14ST caps, the strength of a third 14ST cap with a net area equal to that of the 75ST cap was calculated to be 290,000 lbs. On the basis of equal areas for 14ST and 75ST, the 75ST cap with an average of 27 per cent stronger (coupon) material, would have carried 16 per cent more load with an efficiency of 84.2 per cent. The load carried by the 75ST cap did not increase in proportion to its greater material strength by 11 per cent. This checks closely with the difference in efficiency of the two cap materials.

Fig. 6 is similar to Fig. 5 except that this time a 14ST rolled billet is compared with a 75ST rolled billet. This 75ST billet was used for experimental purposes only since its mechanical properties were not guaranteed. Both caps had the same dimensions and net areas. These results are different from all the others because of the fact that the 75ST carried 2 per cent *less* load than the 14ST although the coupon material in the 75ST cap was 11.8 per cent *stronger* than 14ST. This can be explained by observing that the 11.8 per cent increased material strength of the 75ST was offset by its 11.6 per cent greater stress concentration effect. Therefore, it should have carried about the same load

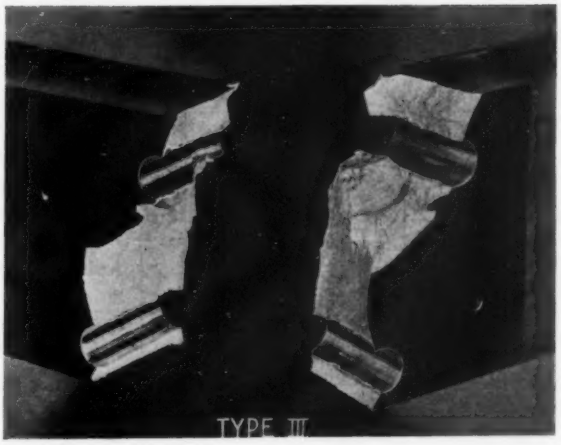

FIG. 7.

as the 14ST cap. The efficiency of the 14ST and 75ST caps was 94.2 and 82.6 per cent, respectively.

A type III test specimen after failure is shown in Fig. 7. Two large holes run vertically through the body of the cap and they are not located symmetrically with the center line of the cap. The two small holes were placed in the cap in order to simulate actual conditions on the airplane; they had a negligible effect on the test results.

Fig. 8 shows the relation of a 14ST rolled billet to a 75ST extrusion for a type III spar cap. The net areas of the two specimens differed by 1 per cent, the 75ST being the larger. The 75ST cap had 22 per cent stronger (coupon) material and carried 16 per cent more load. This shows that the 75ST cap's load-carrying capacity did not increase in proportion to its greater material strength by 6 per cent. This can be accounted for by the 75ST cap's lower efficiency of 84.5 per cent as compared with an efficiency of 89.8 per cent for the 14ST cap.

The various spar cap combinations have been compared on the basis of their efficiencies, S_N/S_U. Fig. 9 shows the efficiency of spar caps with respect to Jensen's curves for 2.0 by 0.50 specimens with single

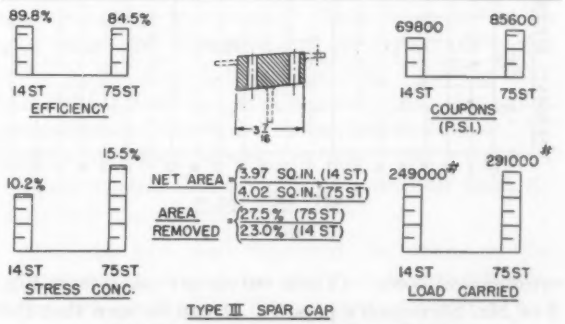

FIG. 8.

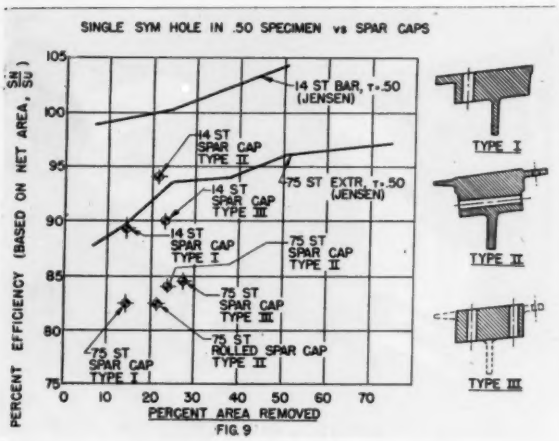
SINGLE SYM HOLE IN .50 SPECIMEN vs SPAR CAPS
PERCENT EFFICIENCY (BASED ON NET AREA, SN/SU)
105
100
95
90
85
80
75
0 10 20 30 40 50 60 70
PERCENT AREA REMOVED
14 ST BAR, T=.50 (JENSEN)
14 ST SPAR CAP TYPE II
14 ST SPAR CAP TYPE III
14 ST SPAR CAP TYPE I
75 ST EXTR. T=.50 (JENSEN)
75 ST SPAR CAP TYPE II
75 ST SPAR CAP TYPE III
75 ST ROLLED SPAR CAP TYPE III
75 ST SPAR CAP TYPE I
TYPE I
TYPE II
TYPE III
FIG. 9

FIG. 9.

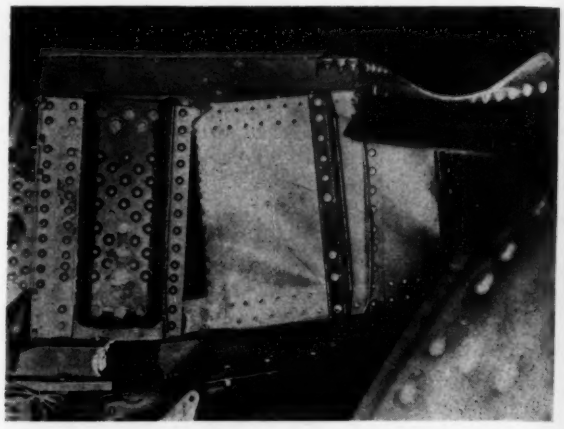

FIG. 12.

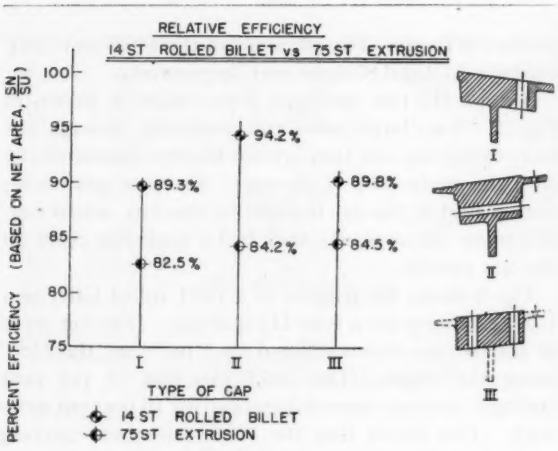

FIG. 10.

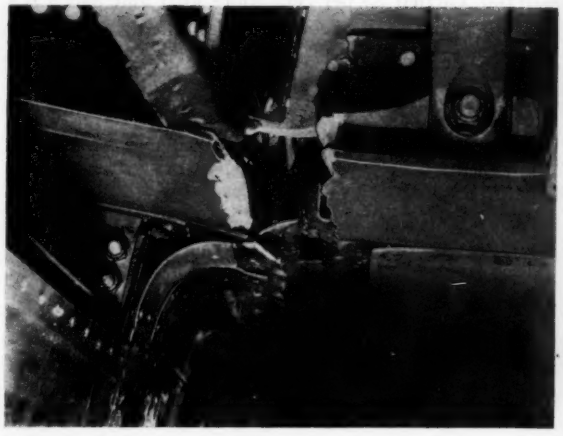

FIG. 13.

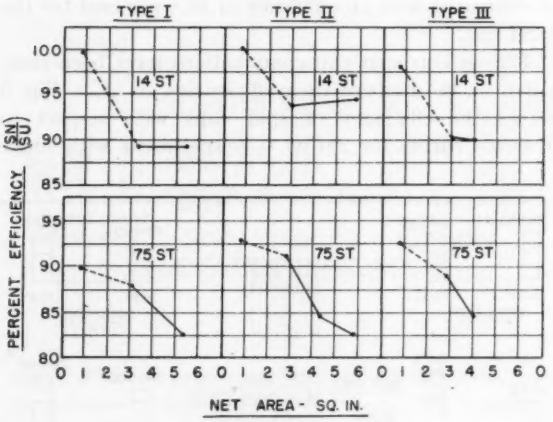

FIG. 11.

symmetrical holes. (These curves are taken from Fig. 2 of Mr. Stevenson's paper.) It can be seen that the type I cap has 7.5 to 10 per cent less efficiency than the small specimens of corresponding material. The type II spar caps showed 6 to 9 per cent lower efficiency for 14ST and 75ST (extrusions), respectively. The 14ST and 75ST caps, type III, had an efficiency 10 per cent lower than the corresponding small specimens.

Apparently the greater mass and eccentricity effects of the spar caps were the contributing factors to the lower efficiencies with respect to Jensen's curves.

Fig. 10 shows the relative efficiencies of 14ST and 75ST (extrusions) for the three different types of caps investigated. The 14ST rolled billet averages about 91 per cent in efficiency and the 75ST extrusion averages approximately 83 per cent in efficiency for the three types of caps.

The net areas have been plotted against efficiency for 14ST and 75ST in order to show mass effects. In Fig. 11 the three types of caps have been arranged so that their mass effects can be compared. The dotted lines connect spar cap data with the small 2.0 by 0.50 specimen data. For the range of specimens investigated, it can be seen that increasing the size causes decreasing efficiency. For the 14ST caps, there was small change in efficiency due to increased mass, but for

75ST a more rapid decrease in efficiency takes place with increased mass.

Static tests were conducted on two wings. One wing had all of its spar caps made of 14ST; the other had 14ST upper spar caps and 75ST extruded lower spar caps. The upper spar caps were exactly the same size in both wings and the only difference in the size of the lower caps was that the 75ST extrusions had more local area in the region of large bolt holes. In both wings the lower caps failed in tension. The failure in the front 75ST cap is shown in Fig. 12; this was a type I section. Fig. 13 shows the failure in the rear spar near a type II section. The wing with the 75ST caps carried 25 per cent more load than the wing with 14ST caps. Since the guaranteed minimum tensile strength of 75ST extrusion is 20 per cent greater than 14ST bar, this order of increased strength was expected with the provision that proper allowance was made for the greater stress notch sensitivity of 75ST material. (Coupons taken from the spars of these wings showed that 75ST material had 28 per cent greater strength.)

Conclusions

The results of these tests lead to the following conclusions: (1) In some cases, stress concentration effects have caused parts made from a high-strength aluminum alloy to have equal or slightly less strength than parts made from a lower strength aluminum alloy. (2) In overcoming the effects of stress concentrations, the 75ST alloy will require the addition of more material at the hole than the 14ST alloy. (3) Eccentricity, of course, is to be avoided. Holes through structural members should not come too near the surface. (4) Test results show that there is a trend toward decreasing efficiency as the mass of the spar cap increases. (5) Small local increases in area take care of the notch effects caused by bolt holes, making it possible to take advantage of the greater strength in the remainder of the 14ST or 75ST member. (6) In view of the limited number of tests, there is a need for further investigation of large-size specimens of high-strength aluminum alloys for the effects of stress concentrations.

Part IV. The Effect of Notches upon Limiting Strain in High-Strength Aluminum Alloys

O. A. WHEELON AND ST. J. BARRETT

Douglas Aircraft Company, Inc.

Abstract

Bending tests were conducted on $^1/_2$-in. square, notched bars of 14ST, 24ST, and 75ST. It was found that notches of any depth drastically reduce the limiting strain for all materials tested and for all testing temperatures. The effect of notches upon the formability in bending is more severe in the case of 75ST than in the case of 24ST. Heating appreciably increases the limiting strain under notch conditions for the two artificially aged alloys, 14ST and 75ST. A true solution of the notch problem is dependent upon a fuller knowledge of rupture conditions under triaxial stresses and upon knowledge of the effect of notch geometry upon the stress state.

Introduction

THE EARLIEST EXPERIENCE of Douglas Aircraft in forming 75ST parts showed the strain limits of that material to be extremely sensitive to scratches. It was found that if excessive breakage during forming was to be avoided, it was necessary to polish the critical regions of all parts to be formed. This shop experience indicated that the relative effect of notches upon the strain limits of 24ST and 75ST was exactly the opposite of their effect upon the ultimate tensile strength of the two alloys.

Test Work

A series of tests was conducted to determine under controlled conditions the quantitative effect of notches upon fabrication or strain limits. The tests were confined to the bending of $^1/_2$-in. square bars cut from 14ST, 24ST, and 75ST extrusion. The 14ST and 75ST bars were bent at elevated as well as at room temperature. At least two bars of each alloy were set aside as control specimens and a 60° V notch was machined across one face of each of the others. Three depths of notch were used. For the 24ST and 75ST bars the radius at the root of the notch was 0.0025 in. For the 14ST bars, which were run in a separate test, the radius was 0.0005 in. The bars were supported by two $1^1/_2$-in. radius rollers with centers 5 in. apart, and a load was centrally applied through a $^1/_2$-in. radius die block directly over the notch.

After the bars were fractured the strain on the tension surface of each bar was read from a 100-line-to-the-inch photogrid. The greatest strain that had been attained away from the notch was taken as the "limiting strain" or fabrication limit for that particular

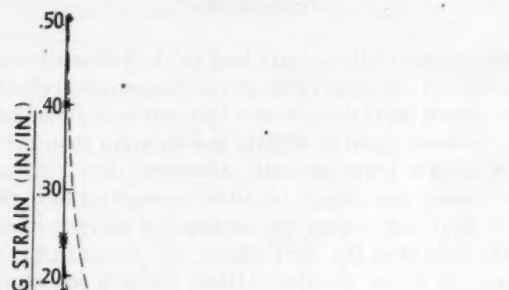

FIG. 1. Limiting strain vs. notch depth (24ST, 75ST).

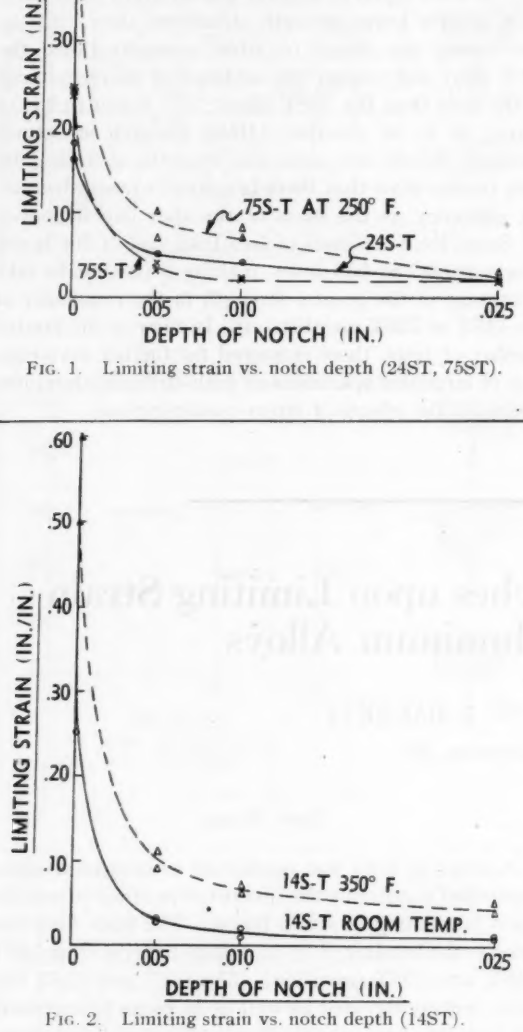

FIG. 2. Limiting strain vs. notch depth (14ST).

FIG. 3. Limiting strain vs. notch depth. Per cent of control specimen (24S, 75S).

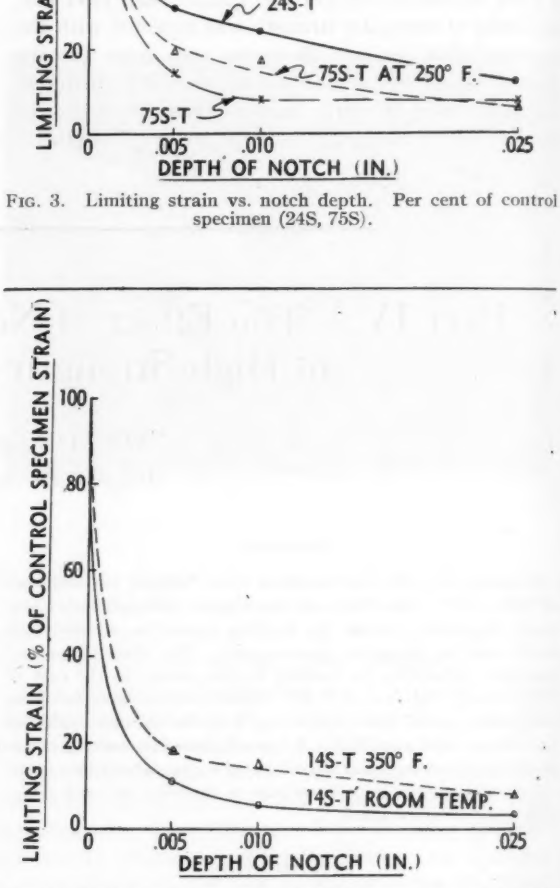

FIG. 4. Limiting strain vs. notch depth. Per cent of control specimen (14ST).

operation and notch condition. In Fig. 1 the limiting strain for the 24ST and 75ST bars is plotted against notch depth. It can be seen that under notch conditions the limiting strain of 24ST exceeds that of 75ST at room temperature, while the limiting strain of 75ST at 250°F. is higher than either of the other two. Fig. 2 shows the limiting strain for the 14ST bars. These are not compared directly with the data from the 24S and 75S bars because of the difference in root radii.

EFFECT OF TEMPERATURE

For both 14S and 75S, heating increased the limiting strain under notch conditions. At any strain level the horizontal distance between the "hot" and "cold" curves for the same material indicates the range of notch depths that would precipitate failure in cold bending but not in hot bending. This distance is a measure of the relative advantage of hot bending at the various strain levels. The vertical distance between the two curves indicates the difference in strain level permissible

at the two temperatures for a surface condition simulating a notch of any given depth.

Notch Effect not Isolated

In an attempt to isolate the notch effect the limiting strains of the notched bars were expressed as percentages of the limiting strains attained in the corresponding unnotched bars. In Fig. 3, these values are plotted against notch depth.

On first analysis it appeared that this per cent of the control specimen strain determined the relative bending strain "notch sensitivity" of the materials. On this basis, the limiting strain of 24ST appears least affected by notches; that of 75ST at 250°F. next; and 75ST at room temperature most affected. Fig. 4 indicates that the performance of the 14ST bars is also improved by heating. A re-examination of the data, however, shows the fallacy of this reasoning. Work conducted by Sachs[1] has indicated that the limiting strain in bending unnotched bars is related to a stability phenomenon similar to that of necking in tensile test coupons. This stability factor varies both with material and with specimen geometry. Hence, the basis from which the notch effect is measured is not a true material constant but rather is a sliding yardstick whose change with specimen geometry differs for different materials.

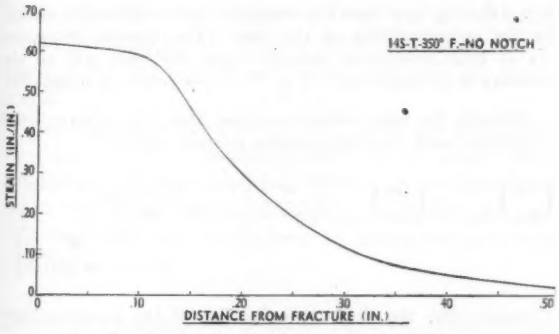

Fig. 5. Strain distribution unnotched specimen.

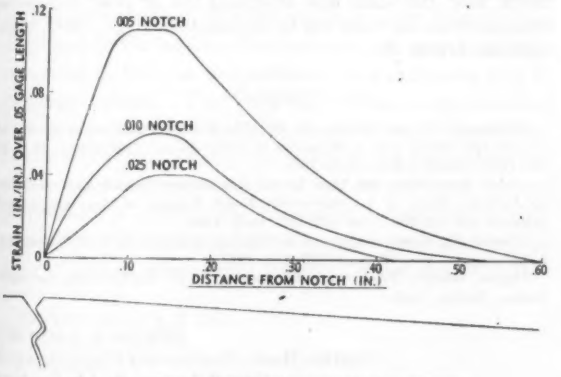

Fig. 6. Strain distribution notched specimen.

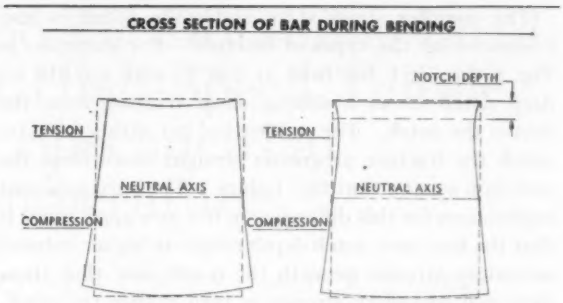

Fig. 7. Cross section of bar during bending. (a, *left*) Unnotched. (b, *right*) Notched.

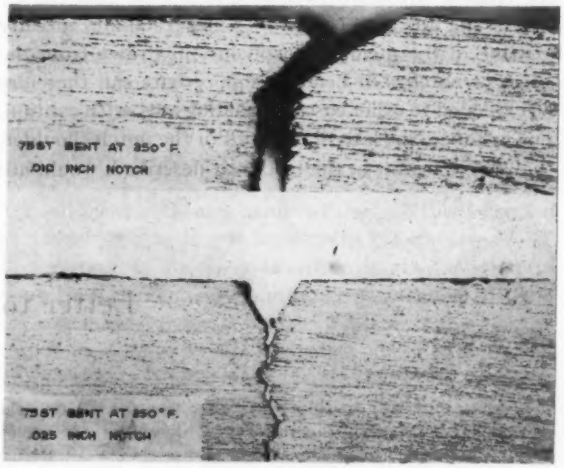

Fig. 8. Sections of fractured bars.

Triaxial Stress State

Further study reveals another obstacle to any general application of the data. This obstacle lies in the triaxial stress state induced by the notch. The existence of such a stress state is deduced from photogrid analysis. The distribution of strain along the surface of an unnotched bar bent to fracture is shown in Fig. 5. The region of greatest strain is directly adjacent to fracture. The distribution of strain along the surface of similar bars with notches is shown in Fig. 6. For these there is zero strain at the edge of the notch, and this zero strain in the notch shoulder has an important effect upon the stress state at the notch root.

Normally, when a bar is bent the material on the tension side of the bend contracts laterally to preserve constant volume, so that the cross section changes from that shown by the dotted lines of Fig. 7a to that shown by the solid. When there is a notch in the tension surface of the bar, however, the unstrained material in the shoulder of the notch does not contract laterally and tends to restrain the highly stressed material at the notch root as shown in Fig. 7b. Thus, the notch shoulder produces an increased lateral stress.

The complex stress state under the notch is also evidenced by the types of fracture. For example, in Fig. 8 the 75ST bar bent at 250°F. with a 0.010 in. deep notch shows a sliding, shear fracture from the root of the notch. For an identical bar with a 0.025 in. notch the fracture progresses straight down from the root in a square, "brittle" failure. The only apparent explanation for this difference in fracture appearance is that the increased notch depth results in higher induced secondary stresses beneath the notch, and that these increased secondary stresses in turn change the conditions of rupture.

Since a significant part of the notch effect is found in the triaxial stresses it produces, it is clear that the effect of the notch will vary with the triaxiality already existing in the member. Conclusions drawn from the effect of notches in bending square bars can therefore be extended to other cases of bending only with caution. For instance, the lateral restraint of the notch shoulder, though important in the tests just described, would not influence the bending of wide sheet where there is already complete lateral restraint.

In brief, it must be concluded that the notch effect cannot be isolated in tests such as these until we have a more thorough understanding of the variables affecting the bending process itself, the effect of notch geometry upon the stress state, and the effect of triaxiality upon rupture conditions.

However, despite these difficulties the tests have shown how seriously strain limits are reduced by discontinuities and the need for polishing critical items. The benefit of heat is well demonstrated for those materials whose local elongation improves at elevated temperatures.

Reference

[1] Sachs, George, Lubahn, J. D., and Taub, J. B., *Correlation of Information Available on the Fabrication of Aluminum Alloys (NA-126): Section V, Formability of Aluminum Alloys for Use in Military Aircraft, Part V—Simple Bending of Rectangular Shapes by Means of Dies*, N.D.R.C. Report O.S.R.D. No. 5014, Serial No. M-487 (1945).

Letter to the Editor

Dear Sir:

It seems important at the present time to point out that the linearized compressibility correction of $1/\sqrt{1-M^2}$ applies only to two-dimensional flows. The factor $1/\sqrt{1-M^2}$ has been improperly introduced as a correction for axially symmetric three-dimensional flows in many recent papers (see, for example, references 1 and 2).

As early as 1937 Ferrari[3] pointed out that to the first order or linear approximation a given body of revolution has the same pressure distribution in either a compressible or an incompressible fluid as long as the flow remains subsonic. The incorrect derivation of the factor $1/\sqrt{1-M^2}$ for three-dimensional flows has been based on the assumption that the linearized perturbation potential ϕ' varies directly with the geometry of the flow. This, however, is only true for two-dimensional flows as may be seen by comparing the potential for a source in the two cases.

$$\phi(x, y) = Ux + (m/2\pi)\log r$$
$$\phi'(x, y) \backsimeq (m/2\pi)\left\{\log a + [(r-a)/a]\right\}$$

for $|r-a| < |a|$.

$$\phi(x, y, z) = Ux + (m/4\pi)(1/r)$$
$$\phi'(x, y, z) \backsimeq \frac{m}{4\pi}\left(\frac{1}{a} - \frac{r-a}{a^2}\right)$$

for $|r-a| < |a|$.

The analysis of a source sink system in a compressible subsonic flow shows that, for a given small symmetric body in an axially symmetric flow, the increase of Δu the velocity component along the x axis (free stream direction) due to compressibility effects will be approximately

$$\left(\frac{\Delta u}{u_\infty}\right)_{\text{Comp.}} \approx \left(\frac{\Delta u}{u_\infty}\right)_{\text{Incomp.}} \left[\frac{2x^2-(1-M^2)y^2}{2x^2-y^2}\right] \times \left[\frac{x^2+y^2}{x^2+(1-M^2)y^2}\right]^{3/2}$$

at large distances from the body. As a first approximation the velocity increment Δu along the body or along the streamline $y = 0$ flowing to or from the stagnation point will not be altered by the compressibility of the fluid. The velocity increment Δu at great transverse distances from the body will on the contrary be increased by $1/(1-M^2)^{3/2}$ (see reference 4, page 33).

Similarly, for plane two-dimensional flows over a given small symmetric body the corresponding relation will be

$$\left(\frac{\Delta u}{u_\infty}\right)_{\text{Comp.}} \approx \left(\frac{\Delta u}{u_\infty}\right)_{\text{Incomp.}} \left[\frac{x^2-(1-M^2)y^2}{(x^2-y^2)\sqrt{1-M^2}}\right] \times \frac{x^2+{}^2y}{x^2+(1-M^2)y^2}\Bigg]$$

Consequently, the first approximation of the compressibility effects is to increase the velocity increment Δu along the given body or along the streamline flowing to or from the stagnation point by the factor $1/\sqrt{1-M^2}$. Similar to the axially symmetric flow, the plane flow increment Δu at great transverse distances from the body will be increased by $1/(1-M^2)^{3/2}$ (see reference 4, page 29).

References

[1] Goldstein, S., and Young, A. D., *The Linear Perturbation Theory of Compressible Flow, with Applications to Wind Tunnel Interference*, R & M No. 1909, British A.R.C., July, 1943.

[2] Tsien, Hsue-Shen, and Lees, Lester, *The Glauert-Prandtl Approximation for Subsonic Flows of a Compressible Fluid*, Journal of the Aeronautical Sciences, Vol. 12, No. 2, pp. 173–187, April, 1945.

[3] Ferrari, C., *Campi di Corrente Impersonora Attorno a Solidi di Rivolusione*, L'Aerotecnica, Vol. 17, pages 507–518, 1937.

[4] Sauer, Robert, *Theoretische Einführung in die Gasdynamik*, Springer-Verlag, Berlin, 1943.

Edmund V. Laitone
Section Head—Engineering Flight Research
Cornell Aeronautical Laboratory

An Autographic Method for Obtaining Load-Extension Records of High-Speed Tensile Tests on Sheet Specimens at Elevated Temperatures

ALAN E. FLANIGAN,* LESLIE F. TEDSEN,† JOHN E. DORN,‡ AND H. R. KAISER†

University of California

ABSTRACT

An apparatus has been developed for obtaining load-extension records of tensile tests on sheet specimens at elevated temperatures. It has been used successfully at temperatures up to 900°F. and at strain rates as high as 1 per sec. Difficulties are encountered, however, in determining the load at fracture. Typical results are shown to illustrate the effects of testing temperature and strain rate on the load-extension curves for XB75S-O Alclad sheet.

INTRODUCTION

IN CONNECTION WITH A RECENT STUDY of the formability of aluminum-alloy sheet at elevated temperatures, it was necessary to investigate the elevated temperature tensile properties related to formability.[1] Since the testing speeds were considerably higher than those ordinarily used in tensile testing, an autographic method was required. The problem was further complicated by the need to use sheet materials for specimens.

The apparatus described in this paper was developed to obtain complete load-extension records under these conditions. It was used successfully at temperatures up to 900°F. and at strain rates as high as 1 per sec. It is probably suitable for tests at higher temperatures and higher rates.

GENERAL DESCRIPTION OF LOAD-EXTENSION RECORDER

Electrical methods are employed to measure both load and extension. An a.c. voltage is regulated in such a manner that changes in voltage are directly proportional to the load on the specimen. A second voltage is caused to vary in proportion to the extension in a 2-in. gage length. The resulting voltages are rectified and applied across the deflecting plates of a cathode-ray oscilloscope, causing the beam of the latter to trace out a load-extension curve which is recorded photographically. During the course of a test the oscilloscope beam is extinguished at regular intervals to produce a dashed curve from which it is possible to determine variations in strain rate. The frequency of interruption may be adjusted over a wide range. Upon final parting of the specimen the beam is automatically extinguished permanently. A block diagram of the apparatus and a photograph of the recorder are shown in Figs. 1 and 2.

LOAD MEASUREMENT

Load measurement is achieved through the deflection of a steel proving ring in series with the specimen (Fig. 3). A pair of SR-4, A-11 strain gages mounted in opposition on the inner and outer surfaces of the ring are connected to an a.c. bridge circuit so that when the ring is loaded the bridge is thrown out of balance. A 12,000-cycle oscillator is used to feed the bridge, and the alternating voltage resulting from unbalance is amplified and rectified, yielding direct voltage proportional to the load. This voltage is applied to the vertical deflecting plates of the oscilloscope.

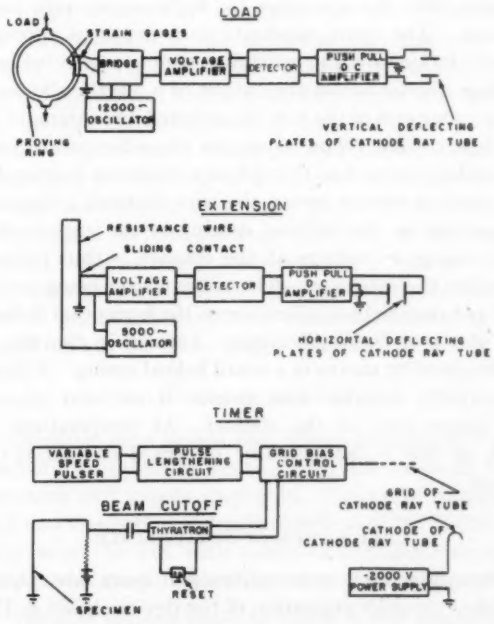

FIG. 1. Block diagram of load-extension recorder.

Received January 8, 1946.

* Research Engineer.
† Engineer.
‡ Associate Professor.

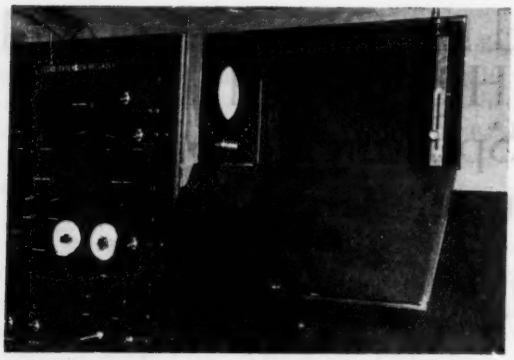

FIG. 2. Load-extension recorder.

FIG. 3. Proving ring and loading device used in calibration of load scale.

A load calibration is carried out immediately preceding each test. In this process spots corresponding to known loads are photographed on the screen of the oscilloscope. True values of the loads used in calibration are obtained by means of a second set of strain gages mounted on the ring and connected to an SR-4 strain indicator. Previous calibration of the proving ring is, of course, required.

MEASUREMENT OF EXTENSION

The extensometer is somewhat similar to a device used at room temperature by Jones and Moore.[2] It consists of two steel yokes, a 30-gage Nichrome resistance wire, and a sliding contact made of nickel rigidly attached to the upper yoke. Details are shown in Figs. 4 and 5.

In testing, the yokes are secured to the specimen at each end of the gage length by means of sharp cones pressed into the specimen by high-temperature steel springs. The cones penetrate to a depth of approximately 0.007 in. The resistance wire is connected as a voltage divider across the output of a 5,000-cycle oscillator. One end of the wire is anchored and grounded at the lower yoke. The remainder extends upward past the sliding contact so that when a specimen is extended the contact sweeps across the wire through a distance dependent on the relative spacing of the gage points. The change in voltage at the contact is thus proportional to the extension. The voltage after being amplified and rectified is applied across the horizontal deflecting plates of the oscilloscope. Tension in the wire is maintained by means of a small helical spring. A slight eccentricity of the wire causes it to bear against the sharp edge of the contact. At temperatures as high as 900°F. satisfactory electrical contact is obtained.

CALIBRATION OF STRAIN SCALE

Preceding each test calibration spots are photographed through utilization of the device shown in Fig. 5. To effect calibration the sliding contact is discon-

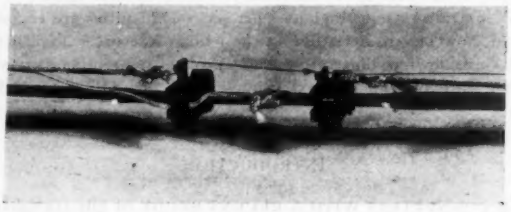

FIG. 4. Extensometer mounted on specimen.

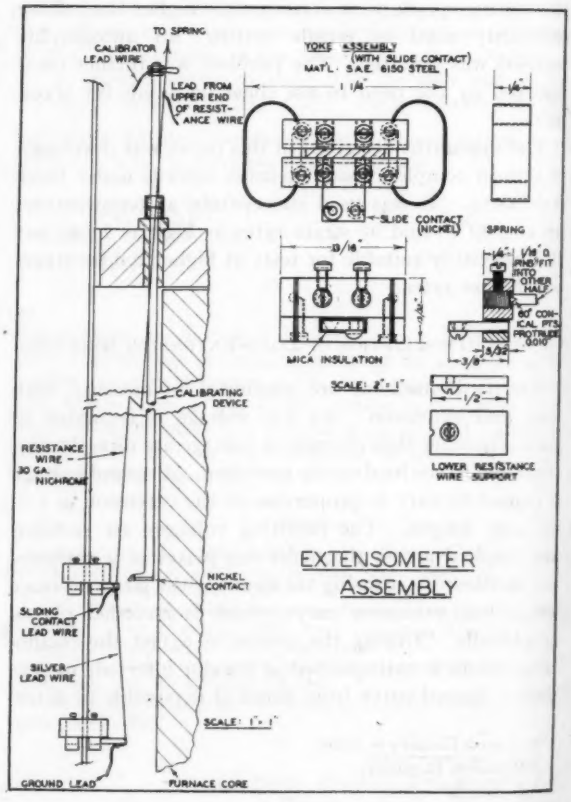

FIG. 5.

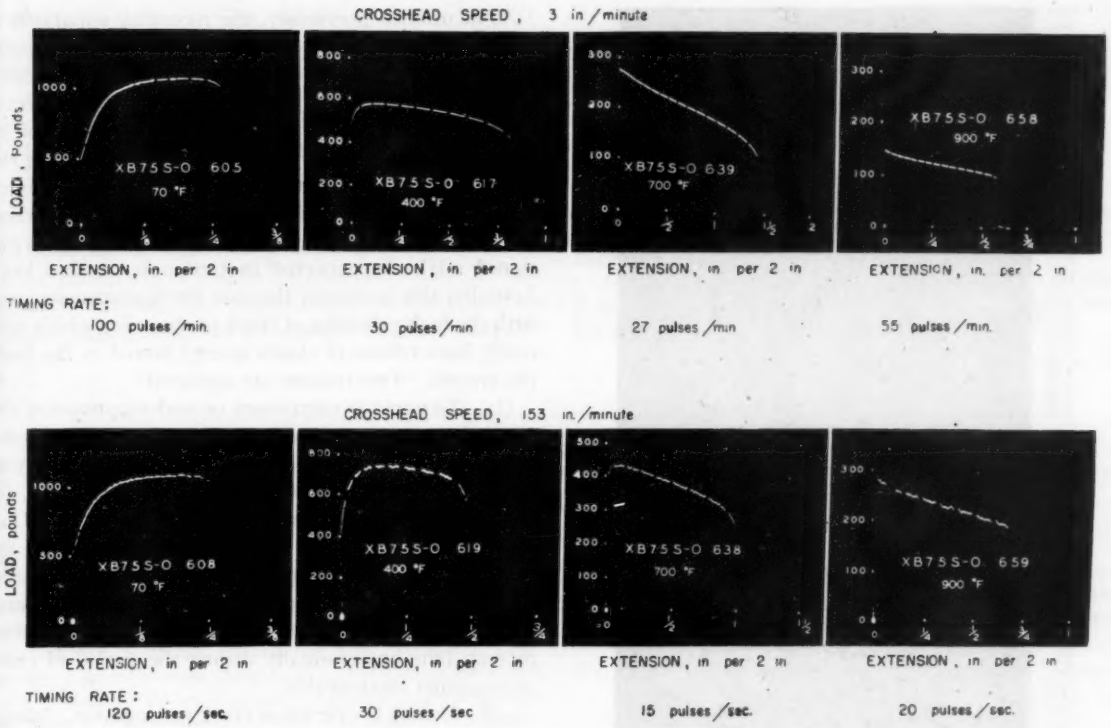

FIG. 6. Typical load-extension records for XB75S-O Alclad sheet.

nected from the oscilloscope circuit and the "calibrator" substituted. The nickel contact edge of the latter is positioned on the resistance wire slightly above the upper yoke and a spot corresponding to zero extension is registered. The calibrator is then moved upward along the wire and additional spots are photographed at known distances, a step gage being used to insure accurate control of the movement. In elevated temperature tests motion of the calibrator is controlled from outside of the furnace.

After calibration, the calibrator is withdrawn and the original connections are restored. The point on the oscilloscope screen representing zero elongation for the following test is then made to coincide with that for the calibration by means of a zero positioning control in the circuit. Thus, it is not necessary that the initial position of the calibrator on the wire coincide with that of the moving contact.

In tests at elevated temperature, calibrations should be made after specimen and extensometer have attained temperature, so that no change in temperature occurs between calibration and testing. Heating currents must be shut off during both operations to eliminate electrical interference.

Typical Load-Extension Records

A set of typical records shown in Fig. 6 reveals the effects of temperature and strain rate in tests on XB-75S-O*Alclad sheet. The individual curves are combined and plotted to a common scale in Fig. 7.

Although each of the tests was run at constant crosshead speed, it may be seen from the timing pulses in Fig. 6 that the strain rate varied in the course of a test, the rate in the elastic region being considerably lower than that attained in the plastic portion. The variation is attributed to the design of the specimen employed. The reduced section (including the 2-in. gage length) was $3^1/_2$ in. long in a total specimen length of 24 in. In the early stages of a test both the reduced section and the much longer grip section were strained elastically, so that only a small part of the crosshead motion was concentrated in the gage length. Because of its smaller section, however, the latter flowed plastically at loads at which the remainder of the specimen was below the elastic limit. Thus, an increasing proportion of the crosshead motion was concentrated in the gage length in the latter stages of a test.

Evaluation of the Method

Extensive tests reveal that the apparatus produces reliable load-extension records over the range of temperatures and speeds employed. Values of maximum load and elongation at fracture indicated by the curves have been checked with values determined independently and found in good agreement. The reproduci-

* The alloy formerly known as XB75S is now designated as 75S by its producer, the Aluminum Company of America.

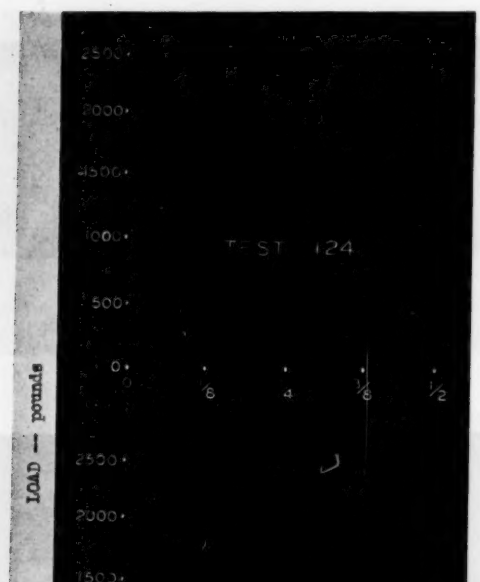

FIG. 7. Load-extension curves for bare XB75S-O sheet (replotted from Fig. 6).

bility of records is excellent, as indicated in Fig. 8. As noted later, however, serious difficulties are met in determining the precise load at fracture.

A modified extensometer incorporating a resistance wire on each side of the specimen has been used to determine yield stress and the modulus of elasticity at elevated temperatures. While acceptable for determination of yield stress, the method is not regarded as satisfactory for the modulus of elasticity. Rather smooth curves were obtained but scatter in the modulus values was of the order of ±5 per cent. Lack of flatness on the part of the oscilloscope screen contributed to the difficulty.

DIFFICULTIES ATTENDING DETERMINATION OF THE LOAD AT FRACTURE

In the study of formability true stress-true strain curves are often desired. To derive such information from a load-extension record it is necessary to know both the load at fracture and the corresponding local strain. The latter may be obtained from the fractured specimen by measurement of the reduction in area but the load at fracture in a high-speed test presents more difficulty.

As mentioned previously, the recording apparatus is so constructed that the oscilloscope beam is automatically extinguished upon final parting of the specimen, this action depending on the breaking of a circuit through the specimen itself. Thus, after initiation of fracture, the apparatus continues to record during the period of crack propagation. The load on the specimen tends toward zero at the instant of complete parting since the remaining section vanishes. As a result, the record might be expected to terminate at zero load. Actually, this is seldom the case for reasons associated with the high velocities of crack propagation which may result from release of elastic energy stored in the loading system. Two reasons are apparent:

(1) To avoid overexposure or underexposure of the film it is necessary to select an intensity of the oscilloscope beam suitable for the crosshead speed employed. A greater intensity is needed in a high-speed test, for instance, than in one conducted at a lower speed. During the period of crack propagation the travel of the beam may become relatively rapid, resulting in a decrease in the intensity of the record. The latter may vanish abruptly upon initiation of fracture (desirable) or may fade out gradually during the period of crack propagation (undesirable).

(2) During the period of crack propagation, changes in the load on the proving ring may lag simultaneous changes at the fracture, the difference depending on such factors as the distance from the fracture to the proving ring and the relative velocities of crack propagation and the stress wave. The final point on the record may, therefore, lie between zero load and the actual load at fracture. When the velocity of crack propagation is sufficiently great, the last point may correspond closely to the load at fracture (desirable). Otherwise, the record may continue past this point (undesirable). In cases where the load-extension record continues beyond the initiation of fracture, a more or less abrupt change

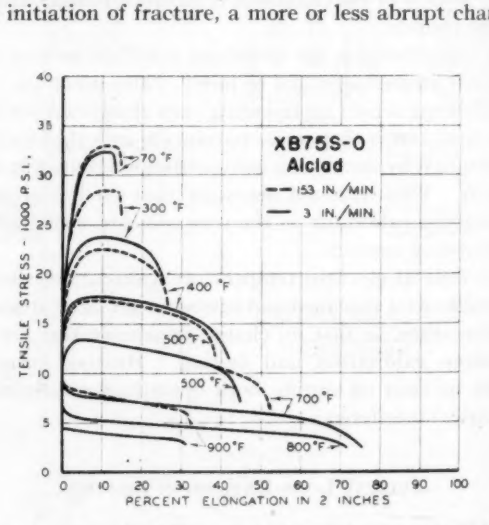

FIG. 8. Reproducibility of load-extension records. Material: 24S-T sheet. Crosshead speed: 3 in. per min. Timing rate: one pulse per sec. Test temperature: 69 °F.

in slope might be expected to mark the actual fracture. In practice, such changes are often not evident or are poorly defined.

In conclusion, it may be said that the method as employed to date may fail to clearly define the fracture load but that it is otherwise satisfactory.

ACKNOWLEDGMENT

The apparatus described in this paper was developed at the University of California as a portion of the "restricted" Project NRC-548 financed by the War Production Board's Office of Production Research and Development and supervised by the War Metallurgy Committee. The program was devoted to the study of the formability of aluminum-alloy sheet at elevated temperatures. This paper has been released for publication by the O.P.R.D.

REFERENCES

[1] Flanigan, A. E., Tedsen, L. F., and Dorn, J. E., *Tensile Properties Affecting the Formability of Aluminum Alloy Sheet at Elevated Temperatures.* (To be published.)

[2] Jones, P. G., and Moore, H. F., *An Investigation of the Effect of Rate of Strain on the Results of Tension Tests of Metals*, Proc. A.S.T.M., Vol. 40, pp. 610–644, 1940.

Letters to the Editor

Dear Sir:

The paper by G. H. Martin, "A Procedure for Determining the Critical Load for a Column of Varying Section" (JOURNAL OF THE AERONAUTICAL SCIENCES, Vol. 13, No. 3, p. 135, March, 1946) presents a simple method based upon approximating the elastic curve. Whenever found in aircraft structures, good design usually dictates that such columns vary in a more or less regular manner.

In such cases there is available a much shorter method, for which the writer is indebted to Arthur Ogness, of the Douglas Aircraft Company, Inc. It is based upon the usual assumption that the elastic curve is a segment of a sine curve and uses energy methods and a matrix solution to arrive at the following expression for the critical load of a pin-ended column:

$$P_{cr} = 20{,}000(E/L^2)\sum_{0}^{n}(C_n/I_n)$$

in which

n = the number of segments into which the column is divided
I_n = the average moment of inertia of each segment
C_n = a constant whose value for each segment is as follows:

Segment Numbers	C
1 and 10	10.00
2 and 9	84.15
3 and 8	204.05
4 and 7	323.88
5 and 6	397.28

In the classic example of Dinnick, as solved by the author in his Appendix, only one-half of the symmetrical column need be considered. Using a slide rule, the procedure is as follows:

Segment	1	2	3	4	5
Avg. I	0.0322	0.0368	0.0451	0.0491	0.0491
C	10.0	84.2	204	324	397
C/I	310	2290	4520	6600	8090

$$\sum_{0}^{10}(C/I) = 43{,}600$$

$$P_{cr} = 20{,}000E/43{,}600L^2$$

for $I' = 0.0491$ and

$$P_{cr} = 9.35EI'/L^2$$

for any value of I'.

This is the identical result obtained by the author and compares with Dinnick's value of $9.45EI'/L^2$. It is evident that the labor of the above solution is negligible in comparison to the author's method.

FRANCIS V. WAGNER
North American Aviation, Inc.

Dear Sir:

While reading the very interesting paper—"A Method for the Stress Analysis of Helicopter Blades," Journal of the Aeronautical Sciences, April, 1946, by D. O. Dommasch, it occurred to me that it may be of interest in this connection to outline the procedure used by the Jet Helicopter Corporation, of New York, in preliminary stressing of their fixed-blade rotors. Although the solution found here is, in general, a roughly approximate one, nevertheless, because of its relative simplicity, the procedure itself seems to be useful, especially in the preliminary state of design when a quick though approximate answer is most desirable. If such an answer is not available at that time, the design engineer is delayed, or must fill the gap by "rule of thumb."

A number of characteristic stations of the blade are selected. It is clear that the greater the number of stations used, the greater will be the accuracy of the result, but for the preliminary stressing even three properly selected points are sufficient. Let the characteristic stations be at distances r_1, r_2, and r_3 from the rotor axis, and in the state of equilibrium let the values of M/EI be u, v, and w, respectively (see Fig. 1). If at any station (at r_2 and r_3, Fig. 1) a sudden change in the moment of inertia of the

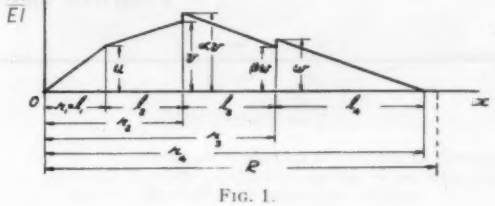

FIG. 1.

blade section due to reinforcing cuffs, etc., is present, then a suitable coefficient (α, β in Fig. 1) should be introduced. This coefficient expresses the ratio of the moment of inertia of sections immediately outboard and inboard of the station in question. It is assumed next that in the state of equilibrium of the blade under loads the function M/EI ($dy/dx = \int (M/EI)dx$, where y is the deflection of the blade neutral axis, and x is the distance from the rotor axis) varies linearly between any consecutive pair of the characteristic stations (Fig. 1). For fixed-blade rotors the rigidity of the hub is usually so great in comparison with the blade itself that it seems to be justified to consider that at the station zero $M/EI = 0$.

Keeping these assumptions in mind and by using simple arithmetic and elementary calculus, there is no difficulty in expressing the deflection y of any point x of the blade neutral axis as a function of the unknown u, v, and w. Between the particular pairs of characteristic stations the deflection y becomes:

From 0 to r_1

$$y = {}^1/_6(x^3/r_1)u \tag{1}$$

From r_1 to r_2

$$y = [{}^1/_6l_1^2 + {}^1/_2l_1(x - r_1) + {}^1/_2(x - r_1)^2 - ({}^1/_6l_2)(x - r_1)^3]u + ({}^1/_6l_2)(x - r_1)^3v \tag{2}$$

From r_2 to r_3

$$y = [{}^1/_6l_1^2 + {}^1/_3l_1l_2 + {}^1/_3l_2^2 + {}^1/_2r_2(x - r_2)]u + [{}^1/_6l_2^2 + {}^1/_2l_2(x - r_2) + {}^1/_2\alpha(x - r_2)^2 - ({}^1/_6l_3)\alpha(x - r_2)^3]v + ({}^1/_6l_3)\beta(x - r)w \tag{3}$$

From r_3 to r_4

$$y = [{}^1/_6l_1^2 + {}^1/_2l_1l_2 + {}^1/_3l_2^2 + {}^1/_2r_2l_3 + {}^1/_2r_2(x - r_3)]u + [{}^1/_6l_2^2 + {}^1/_2l_2l_3 + {}^1/_3\alpha l_3^2 + {}^1/_2(l_2 + \alpha l_3)(x - r_3)]v + [{}^1/_6\beta l_3^2 + {}^1/_2\beta l_3(x - r_3) + {}^1/_2(x - r_3)^2 - ({}^1/_6l_4)(x - r_3)^3]w \tag{4}$$

The further procedure can be carried out through the following steps: (1) The whole blade is divided into a number of elements (say 10). (2) The weight and c.g. position of each element is estimated (r_4 is supposed to coincide with the c.g. of the last element). (3) The centrifugal force produced by each element is computed. (4) Deflection of the blade neutral axis at the abscissae corresponding to the elements' c.g.'s (x) are expressed in terms of u, v, and w with the help of Eqs. (1) to (4). (5) Deflection of the blade neutral axis at the characteristic stations is computed as in step (4). (6) The centrifugal force arms of different blade elements with respect to the c.g. of the characteristic sections are computed from steps (4) and (5), as well as on the basis of the blade geometry (e.g., preconing angle). (7) Sum of moments (due to the centrifugal force) about the neutral axis at the characteristic sections are found from steps (3) and (6). (8) Total bending moments M at the characteristic stations (r_1, r_2, r_3) are expressed by adding to the centrifugal force bending moments $\Sigma M_{c.f.}$ the bending moments due to the aerodynamic loads (M_A), and subtracting the bending moments due to weight, or inertia forces M_W.

Hence, for the characteristic sections the following equations can be set up:

$$EI_{r_1}u = M_{A_{r_1}} + \Sigma M_{c.f._{r_1}} - M_{W_{r_1}}$$
$$EI_{r_2}v = M_{A_{r_2}} + \Sigma M_{c.f._{r_2}} - M_{W_{r_1}}$$
$$EI_{r_3}w = M_{A_{r_3}} + \Sigma M_{c.f._{r_3}} - M_{W_{r_2}}$$

These are three simultaneous linear equations which can easily be solved for u, v, and w. Knowing u, v, and w there is no difficulty in computing the bending moment for any station of the blade. The bending moment found in this way will be, of course, an approximate one, but in special cases the accuracy may be improved by the following conditions: (1) The total bending moment at the characteristic stations is calculated from the known values of u, v, and w. (2) Some plausible shape of curve representing total bending moment as a function of x is drawn passing through the points calculated for r_1, r_2, and r_3. (3) The moments of inertia of intermediate sections are modified to conform to the linear variation of M/EI originally assumed and when, of course, values of M are taken from the graph made in step (2).

W. Z. STEPNIEWSKI
Jet Helicopter Corporation

Changes of Address

To facilitate the prompt receipt of copies of the JOURNAL OF THE AERONAUTICAL SCIENCES, members and subscribers are requested to give the Institute 30 days' notice of any change of address.

Notices should be sent directly to:

Institute of the Aeronautical Sciences, Inc.
2 East 64th Street, New York 21, New York

Jet Propulsion and Its Application to High-Speed Aircraft

D. J. KEIRN* AND D. R. SHOULTS†
Wright Field and Bell Aircraft Corporation

INTRODUCTION

JET PROPULSION as a new mode of aircraft propulsion has aroused general public and technical interest to a degree seldom reached by any technical achievement. The explanation may lie in the simplicity of the principles and the apparatus involved, combined with a certain sense of the mysterious or, perhaps, lack of appreciation of Newton's third law. Among scientists and engineers, jet propulsion is no novelty. Technical and patent literature discloses able thinking on this subject for many years past.[1,8] Why, then, did so many years elapse before jet propulsion was applied to aircraft?

The authors believe the answer to this question is one of timeliness. As will be developed later, jet propulsion is of greatest value at high aircraft speeds, and until top speeds were pushed well over the 400 m.p.h. value there was little need for or practicality in jet propulsion. Another factor often stated in the past is that metallurgical developments have just recently proceeded to the point where a practical gas turbine could be built to operate at the gas temperatures required.

A third and highly important factor was the burning desire of Air Commodore Frank Whittle to produce such a device, and his imagination and design skill which, when applied to the problem, brought forth a practical lightweight power plant. Others working independently have achieved the same end but the incentive provided by Whittle's work has unquestionably been important.

There are many types of jet propulsion equipment but in this paper consideration will be limited to jet propulsion apparatus using the same atmospheric air for propulsion as for the thermal cycle and in which the gas-turbine-driven compressor supplies the major component of pressure for the thermodynamic cycle.

Rocket propulsion and ram jets of the intermittent or continuous-flow types, although true examples of jet propulsion, will not be elaborated upon.

Presented at a closed meeting of the Institute of the Aeronautical Sciences, Hollywood, Calif., August 15, 1945. Released for publication February 25, 1946.

* Colonel, Army Air Forces, Acting Chief—Power Plant Laboratory.

† Vice-President—Engineering.

EARLY DEVELOPMENT

The circumstances surrounding the delivery of the first flight-tested engine of the Whittle design (Fig. 1) to the United States and the initiation of the project here have been related numerous times. The design experience and productive capacity of the General Electric turbosupercharger organization were applied to the problem of reproducing the British production design at the earliest moment. Numerous minor changes were made to adapt the product to United States factory practices but the fundamental design was unaltered. Production proceeded rapidly and in slightly more than 6 months the first engine was placed on test. Following initial factory tests, certain design

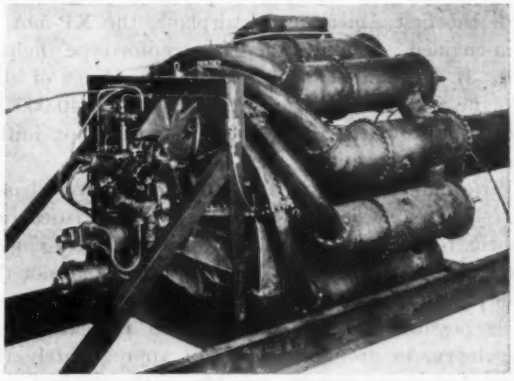

Photograph Courtesy of General Electric Company

FIG. 1. First flight-tested Whittle engine as received in the United States, October 4, 1941.

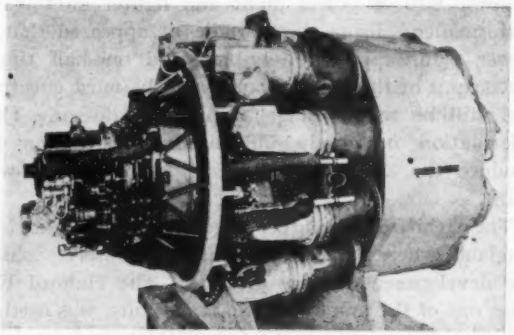

Photograph Courtesy of General Electric Company

FIG. 2. General Electric production design of turbojet engine used in the Bell P-59 interceptor fighter.

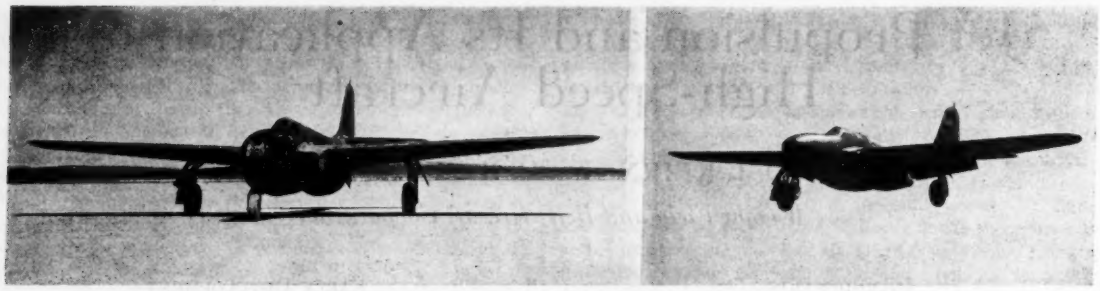

FIG. 3. The left-hand picture shows the XP-59A on the ground at the Muroc test base, and the right-hand picture shows the conclusion of one of the early desert test flights of the first plane.

modifications were required and accomplished prior to flight.

It was soon apparent that the design fell far short of its performance predictions and design revisions were made on both sides of the Atlantic, with close coordination through the A.A.F., the British Air Commission, and the Ministry of Aircraft Production. As experience was gained, both reliability and performance were improved until satisfactory flight articles were obtained (Fig. 2).

Concurrent with the engine program at General Electric, the Bell Aircraft Corporation designed and built the first American jet airplane, the XP-59A, a twin-engined, high-altitude, interceptor-type fighter (Fig. 3). The light wing and span loadings of this airplane favored operation at levels above 40,000 ft. and also provided a maximum of safety for initial flights of these radically new power plants.

Performance predictions for this aircraft were based on estimated design performance characteristics furnished from England in lieu of United States engine test data. Unfortunately, neither the original nor the later production engines produced the output predicted. It is possible today, however, with present design knowledge, to produce engines of approximately the original size and weight, capable of the original predicted performance.

Following the completion of the XP-59 airplanes, studies were completed at Bell for the A.A.F. relating absolute size of power plant and fighter aircraft to performance. From these studies it appeared that a power plant approximately two and one-half times the output of the original one would be most effective and still be within range of practical design. This information materially influenced the decision to produce the larger new General Electric jet power plant.

The trend toward larger engines was also noted in England, where numerous manufacturers were pushing the development of new projects. The Halford Engine, one of the first successful large units, was used in this country to power the first XP-80 single-engined jet fighter. The production design of the P-80 used the large General Electric engine because of its greater output and its availability from United States production.

Other engines and numerous airplanes have been projected in England and the United States. Announcement of these will be made in due course by the interested military service.

THE JET PROPULSION SYSTEM

In passing to the technical aspects of the jet propulsion system, the single most important and basic consideration is that thrust or propulsive force is equal to the time rate of change of momentum of the propelling gas stream.

$$F = [d(Mv)]/dt \tag{1}$$

where

F = force or propelling thrust
M = mass of air or gas
v = velocity of the gas with respect to the aircraft

With steady flow where a weight flow of W_a lbs. per sec. of gas is accelerated from a velocity of V to v_j ft. per sec. the thrust

$$F = (W_a/g)(v_j - V) \text{ lbs.} \tag{2}$$

where the propulsion medium is the atmospheric air acted upon by the aircraft system V = aircraft velocity = initial velocity of the air with respect to the aircraft.

v_j = discharge velocity of the air stream or jet
g = acceleration of gravity

The power output of the propulsive system equals force times velocity

$$(W_a/g)(v_j - V)V \tag{3}$$

The power input to the air stream is equal to the rate of increase of kinetic energy of the air stream. The initial kinetic energy rate is

$$(W_a/g)(V^2/2) \tag{4}$$

The leaving energy rate is

$$(W_a/g)(v_j^2/2) \tag{5}$$

The power added is then

$$(W_a/2g)(v_j^2 - V^2) \tag{6}$$

This power is added to the air or gas in the internal thermodynamic cycle and is applied to the aircraft propulsion as previously discussed. The efficiency with which this power is used, i.e., the propulsive efficiency

$$\left.\begin{aligned} \eta_p &= \frac{\text{output}}{\text{input}} = \frac{(W_a/g)(v_j - V)V}{(W_a/g)(v_j^2 - V^2)} \\ &= \frac{2V}{v_j + V} = \frac{2}{1 + (v_j/V)} \end{aligned}\right\} \tag{7}$$

This relation may be derived also by considering that the only propulsive power loss is that in the excess of velocity of the jet above the airplane velocity or, to state it differently, the velocity of the jet with respect to the ambient air.

This velocity is $v_j - V$ and the energy loss is

$$(W_a/2g)(v_j - V)^2 \tag{8}$$

The efficiency of propulsion is

$$\eta_p = \frac{\text{output}}{\text{output and loss}} = \frac{(W_a/g)(v_j - V)V}{(W_a/g)(v_j - V)V + (W_a/2g)(v_j - V)^2}$$

which also reduces to

$$\eta_p = \frac{2V}{v_j + V} = \frac{2}{1 + (v_j/V)} \qquad (9) = (7)$$

With the assumption of jet velocity and W_a as independent of airplane speed, we find by differential examination of Eq. (3) that maximum output occurs when $v_j = 2V$; at this point $\eta_p = 2/1 + 2 = {}^2/_3 = 66.7$ per cent. Maximum efficiency occurs when $v_j = V$ where output is zero.

The assumption of constant maximum jet velocity and airflow for a given engine holds only approximately as it is influenced by both ambient air temperature and the ram pressure rise resulting from the aircraft velocity. This approach does indicate that the propulsive efficiency may be relatively low where maximum output is striven for or approached.

The momentum change resulting from the velocity increase of the propelling air stream is independent of the manner in which air stream is accelerated while under the influence of the propulsion equipment. The conventional Otto cycle engine driving a propeller extracts power from one stream of gas which is carried through the thermodynamic cycle and applies it to the acceleration of a second larger stream. In this case, the propulsive efficiency may be, and is usually, rather high as a large mass of air is accelerated only a small amount and the losses chargeable to residual velocity are low. The energy absorbed per mass unit of air is low, much lower than the energy produced per mass unit of gas in the engine. The engine and propeller combination thus functions as a power converter transferring high level energy from a small flow of gas to a larger flow of air at lower energy level.

If the energy available from the Otto cycle engine is used solely to produce a high jet velocity of the engine combustion gases, as in the Lorin scheme of 1908,[1] the propulsion efficiency will be low by reason of the great difference between jet velocity and airplane velocity. Furthermore, the output per unit of power plant size or weight will be low at all except extreme air speeds.

The exhaust from such an engine is, however, an effective propulsion agent when properly employed, as is witnessed by the contribution made by the use of individual jet exhaust stacks on many present-day first-line fighter airplanes. Such utilization of the exhaust contributes a significant increase in thrust with little addition in weight or complexity.

Turbojet Engine

Effective use of the jet propulsion principle utilizing atmospheric air for the thermodynamic cycle and as the propulsive agent as well requires an engine capable of handling large flows of air but proportionately light in weight. The turbojet engine with turbine-driven centrifugal or axial flow compressor meets these requirements to a high degree. Both turbine and compressor are well adapted to a high flow per unit of size and, fortunately, the turbine cycle temperatures for best overall (thermal times propulsive) efficiency is much lower than the combustion temperatures in the reciprocating engine and well within the limit of operation of available turbine alloys.

Constant Pressure Cycle

Such an engine operates on the constant pressure cycle, with highly efficient adiabatic compression by ramming intake and compressor action, subsequent heating at constant pressure by burning with fuel in suitable combustion chambers, partial expansion through a turbine to generate sufficient shaft power to drive the compressor, and final expansion to atmospheric pressure with resulting high jet velocity.

In making an exploratory energy analysis of any such specific cycle, certain conditions are either known or assumed. In general, these are

p_{am} = ambient pressure
T_{am} = ambient temperature (°F. abs.)
V = true air speed
η_r = ram efficiency
η_c = compressor efficiency
p_2 = compressor delivery pressure
p_4 = turbine inlet pressure (less than p_2 by burner pressure drop)
η_t = turbine efficiency
η_n = nozzle efficiency

T_4 = permissible turbine inlet temperature (°F. abs.)
c_p = specific heat at constant pressure
c_v = specific heat at constant volume
k = ratio of specific heat = c_p/c_v
J = Joule's constant

Ram Intake

The temperature rise by ram impact

$$\Delta T = T_2 - T_{am} = V^2/2gJc_p \tag{10}$$

where T_2 = total temperature at compressor inlet.

The isentropic pressure rise by ram impact may be calculated

$$\left[\left(\frac{p_2'}{p_{am}}\right)^{(k-1)/k} - 1\right]T_{am} = T_2 - T_{am} = V^2/2gJc_p \tag{11}$$

$$\frac{p_2'}{p_{am}} = \left(1 + \frac{V^2}{2gJc_pT_{am}}\right)^{k/(k-1)} \tag{12}$$

where p_2' is total ram pressure with isentropic compression.

The ideal pressure rise

$$\Delta p' = p_2' - p_{am} \tag{13}$$

The actual ram pressure p_2 will be less than p_2' and the actual ram pressure rise Δp less than $\Delta p'$ by reason of inlet losses.

Ram efficiency η_r is defined

$$\eta_r = \frac{\Delta p}{\Delta p'} = \frac{p_2 - p_{am}}{p_2' - p_{am}} = \frac{(p_2/p_{am}) - 1}{(p_2'/p_{am}) - 1} \tag{14}$$

The actual pressure ratio for an assumed efficiency

$$\frac{p_2}{p_{am}} = \left(\frac{p_2'}{p_{am}} - 1\right)\eta_r + 1 \tag{15}$$

Compressor

The compressor pressure ratio is either known or assumed.

The temperature rise (ΔT) in compression is calculated

$$\Delta T \text{ compressor} = T_3 - T_2 = \frac{T_2}{\eta_c}\left[\left(\frac{p_3}{p_2}\right)^{(k-1)/k} - 1\right] \tag{16}$$

where T_3 and p_3 are total temperature and pressure conditions at compressor discharge and η_c is the compressor efficiency.

The compressor energy for each pound of air compressed

$$= c_p(T_3 - T_2) \tag{17}$$

Combustion

The pressure drop in the combustion chamber may be a few per cent of the total pressure at that point. This is estimated or determined from test. The turbine inlet pressure, p_4, is consequently then known.

The turbine inlet temperature, T_4, at the design point may be any selected value appropriate to the turbine stresses, materials available, and the life desired.

The fuel-air ratio or the pounds of fuel per pound of air is determined knowing the combustion efficiency and lower heating value of the fuel:

$$\frac{\text{fuel}}{\text{air}} = \frac{c_p(T_4 - T_3)}{\text{lower heating value} \times \text{combustion efficiency}} \tag{18}$$

The total gas flow rate through the turbine is increased over the airflow rate through the compressor by the amount of fuel added. Thus, the gas flow is

$$W_g = [1 + (\text{fuel/air})]\,W_a \tag{19}$$

where W_a = air flow in lbs. per sec. and W_g = gas flow in lbs. per sec.

Turbine

In the ideal case the power developed by the turbine is equal to the power input to the compressor. Practically, it must be greater by the amount of the bearing losses, accessory power and air leakage losses, all of which are of small magnitude. Neglecting these factors

Turbine energy output = compressor energy input

$$c_{pt}(T_4 - T_5)(1 + \text{fuel/air}) = c_{pc}(T_3 - T_2) \tag{20}$$

where T_5 = turbine discharge temperature.

The values of c_p will vary with the temperature range, and the values of c_p for the turbine (c_{pt}) and compressor (c_{pc}) above will not be identical or constant.

The total available energy per pound of air in the expansion from p_4 to p_{am}

$$= c_{pt}T_4\left[\frac{(p_4/p_{am})^{(k-1)/k} - 1}{(p_4/p_{am})^{(k-1)/k}}\right]\left(1 + \frac{\text{fuel}}{\text{air}}\right) \tag{21}$$

This is divided between the turbine and the jet energy.

Nozzle

The efficiency of the turbine may be defined as

$$\eta_t = \frac{\text{energy output}}{\text{total available energy} - \text{energy available to jet nozzle}}$$

Thus, the energy available to nozzle = total available energy − turbine output ÷ turbine efficiency

$$= c_{pt}T_4\left[\frac{(p_4/p_{am})^{(k-1)/k} - 1}{(p_4/p_{am})^{(k-1)/k}}\right]\left(1 + \frac{\text{fuel}}{\text{air}}\right) - \frac{c_{pc}(T_3 - T_2)}{\eta_t} \tag{22}$$

The final kinetic energy of the jet will be less than the total available at the nozzle by reason of turbulence; therefore, a nozzle efficiency factor η_n must be considered.

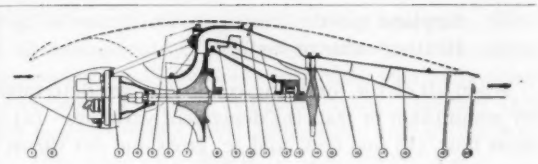

Diagram Courtesy of General Electric Company

FIG. 4. Schematic arrangement of centrifugal compressor type turbojet engine.

(1)	Accessories fairing	(11)	Ignition plug
(2)	Accessories	(12)	Combustion chamber
(3)	Accessory gear drive	(13)	Turbine bearing
(4)	Front bearing	(14)	Turbine wheel
(5)	Mounting trunnions	(15)	Turbine nozzle
(6)	Compressor casing	(16)	Inner exhaust cone
(7)	Impeller	(17)	Strut
(8)	Balancing drum	(18)	Exhaust cone
(9)	Fuel manifold	(19)	Tailpipe
(10)	Burner tip	(20)	Final nozzle

Thus, the energy in the jet

$$= \eta_n \times \text{energy available to jet} \qquad (23)$$

The jet velocity v_j may now be determined by considering

$$\frac{v_j^2}{2gJ} = \eta_n \times \text{energy available to jet}$$

thus

$$v_j = \sqrt{2gJ\eta_n\left\{c_{pt}T_4\left[\frac{(p_4/p_{am})^{(k-1)/k} - 1}{(p_4/p_{am})^{(k-1)/k}}\right] \times \left(1 + \frac{\text{fuel}}{\text{air}}\right) - \frac{c_{pc}(T_3 - T_2)}{\eta_t}\right\}} \qquad (24)$$

In the original Whittle design and in designs with similar configuration this cycle has been effectively used in obtaining a high-flow, small, lightweight jet power plant (Fig. 4).

Operation

The compressor is of a high-speed, single-stage, double-ended centrifugal type emphasizing high flow for a given size. The tip speed of the aluminum-alloy impeller is of the order of 1,500 ft. per sec. Tip speed is limited to some extent both by allowable stresses and by a rapid drop in efficiency as speed is increased beyond this value. At the present stage of the design art for this type of compressor, the design is substantially optimum considering construction problems, size, weight, and performance.

The diffuser section is divided into a number of individual channels, one leading to each of the cylindrical combustion chambers. Streamlined turning vanes are employed to turn the tangential flow of air to an axial direction. The use of divided channels assists materially in stabilizing and equalizing the flow in the multiple combustion paths.

The overall compressor efficiency is of the order of 75 per cent at the design point, with compressor pressure ratio of from 3.5 to 4.0, depending upon inlet temperature.

The combustion chambers, consisting of tubular pressuretight outer cylinders with perforated inner coaxial cylinders, have presented some of the most difficult development and design problems. The rate of heat release per unit of volume and the shortness of the flame path are outstanding in comparison with other combustion equipment. The heat release may be as high as several million B.t.u. per hour for each cubic foot of combustion space.

The incoming air enters the end of the chamber flowing in the annular space between the chamber and inner liner until it enters the flame chamber through the perforations in the liner. The fuel is sprayed into one end of the liner and combustion takes place within the liner, the hot gases exiting at a high velocity at the opposite end. The many small jets of air impinging on the flame create high turbulence, promote mixing of fuel and air, and thus complete the combustion with short flame length.

Combustion chamber pressure drop is of the order of 3–5 per cent of the total pressure. Combustion is substantially complete, the combustion efficiency generally exceeding 98 per cent.

The hot gas from the combustion chamber flows through the turbine nozzles, impinges on the buckets of the single-stage turbine wheel, and exits to the tail cone with a substantial axial velocity of the order of 1,000/1,200 ft. per sec. This high exit velocity would incur a heavy penalty in efficiency were it not for the fact that the high-velocity gas stream is the end product of this power plant. It is thus important that the energy of the gas stream be conserved. Losses in total pressure head at this point give a significant decrease in performance. Bends or obstructions or excessively long tail pipes are to be avoided.

Final expansion to atmospheric pressure takes place in the tail pipe nozzle with consequent increase in velocity.

Final jet velocities are of the order of 1,600 to 2,100 ft. per sec. depending on ram and inlet temperature conditions. At the exhaust temperature prevailing the jet velocity varies from subsonic to supersonic.

A typical cycle is shown in Fig. 5, a P-V diagram for operation at 20,000 ft. altitude, 500 m.p.h., and for

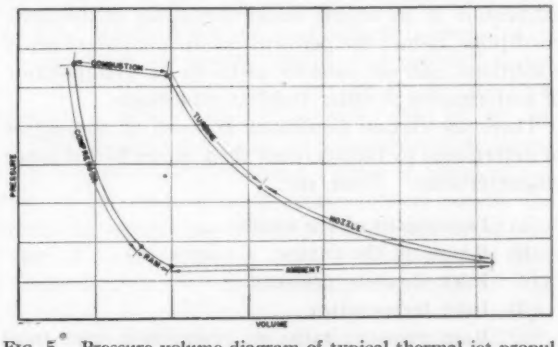

FIG. 5. Pressure volume diagram of typical thermal jet propulsion cycle.

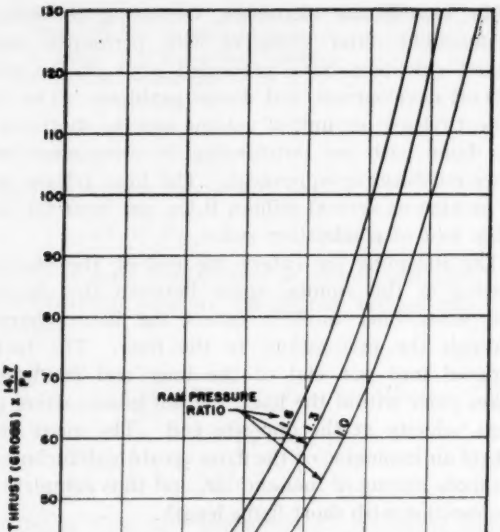

FIG. 6. Relationship of gross thrust vs. a function of engine Mach Number for various pressure ratios.

typical pressure ratios and efficiencies. Final jet velocity is 2,100 ft. per sec., with 42.5 lbs. thrust per lb. airflow per sec. Specific fuel consumption is 1.1 lbs. per thrust hp.-hr.

Specific Engine Performance

The calculation of specific power-plant performance under various operating conditions is rather involved and final solutions are questionable in absolute accuracy by reason of the numerous variable efficiency factors whose value must be estimated at each point. Experience has proved that the most satisfactory method of presenting specific engine performance under a wide variety of conditions is to obtain a test-stand calibration of an engine under prevailing atmospheric conditions, reduce the performance to a standard set of conditions, and use suitable methods for extrapolation of performance to other ambient conditions.

There are certain conditions imposed on the engine or determined by factors other than engine performance characteristics. These are:

(a) Dimensions of the engine.
(b) R.p.m. of the engine.
(c) Inlet absolute pressure.
(d) Inlet temperature.
(e) Ram pressure ratio = compressor inlet total pressure ÷ ambient (atmospheric) pressure.
(f) Airplane speed.
(g) Heating value of fuel.

When all of the foregoing conditions are determined by assumption or test, the dependent variables—(a) air mass flow, (b) fuel flow, and (c) gross and net thrust—may be determined by simple calculation from the performance curves. Figs. 6, 7, and 8 express, in per cent of standard atmosphere static sea-level rating, the relationship of gross thrust, airflow, and fuel flow with variations in engine speed, inlet temperature, inlet pressure, and ram pressure ratio.

These curves express the characteristic variations of a particular engine but are typical of many others in general trends and in effects of ram pressure ratio. Curves for a specific engine are most usefully presented with actual values of thrust, W_a and W_f, rather than percentage values as given herein.

In calculating net thrust at operating speed V the ram drag of the inlet airflow, as determined from Fig. 7, is subtracted from the gross thrust as obtained from Fig. 6

$$\text{Ram drag} = \frac{W_a}{g} V \text{ lbs.} \qquad (25)$$

In the curves of Figs. 6, 7, and 8 the independent variable is $\%N\sqrt{518.4/T_2}$, which has been derived by dimensional analysis.[14] This variable is a basic expression directly proportional to Mach Number (since N is connotative of impeller tip speed and $\sqrt{T_2}$ defines the

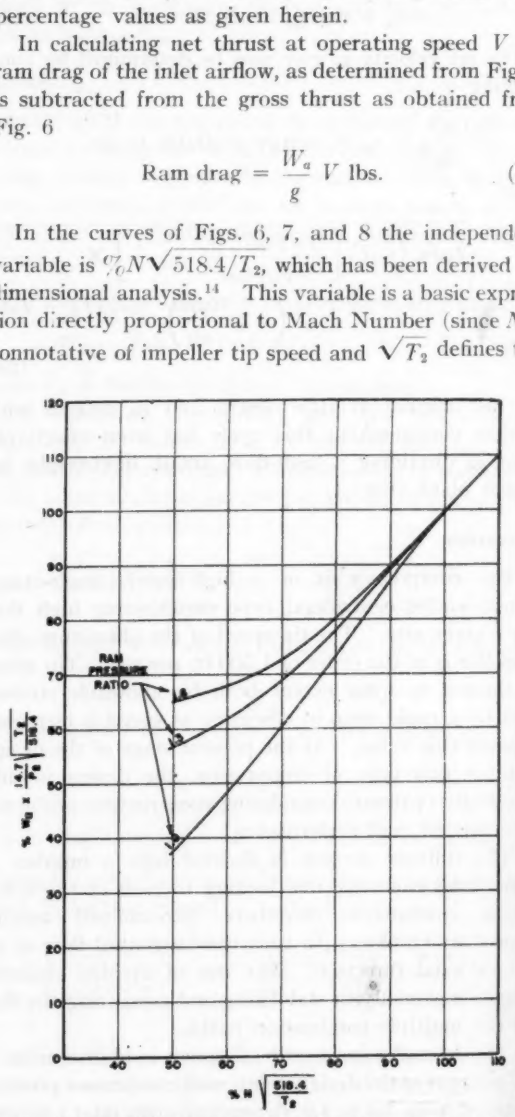

FIG. 7. Relationship of airflow vs. a function of engine Mach Number for various pressure ratios.

speed of sound) which determines the operating point of all components of the power plant. Experience and analysis indicate that component part efficiencies are constant for fixed values of Mach Numbers and that pressure ratios and temperature ratios throughout the cycle are similarly determined when the Mach Number is determined.

The dependent variables—thrust, airflow, and fuel flow, are influenced by ram pressure ratio, and for most convenient use performance curves for a number of pressure ratios are supplied.

With Mach Number and ram pressure ratio established, gross thrust output is then finally determined as a direct function of atmospheric static pressure. Net thrust is then calculated by subtracting the ram drag for the given air flow.

The airflow under particular operating conditions is determined by Fig. 7. This type of chart permits airflow to be calculated on the basis of known operating Mach Number and ram pressure ratio. With these factors determined, the air flow (W_a) is determined under conditions of standard atmospheric pressure. For conditions other than standard the flow is modified in direct proportion to the variation of the ambient pressure and in inverse square root relation with the change in absolute temperature.

The fuel flow is determined from a similar set of curves (Fig. 8). The fuel flow for conditions other than standard atmospheric conditions is modified in direct relation with the static pressure and inverse relation with the square root of the absolute temperature.

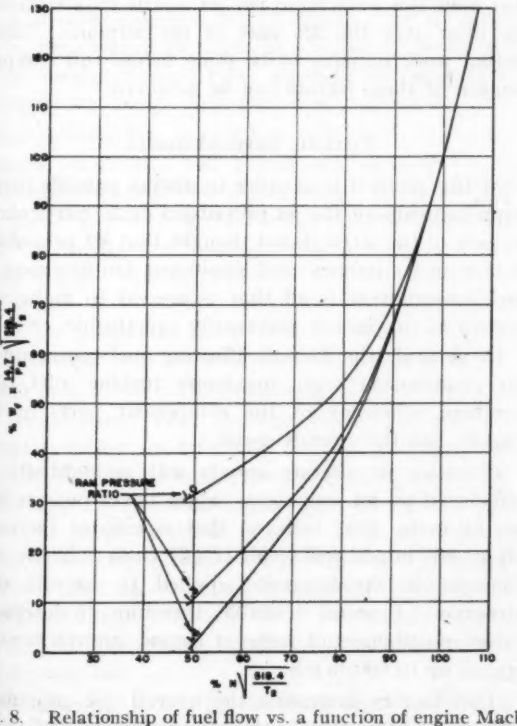

FIG. 8. Relationship of fuel flow vs. a function of engine Mach Number for various pressure ratios.

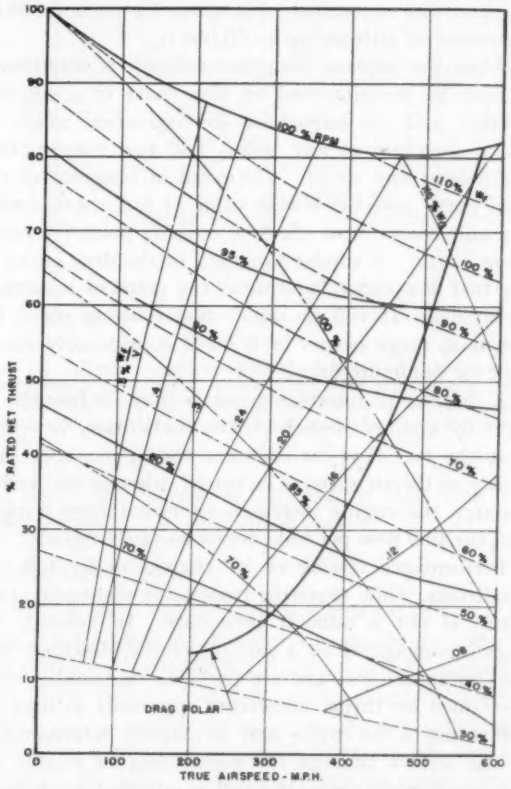

FIG. 9. Composite chart relating true air speed, per cent rated thrust, per cent fuel flow, per cent airflow, and fuel flow per mile (per cent W_f/V) for a typical jet engine for standard atmospheric sea-level conditions, 85 per cent ram efficiency. Superimposed is the drag polar of a typical high-speed jet-propelled airplane.

With these data, performance may be calculated under various altitude, temperature, speed, and ram conditions. In carrying out preliminary aircraft designs it is convenient to present performance as a function only of aircraft speed for standard atmospheric conditions for each particular altitude using a fixed reasonable value of ram efficiency. A typical presentation of this type is given in Fig. 9, which shows the performance of a representative turbojet engine at sea level, standard pressure and temperature conditions for air speeds up to 600 m.p.h. The ordinate is the per cent of rated standard atmosphere static sea-level thrust. A series of thrust curves for 100, 95, 90, 80, and 70 per cent rated r.p.m. of the engine relate thrust to air speed and engine speed. Lines of constant airflow, in per cent of rated static airflow, permit the determination of this quantity for any air speed and value of thrust. Similar lines of constant fuel flow permit this quantity to be equally ascertained. For convenience in estimating speeds for maximum range, lines of constant fuel consumption per mile (W_f/V) are superimposed on the chart. Such charts have been

prepared for a number of engines for each 5,000-ft. increment of altitude up to 50,000 ft.

When the airplane drag characteristic is determined it may be superimposed on this chart in a suitable overlay and an immediate determination made of $V_{max.}$, fuel flow at any speed, and fuel consumption per mile at any speed. The point of tangency of the drag curve and the lowest value of fuel consumption per mile shows most effective cruising point for maximum range. A similar tangency of the drag curve to the fuel flow curve determines the point of maximum endurance. It will be noted that cruising speed for optimum range occurs at a speed considerably above that for minimum drag.

A number of interesting points may be brought to light by a study of such charts, particularly in noting that the fuel flow for constant thrust increases only slowly as the air speed is increased, whereas the airflow through the engine increases somewhat more rapidly and the fuel flow per mile decreases fairly rapidly.

Performance testing of jet engines under test cell conditions, while requiring reasonably elaborate apparatus, is not a difficult procedure. In general, the engine is mounted on a suitable cradle, designed with the minimum fore-and-aft friction, the cradle being restrained by thrust measuring apparatus so that the full thrust of the engine may be directly determined.

The airflow through the engine may be readily determined by measuring the airflow into the test chamber by suitable flow nozzles. Air leakage to the test chamber must be held to a low value. Fuel flow rates may be obtained from flowmeters or weighing apparatus. Inlet air pressures and temperatures must be accurately determined, and it is particularly important to prevent recirculation of the air in the test chamber which might give unequal distribution in the compressor inlet.

When the engines are installed in the airplane and operated under flight conditions, the aircraft manufacturer will wish to determine thrust under actual operating conditions. Inasmuch as the forces due to ram drag appear partly on the inside of the nacelle structure and partly on the engine, a direct thrust measurement obtained from the engine support reactions will not give true values of thrust output. The most practical method of determining thrust in flight is to make a direct measurement of the total momentum of the jet and subtract the ram drag.[14] Such a measurement may be made in a variety of ways but, basically, it is necessary to determine only the average jet velocity and the gas flow rate through the jet nozzle. The determinations made in this connection are (a) area of the nozzle, (b) temperature of gas through the nozzle, (c) average velocity of gas through the nozzle, (d) pressure in the nozzle, and (e) ambient pressure.

In many cases it may be expedient to measure these quantities directly; in other cases measurements of temperature and pressure may be made in the tail pipe and the nozzle conditions calculated from the pressure ratio between the gas in the tail pipe and the static pressure at the discharge point.

Jet thrust may be determined by this method under test-stand conditions, so that an opportunity is afforded to calibrate instrumentation and check the calculation method against the test stand thrust measurements.

The thrust of the engine in flight may also be calculated using the method previously described for initial calculation performance. Inlet conditions of the compressor, including temperature, total pressure, ram pressure ratio, and engine and airplane speed, should permit complete determination of net thrust of the unit. Fuel flow may be measured by flowmeter as a check against test stand conditions. This method is valuable as a check on the performance obtained by jet pipe survey. It has been determined, however, that the performance of the engines will vary over a period of time because of changes in combustion efficiency introduced by possible unbalance in fuel flow to the various combustion chambers, changes in surfaces by dirt or oil deposits, and slight changes in contour of the combustion chamber liners, turbine nozzles, and turbine buckets.

If the drag characteristics of the aircraft under test are determinable by glide test or full-scale wind-tunnel test, close correlation of thrust available and thrust required should be obtained. However, in making drag determinations of the aircraft it is difficult to ascertain the true value of external drag without normal airflow through the nacelle entrance and it is possible, also, that the wake from the jet nozzle may influence the drag over the aft part of the airplane. Much testing work remains to be done before full comprehension of these factors can be achieved.

Future Improvements

At this point it is in order to discuss possible future improvements for the jet propulsion cycle, particularly in view of the often stated thought that jet propulsion is now in its infancy and significant improvement in fuel consumption is all that is needed to make this system of propulsion universally practicable.

In general, the factors affecting fuel consumption are compression ratio, maximum turbine inlet temperature, efficiency of the component parts of the engine, and the aircraft speed.

Increases in aircraft speeds will undoubtedly be influenced by jet propulsion engine developments but, in the main, it is believed that significant increases above 600 m.p.h. will result chiefly from radically new concepts in aerodynamics applied to aircraft construction. It seems desirable, therefore, to determine future possibilities of turbojet engine improvement at speeds up to 600 m.p.h.

Two factors determine the overall jet propulsion efficiency. The first is the thermodynamic efficiency

with which the energy in the fuel is converted to the kinetic energy of the exhaust gas stream. This is influenced by component part efficiencies, combustion temperatures, and compression ratios. The second factor is the propulsive efficiency, which is determined by the relationship of jet velocity to air velocity.

Considering the large number of independent variable conditions, and the permutations and combinations of all these, it is difficult to either secure or present any accurate wide-range study. It is possible, however, to determine the major trends in efficiency by making a few assumptions. The authors have approached this problem with the thought of determining the major trends in efficiency considering variations in pressure ratio, turbine inlet temperature, and turbine and compressor efficiencies. Turbine and compressor efficiencies have been assumed to be of equal value and losses in the combustion chamber or tail pipe are assumed to be part of turbine or compressor losses.

Thermal Efficiency

A series of computations were made varying compression ratio and machine efficiencies for constant turbine inlet temperatures for sea-level static conditions and also for a flight condition of 600 m.p.h., 40,000 ft., standard atmosphere, 85 per cent ram efficiency. These data were plotted as indicated typically by Fig. 10 for the sea-level static condition, showing thermal efficiency versus net thrust output per pound of air flow per second. For equal pressure ratio an increase in thermal efficiency is accompanied by an increase in thrust output, but in order to obtain this higher thermal efficiency at a higher thrust output at a given compression ratio, a corresponding increase in compressor and turbine efficiency is required.

In examining Fig. 10 it will be noted that for a given constant compressor and turbine efficiency the point of operation for maximum thrust per unit of air flow and the point representing maximum thermal efficiency occur at nearly the same pressure ratio. A single optimum point may be picked on the curve of constant compressor and turbine efficiency which represents nearly the maximum thrust output per pound of air per second and also the maximum thermal efficiency.

Such points selected from a series of charts for varying temperatures and machine efficiencies may be plotted together as indicated in Fig. 11. Lines of constant compressor and turbine efficiency show the relationship of the compression ratio to thermal efficiency for these optimum points. Lines of constant turbine inlet temperature are superimposed to illustrate the point that as compression ratio is increased, the optimum thermal efficiency for a given machine efficiency is obtained with a rapidly increasing turbine inlet temperature.

The foregoing charts for sea-level static conditions relate only to thermal efficiency—that is, the efficiency

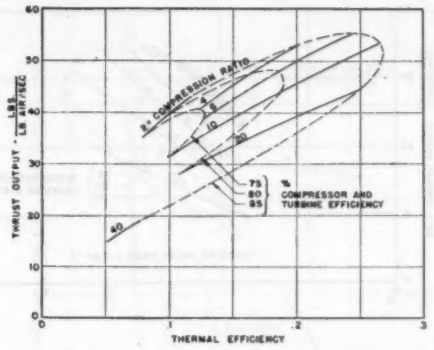

FIG. 10. Thrust output vs. thermal efficiency for various compression ratios under static sea-level standard atmospheric conditions and a constant 1,500°F. turbine inlet temperature. Lines of constant required turbine and compressor efficiency are also shown.

with which the energy in the fuel is converted to kinetic energy of the discharged gas.

Overall Efficiency

A similar set of information is displayed in Fig. 12, which relates overall efficiency to net thrust output per pound of air per second for high-speed, high-altitude flight at 600 m.p.h., 40,000 ft., under standard atmospheric conditions and assuming an 85 per cent ram efficiency. A series of optimum points is selected as indicated in the figure and these points are summarized in Fig. 13, which compares compression ratio with optimum output per pound of air per second, and in Fig. 14, which compares compression ratio with optimum overall thrust horsepower efficiency.

It will be seen that with these optimum conditions, and with a constant machine efficiency, output is relatively sensitive to variations in compression ratio, but that if compression ratio is increased turbine inlet temperature must be correspondingly increased to maintain the optimum output.

In considering, in Fig. 14, the relation of compression ratio to thrust efficiency (which includes both thermal efficiency and propulsive efficiency), several observations may be made:

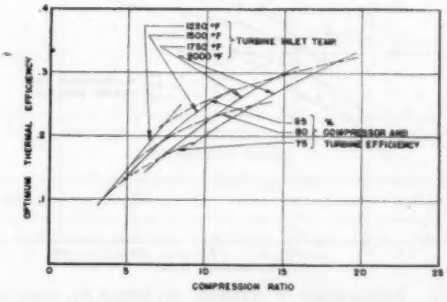

FIG. 11. Relationship of optimum thermal cycle efficiencies vs. compression ratio for static sea-level standard atmospheric conditions. Per cent curves represent performance for stated value of compressor and turbine efficiency (no other losses). Temperature curves show related turbine inlet temperatures.

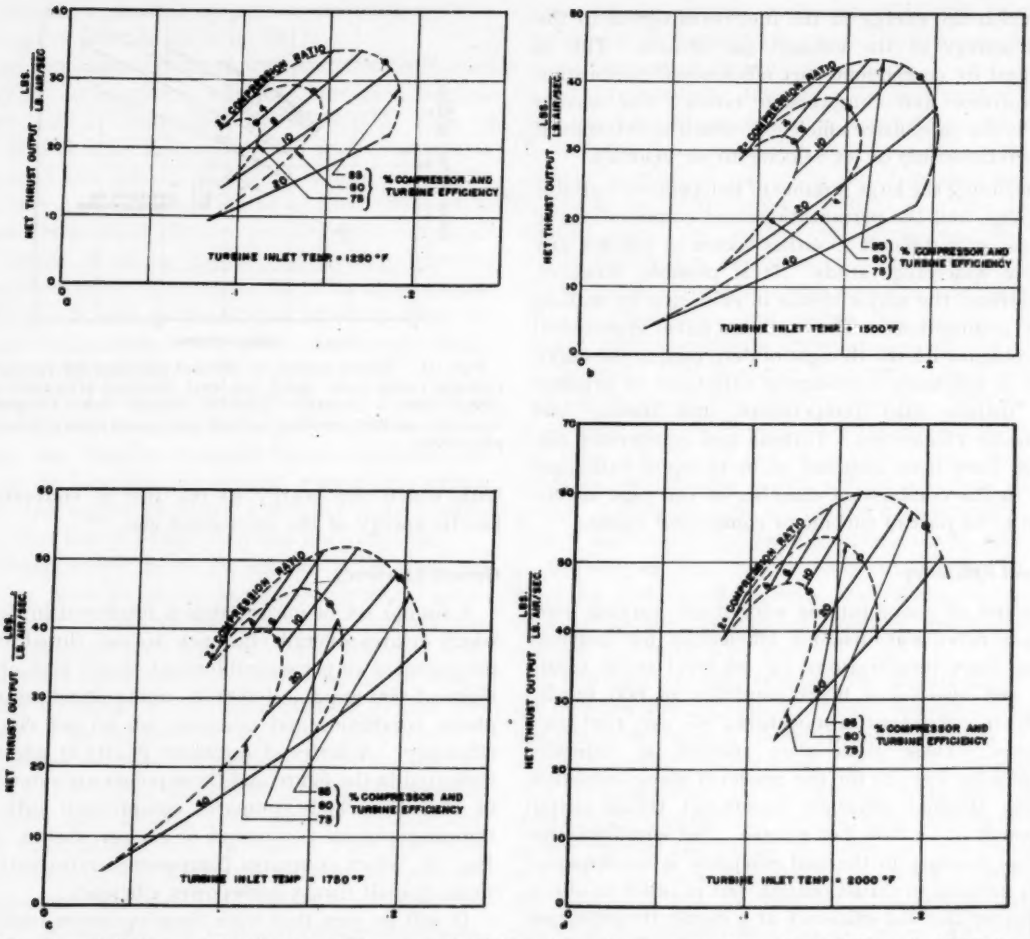
NET THRUST OUTPUT LBS. / LB. AIR/SEC.
P2 COMPRESSION RATIO
% COMPRESSOR AND TURBINE EFFICIENCY
TURBINE INLET TEMP = 1250 °F
TURBINE INLET TEMP = 1500 °F
TURBINE INLET TEMP = 1750 °F
TURBINE INLET TEMP = 2000 °F

FIG. 12. Overall efficiency. Net thrust output vs. overall efficiency for various compression ratios at 600 m.p.h. 40,000 ft. standard atmospheric conditions and a constant 1,500 °F. turbine inlet temperature. Lines of constant required turbine and compressor efficiency are shown and optimum points as shown (⊙) are equal percentages of maximum efficiency and net thrust per pound of air.

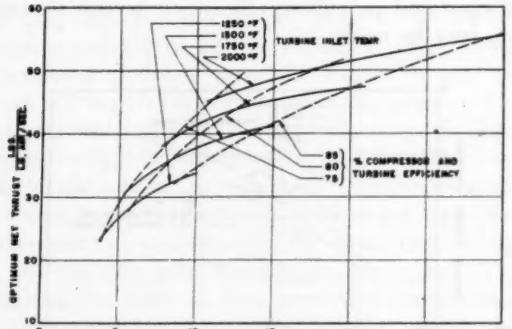

FIG. 13. Relationship of optimum net thrust vs. compression ratio for 600 m.p.h. 40,000 ft. standard atmospheric conditions. Per cent curves represent performance for stated value of compressor and turbine efficiency and 85 per cent ram efficiency (no other losses). Temperature curves show related turbine inlet temperatures.

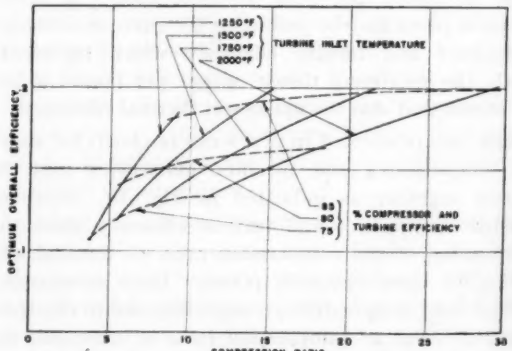

FIG. 14. Relationship of optimum overall efficiencies vs. compression ratio for 600 m.p.h. 40,000 ft. standard atmospheric conditions. Per cent curves represent performance for stated value of compressor and turbine efficiencies and 85 per cent ram efficiency (no other losses). Temperature curves show related turbine inlet temperatures.

(a) For a constant compression ratio the higher value of machine efficiency results in a higher value of thrust efficiency. It should be noted, however, that this is accompanied by a substantial decrease in turbine inlet temperature. It should also be borne in mind from reference to Figs. 12a, 12b, 12c, and 12d, that, for a constant value of turbine inlet temperature and for constant compression ratios, a higher machine efficiency gives both a higher output and a greater overall efficiency.

(b) The most significant increase in thrust efficiency is obtainable by increase of machine efficiency. Increase in temperature or compression ratio serves mainly to increase the specific output. This condition will serve as a challenge to engine designers to find ways of increasing machine efficiencies.

These conditions may be examined from a different set of charts shown in Figs. 15 and 16, which, for sea level and 40,000 ft., relate compression ratio to the minimum specific fuel consumption in pounds of fuel per hour per pound of thrust at various air speeds from 0 to 600 m.p.h. These curves show, as did the previous ones, that as compression ratio is increased with constant machine efficiency, the turbine inlet temperature for best specific fuel consumption must also be increased.

It should be borne in mind in studying these curves, as well as the previous ones, that they do not represent performance of a particular machine but are rather a summarization of the optimum relationships existing in a series of machines at particular points giving efficiency and temperature conditions specified.

All of the foregoing studies show a gain, particularly at high speed, by increasing the pressure ratio from the present prevalent value of approximately 4 or 5 to 1 to values as high as 10 or 20 to 1. The percentage fuel consumption decrease may not be adequate to compensate for increased power-plant weight and size required by the high compression ratio. It should also be considered that from a design standpoint it may be difficult to maintain component part efficiencies at higher compression ratios.

From studies such as these, the authors conclude that reductions in fuel consumption can and will be made as component part efficiencies are improved and it becomes possible to make moderate increases in compression ratio without undue weight or efficiency penalties.

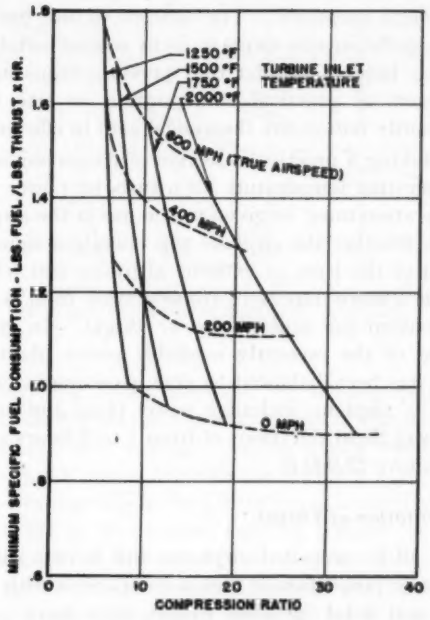

FIG. 15. Minimum obtainable specific fuel consumption vs. compression ratio for 80 per cent turbine and compressor efficiency and 85 per cent ram efficiency (no other losses) at various air speeds, and showing resulting turbine inlet temperatures. Sea-level standard atmospheric conditions.

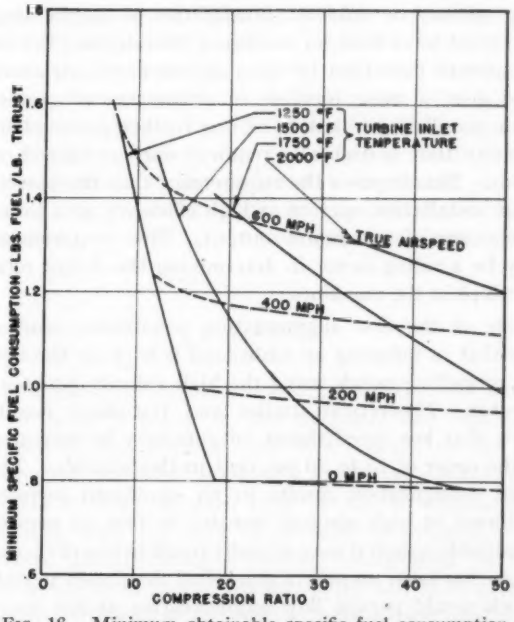

FIG. 16. Minimum obtainable specific fuel consumption vs. compression ratio for 80 per cent turbine and compressor efficiency and 85 per cent ram efficiency (no other losses) at various air speeds, and showing resulting turbine inlet temperatures. 40,000 ft. standard atmospheric conditions.

Turbojet Power Plant

Thus far the cycle considered has been a basic one without intercooling during compression, heat transfer following compression, or reheating during expansion. Others[2–6, 8, 11] have studied the possibilities of the gas turbine in this connection in considerable detail and have shown significant reductions in fuel consumption by taking advantage of such cycle variations. In studying these variations for application to high-speed aircraft it has thus far not appeared practical to add them to the aircraft jet power plant. The turbojet power plant has been most attractive for aircraft use by reasons of its light weight, small size,

and general simplicity. The addition of heat exchangers of significant size seems to incur serious installation penalties besides the fact that pressure drops in heat exchangers of practical configuration or size would significantly reduce the theoretical gain in efficiency.

In making a practical selection of compression ratio and operating temperature for a turbojet power plant, consideration must be given to the use in the airplane; that is, whether the airplane will operate a significant portion of the time at extreme altitudes and whether range is a more important consideration than is maximum output per unit of size or weight. In general, in most of the presently available power plants, the design has been balanced to give a minimum take-off weight of airplane, including power plant and fuel, for full power flight durations of from 1 to 2 hours at altitudes above 25,000 ft.

Augmentation of Thrust

The all-jet-propelled airplanes will have a different and larger proportion of fuel in comparison with power plant and total airplane weight than have present conventional planes. The maximum fuel carried is limited by considerations of take-off run and initial climb; consequently, means of augmenting the present maximum thrust output at low speeds and low altitudes are of importance in new aircraft design.

A number of different possibilities of augmenting the thrust have been, or are being, investigated but at the present date none of them appear more attractive than does a mere increase in proportion of power-plant installation—that is, adding further power-plant capacity that is usable or required only at takeoff or climb. This imposes the requirement that the power-plant installation operate at high efficiency at a lower percentage of maximum output. This requirement may be a ruling factor in determining the design relationships in the machines.

One of the first augmentation possibilities studied was that of inducing an additional flow of air through the propelling nozzle using the high velocity jet as an injector. Theoretical studies and test-stand results show that low-speed thrust outputs may be increased in the order of 15 to 20 per cent in this manner. The same configuration results in no significant increase in thrust at high airplane speeds; in fact, at present obtainable speeds it may actually result in loss of thrust. There has been no practical method developed to date which would permit flow augmentation at low speed which would not adversely affect the high-speed drag of the airplane.

There remains the possibility that the tremendous pumping action of the high-speed jet may be profitably employed for boundary layer control to obtain high lift coefficients valuable in shortening the take-off run. Absorption of the boundary layer over wing or fuselage into the jet stream may possibly be made in high-speed cruising as a means of bettering the fuel consumption for long flights. Use of boundary layer for compressor air supply operates adversely on the thrust available but favorably with regard to specific fuel consumption, for under this condition the gross thrust, although reduced in magnitude, is the net thrust from an efficiency standpoint, the boundary layer having been already inevitably accelerated to aircraft velocity.

Cooling of the inlet air by evaporation of fluids injected into the compressor has been suggested and studied as a means of augmentation. Fluids such as water, ammonia, liquid air, liquid ammonia, and the hydrocarbon fuel being used, all have possibilities. If evaporation takes place prior to compression, the advantage gained by more efficient compression of the lower temperature air is partially offset by the requirement for compression of the added vapor. Water with its high heat of vaporization might be attractive except for the attendant problem of freezing. Injection of ammonia or other fuel may add explosive hazard. In any event, the power plant is made more complex, the power-plant control problem is made more difficult, and provisions must be made for carrying the secondary fluid. The flow rates will be high, so that such a method is practical only for short periods of time, such as at take-off.

The third possibility in augmentation is to burn additional fuel in the gas stream between the turbine and the propelling nozzle. This method has attractive theoretical possibilities but some extremely practical disadvantages. In order to efficiently add heat at this point the total pressure head must be essentially static, which requires either a low exit velocity turbine or an efficient diffusion aft of the turbine. Combustion must be carried out with low pressure drop and with short flame length, and experiments thus far conducted have not been markedly successful in either particular. Further development and experimentation in this connection should be carried out since it is believed that there is a significant possibility of practical success.

Higher Powered Engines

Conjecture about the future of jet-propelled aircraft almost inevitably leads to consideration of higher and higher power engines. As mentioned earlier, outputs have increased approximately two and one-half times in the last 3 years. As airplane studies have progressed to where consideration is given to large, long-range, jet-propelled airplanes, it appears that still higher powered units could be used to advantage. Thus far, increases in size have been accomplished with little significant increase in specific weight, although such power plants should theoretically obey the three-halves power law; that is, the weight should increase as the cube of any principal dimension while output increases only as the square. It is fortunate however, that these power plants, like airplanes, do

not rigorously follow such a law. As engines are made larger, many of the parts, which were originally selected for sturdiness rather than actual strength, increase in weight only slightly. Some design modifications may be made which are practical only in larger sizes, all of which compensate for the more or less inevitable increase in specific weight of the main rotating parts.

At the present time it is believed that the maximum effective size of machine that could be built depends primarily upon the manufacturers' ability to secure sufficiently large turbine wheel forgings with suitable properties and not upon the adverse operation of the three-halves power law.

Design

In the past 3 years jet propulsion has exerted a profound influence on new aircraft design and it is evident that in the future aircraft design will be even more influenced by such characteristics. At constant thrust both horsepower output and miles traveled per unit of fuel consumed increased in almost direct ratio to the aircraft speed. Consequently, the parasitic component of drag should be minimized by every practical design expedient. Cleanliness of shape or contour is the first requisite of a successful jet-propelled aircraft.

The high powers available in small packages with turbojet engines permit the design and construction of airplanes with performance nearing sonic velocity. In several airplanes flying today compressibility is the essential factor determining maximum velocity. For the first time in aircraft history problems of aerodynamics rather than power-plant availability determine the maximum performance.

With the turbojet power plant the altitude-power characteristic is more favorable to operation at high altitudes than for conventional power plants. The lower temperatures at high altitude result in higher thermodynamic efficiency and, as the power available does not decrease in proportion to the decreased density ratio (Fig. 17), speeds, unless limited by compressibility, will be higher at altitude than at sea level. Maximum range of a jet-propelled plane occurs at an altitude only slightly lower than the ceiling under any particular loading condition. Maximum range also occurs at an air speed much nearer the maximum than is the case in conventional powered planes. These two factors will undoubtedly operate to the end that future jet-propelled bomber or transport airplanes will be of the stratosphere type with supercharged cabins. Cabin supercharging will be somewhat less of a problem than with other types of power plants since the required amount of air may be taken from the compressor, where it is available after compression at high efficiency.

Much research and design work remains to be done to determine the optimum power-plant location within the airplane to obtain best ram efficiency and to minimize tail pipe losses, and also to achieve minimum external drag with the large variations of flow through the internal flow system. As previously mentioned, large airflows carried through the turbojet plants may prove advantageous in the utilization of boundary layer for high lift or to decrease cruising specific fuel consumption.

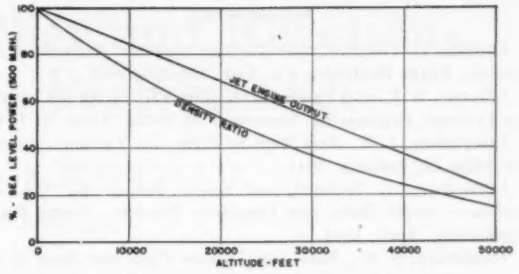

FIG. 17. Output vs. altitude relations for jet propulsion cycle at 500 m.p.h. density ratio shown for comparison.

The jet propulsion power plant need not be limited in its operation to high-altitude travel for it is possible that short-range, high-speed operations at low altitudes will also be attractive. Fuel consumption, although greater in amount, will not necessarily be more costly, and for short-range missions pay load carried per day may be greater with jet propulsion than with propeller-powered airplanes. In order to realize this objective with the jet-propelled airplane, significant design modifications and operating procedures must be made. Cruising speeds will be much higher and flight control must be more rigorous. Radar and radio aids must be found to eliminate the necessity for alternate airports of destination. In general, the entire present conception of flight must be revised to achieve maximum benefit from the jet propulsion principle.

CONCLUSION

The authors have attempted herein to cover somewhat broadly many of the technical and practical aspects of this exciting new field. Much of the information presented is already known to aircraft designers working on such projects and is summarized partially with the hope of stimulating discussion on some of the interesting or possibly controversial points. Many engineers, both in this country and in England, have contributed to the fund of information, and it is at this time almost impossible to single out the contributions made by specific individuals. It is hoped that as secrecy becomes less important and restrictions less stringent, many of the technical phases of the problem may be treated openly and in greater detail. The numerous problems remaining to be solved will serve as a challenge to aeronautical engineers for many years.

REFERENCES

[1] Smith, G. Geoffrey, *Gas Turbines and Jet Propulsion for Aircraft*, Flight Publishing Co., Ltd., London, 1942.

[2] Davies, S. J., and Fawzi, M. I., *The Efficiencies of Combustion Turbines*, Engineering, November 19, 1943; March 10, 1944.

[3] Rettaliata, J. T., *Next Steps in Using Gas Turbines*, Power, Vol. 88, p. 30, January, 1944.

[4] Soderberg, C. Richard, and Smith, Ronald B., *The Gas Turbine—Present Status and Immediate Prospects*, Power Plant Engineering, April, 1944.

[5] Salisbury, S. K., *Basic Gas-Turbine Plant and Some of Its Variants*, General Electric Review, Vol. 47, pp. 23–33, May, 1944.

[6] Fischer, F. K., and Meyer, C. A., *Combustion Gas Turbine*, Electrical Engineering, Vol. 63, pp. 163–169, May, 1944.

[7] Eksergian, Rupen, *On the Reaction of Fluids and Fluid Jets*, Journal of The Franklin Institute, Vol. 237, No. 5, pp. 401–407, May, 1944.

[8] Moss, Sanford A., *Gas Turbines and Turbosuperchargers*, Transactions of the A.S.M.E., July, 1944.

[9] Puffer, S. R., and Alford, J. S., *The Gas Turbine in Aviation, Its Past and Future*, Submitted to the A.S.M.E., October 14, 1944.

[10] Warner, D. F., and Auyer, E. L., *Contemporary American Jet Propulsion Gas Turbines for Aircraft*. A paper presented at a closed meeting of A.S.M.E. in Washington, D.C., October, 1944.

[11] Warren, G. B., *Potentialities, Limitations of the Combustion Gas Turbine*, Electric World, Vol. 122, pp. 83–85, October 28, 1944; pp. 99–101, November 11, 1944.

[12] *Second Report of the Commanding General of the Army Air Forces to the Secretary of War*, Section 3, pp. 75–76, February 27, 1945.

[13] Hamlin, Benson, and Spenceley, F., *Comparison of Propeller and Reaction-Propelled Airplane Performance*, Journal of the Aeronautical Sciences, Vol. 13, No. 8, pp. 425–437, August, 1946.

[14] Hamlin, Benson, *Flight Testing of Conventional and Jet-Propelled Airplanes*. A book being published by The Macmillan Company, New York.

Library Facilities of the
Institute of the Aeronautical Sciences

To serve Institute members and others in the aeronautical industry, the Institute of the Aeronautical Sciences offers the facilities of:

The W. A. M. Burden Library
2 East 64th Street
New York 21, N.Y.

The facilities of this library are available for reference study at the Institute.

The Paul Kollsman Lending Library
2 East 64th Street
New York 21, N.Y.

This library loans books without charge to members and others in the United States over eighteen years of age. Full information will be sent on request.

The Pacific Aeronautical Library
6715 Hollywood Boulevard
Hollywood 28, Calif.

This is a service and reference library for West Coast members and organizations. Full information as to its facilities will be sent on request.

Comparison of Propeller and Reaction-Propelled Airplane Performances

BENSON HAMLIN* AND F. SPENCELEY†

Bell Aircraft Corporation

INTRODUCTION

COINCIDENT WITH the development of successful turbojet power plants for aircraft, a broad new field of propulsion has come to light. Power-plant research and development has progressed so rapidly that a wide choice of power plants is now available to the aircraft manufacturer, who as yet has had little opportunity to demonstrate the practical applications. The purpose of this paper is to evaluate the airplane-performance potentialities of four types of widely differing power plants and to indicate their trends and particular fields of application.

Conventional power plants of the reciprocating, internal-combustion type, both direct and indirect air-cooled, have been extended to compounding with a gas-turbine wheel operated by the normal exhaust gases and delivering the power thus generated back into the crankshaft. The independent gas turbine is also available for use in conjunction with the propeller, in which case approximately 80 per cent of the energy in the gases is absorbed by the turbine to drive the propeller and the remainder is utilized in the form of reaction propulsion. Air-stream engines include the turbojet, reso-jet (or intermittent duct), and the ram-jet (or athodyd), all of which are reaction motors depending upon atmospheric air supply. A third classification of available power plants consists of dry or liquid-fuel types of rocket motors, which are distinguished principally by the fact that atmospheric oxygen is not used for combustion as in the case of other power plants.

For this paper four power plants having distinctly different performance characteristics have been chosen: (1) a V-type, reciprocating, liquid-cooled engine employing water injection for emergency power; (2) a turbojet engine having about 23 per cent less sea-level static thrust than the former; (3) a hypothetical subsonic ram-jet; and (4) a bipropellant liquid-fuel rocket motor. For brevity, these power plants will be referred to as propeller, turbojet, ram-jet and rocket, respectively.

Because these power plants differ so radically in performance characteristics, it is difficult to determine a sound basis for comparison. It has therefore been decided to design a single-engined, single-place fighter or pursuit type airplane employing each type of power plant and limiting the size to some reasonable weight, say less than 14,000 lbs. It is felt that the results submitted, together with the analysis presented, offer sufficient justification for classifying these types of power plants in specialized categories in which they excel. Thus, if a particular type of engine shows outstanding merit in a high-altitude and high-speed performance for a fighter, similar reasoning may be judiciously applied in considering other aircraft types.

The text is divided into three parts. Part A compares the various types of engines independently of airplane characteristics insofar as possible. Part B briefly describes a logical and practicable airplane design configuration for each power plant. In Part C, the results of the airplane performance characteristics are presented from which comparisons and conclusions may be advanced.

PART A—POWER-PLANT CHARACTERISTICS

(1) *Reciprocating Engine and Propeller*

A typical high-performance engine employing water injection is assumed, which delivers 2,000 b.hp. for take-off, the power varying linearly with density to 1,700 b.hp. at an engine critical altitude of 20,000 ft. Typical propulsive efficiencies have been used in converting power to available thrust in order to afford a direct comparison with the other types of power plants in which thrust is the fundamental consideration. Exhaust jet thrust has also been included.

The gas turbine driving a propeller has not been considered because the differences when compared to the remaining three power plants are not radically different from those of the reciprocating engine. Specific engine weight and size are improved, but fuel consumption will be increased in comparison to reciprocating engines. Also, the propeller itself imposes a definite limitation on maximum speed. Both the gas turbine and compound engine may be considered to be alternate developments in relation to propeller-driven airplanes.

(2) *Turbojet Engine*

The turbojet engine selected is typical of the single-stage centrifugal blower type employed in a number of

Presented before a closed meeting of the Institute of the Aeronautical Sciences, Hollywood, Calif., August 15, 1945. Released for publication on March 15, 1946.

* Project Engineer. Formerly Development Engineer.

† Performance Group Aerodynamicist.

aircraft. Performance characteristics represent those already attainable at the present state of development.

(3) *Ram-Jet Engine*

Of the four power plants considered, the ram-jet represents the only hypothetical design under consideration, it being the only type of propulsion not actually known to exist as a flight article. As a basis for the theoretical engine performance, the analysis presented in reference 1 is used herein. This type of power plant will not operate at zero air speed, and consequently cannot take off. Auxiliary take-off means are assumed to launch the airplane and accelerate to a flight speed of 350 m.p.h., at which time the ram-jet is started. Since no logical engine output rating exists in this case, a unit of a size suitable for a 10,000-lb. fighter is assumed.

Combustion temperatures of the order of 3,000°F. are assumed to be structurally possible since moving parts do not exist to complicate the problem. Successful operation in this regime has been demonstrated. Already turbine buckets are operating in a 1,500°F. gas temperature. Kerosene fuel to the engine is provided by a turbine-driven fuel pump.

(4) *Rocket Motor*

The rocket motor, being small and light, has been chosen as a 9,000-lb. thrust unit, which takes advantage of a high thrust output without presenting impractical arrangement or installation problems. An example of actual application is the well-known German Me 163. For practical reasons an existing type of rocket motor using a bipropellant fuel system has been chosen, leaving room for considerable improvement with further research in the relatively near future.

The problem of supplying the fuel and oxidizer to the motor at high pressure is solved by turbine-operated pumps using the same propellants for power.

(5) *Maximum Thrust Available* (*Figs. 1a–1c*)

Immediately apparent is the fact that the conventionally powered airplane will have the lowest maximum speed at all altitudes and, also, that it is essentially a low-altitude power plant. Obviously, the ceiling of this airplane will be inferior. Furthermore, the maximum speed limitation is absolute as indicated by the fact that above 600 m.p.h. the propulsive efficiency limitation due to compressibility effects causes the thrust available to practically vanish. The slope of the curve indicates good acceleration characteristics in level flight below maximum speed and also that climb characteristics will be relatively good.

Considering the rocket airplane, maximum performance is obviously superior under all conditions. Inasmuch as atmospheric pressure variation is but a small percentage of the motor chamber pressure, the small variation in thrust with altitude has been neglected.

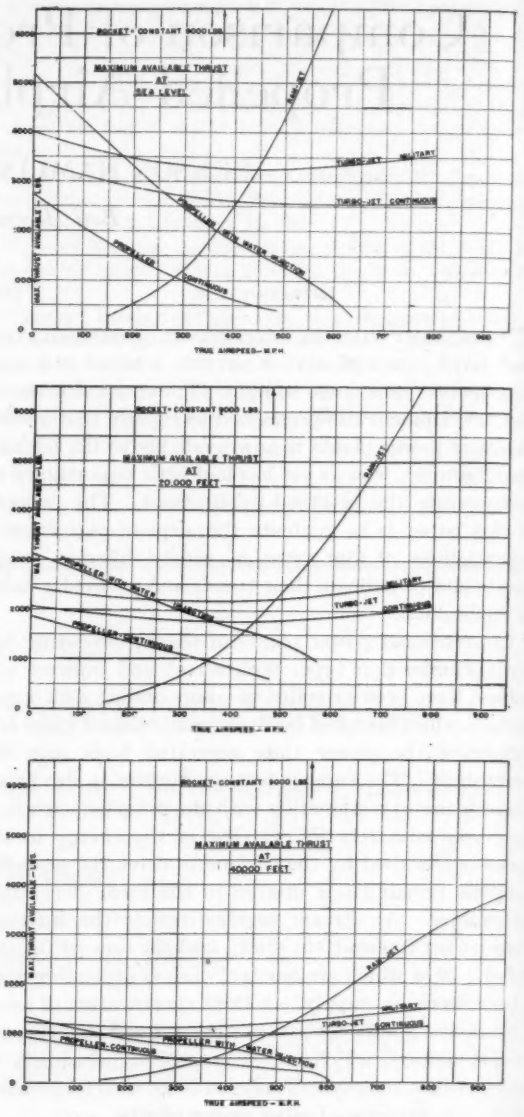

FIGS. 1a (*top*), 1b (*center*), and 1c (*bottom*).

Air speed has no effect upon thrust output. At low altitudes only does the ram-jet offer competition in available thrust, but this is offset by the fact that airplane drag at high air densities is also extremely high. Outstanding is the rocket's complete superiority in performance at high altitudes where airplane drag is greatly reduced. Thus, high-altitude speeds will necessarily be outstanding as will also the high rate of climb at all altitudes.

Relatively constant thrust with speed variation is also apparent for the turbojet. In this case output suffers considerably with altitude, but maximum speed performance compared to the propeller-driven airplane affords a sharp contrast.

From the standpoint of self-sufficiency, the ram-jet is the least desirable since an auxiliary means of pro-

pulsion is required for take-off. Although thrust varies roughly as the velocity to the 2.0 to 2.5 power, it falls off with atmospheric density. In other words, thrust is a direct function of differential pressure, which, in turn, is determined by the airplane drag characteristics. This results in a relatively low airplane ceiling but an excellent maximum speed at sea level where the air forces become prohibitive for sonic air speeds. Loss of energy due to shock waves in the duct entrance has been taken into account.

(6) *Specific Engine Weight (Fig. 2)*

Important in the airplane design configuration is the power-plant installation weight. For comparison, the complete power-plant weight, exclusive of fuel supply system, per unit of maximum available thrust, is presented in Fig. 2 (see also Section 9). When the reciprocating engine is used for high-altitude operation it becomes an extremely complicated and heavy power plant; in fact, beyond 40,000 ft. it becomes prohibitively so. Also, the improvement in specific engine weight with decreasing air speed and altitude again classifies propeller propulsion as best suited for relatively low air speeds and altitudes. Even when compared at low altitudes, the reciprocating power-plant dry weight is some 20 times as heavy as the rocket motor.

The turbojet offers a considerable improvement in engine weight which will probably continue to be improved. Again, with increasing altitude specific engine weight increases, but not to the prohibitive degree evidenced by the propeller type. Also, contrary to the propeller type, specific weight improves at the higher air speeds, which emphasizes the practicability of higher air speeds.

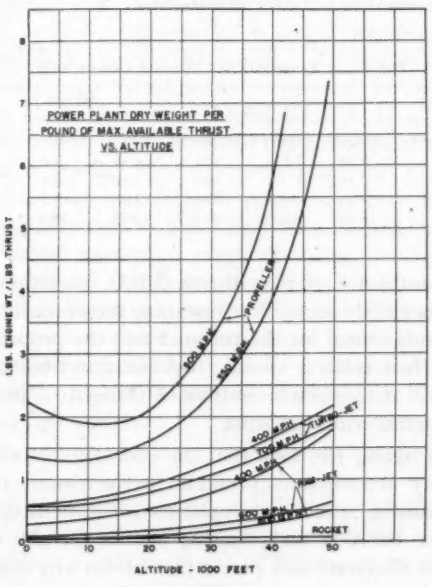

FIG. 2.

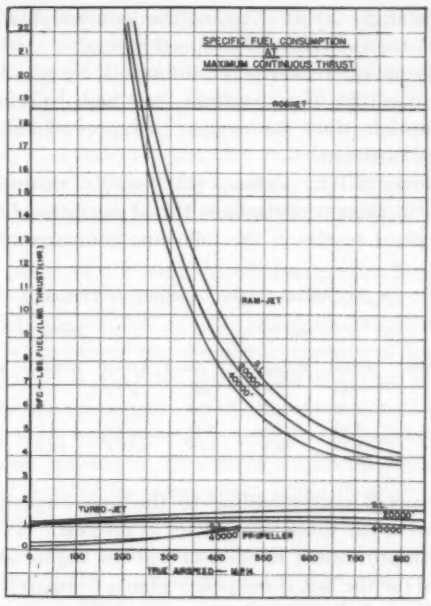

FIG. 3.

Considering the ram-jet, its design depends to a large extent on both speed and altitude. Marked improvement obtains at higher air speeds, and, when considering the reduction of thrust with altitude, it tends to become bulky and heavy for high-powered, high-altitude application. Apparently, the ram-jet is a medium-low-altitude, high-speed type of power plant.

Simplest of all is the rocket, which again makes no compromise for air speed or altitude variation. In terms of specific power plant weight it is unexcelled.

(7) *Specific Fuel Consumption (S.F.C.) at Maximum Continuous Thrust (Fig. 3)*

The propeller-type power plant offers a large saving in fuel, especially at the lower air speeds, as evidenced by its specific fuel consumption at maximum continuous thrust rating. At speeds exceeding 500 m.p.h. this fuel consumption would become greater than that of the turbojet. However, employing this thrust rating, speeds much in excess of 400 m.p.h. are not obtainable. Curves for both the propeller and turbojet are based upon maximum *continuous* available thrust, which, unlike the ram-jet and rocket, are less than the maximum available as shown in Fig. 1. Specific fuel consumption at maximum continuous thrust for the turbojet does not vary significantly with air speed and improves appreciably at the higher altitudes.

In the case of the ram-jet, an entirely different variation is found. Here, efficient operation is decidedly improved at extremely high speeds, in the region of Mach Number = 1.0, while at lower air speeds the fuel consumption is prohibitively high, and, as seen from Fig. 1, the maximum thrust available at low air speeds

is exceedingly small. Again, the ram-jet clearly belongs to the extremely high-speed regime.

As usual, the rocket is not influenced by speed or altitude, resulting in a constant, but high, specific fuel consumption, since the oxygen to support combustion must be included.

Selecting S.F.C. values, (lb. fuel/lb. thrust times hours), maximum continuous thrust operation for each power plant results in the following comparison:

S.F.C. at Maximum Continuous Thrust

	Sea Level			20,000 Ft.		
Power Plant	Actual	Relative	Air Speed	Actual	Relative	Air Speed
Propeller	0.56	1.0	300	0.71	1.0	375
Turbojet	1.72	3.1	520	1.46	2.1	520
Ram-jet	5.10	9.1	650	5.15	7.2	590
Rocket	18.75	33.5	675	18.75	26.4	685

Air speeds corresponding to the four airplanes are included in the table as a matter of interest. A considerable improvement in efficiency at the higher altitude is noted for the last three power plants compared to the propeller and the price that must be paid for increasing air speeds above 500 m.p.h. is painfully evident.

(8) *Variation of S.F.C. with Reduced Thrust (Fig. 4)*

Comparison of specific fuel consumption at various level flight speeds is not possible without considering airplane characteristics, because the thrust required depends directly upon the airplane drag. Therefore, the curves drawn in Fig. 4 necessarily coincide with the particular airplanes to be considered later but the general trends and comparisons are valid in other applications.

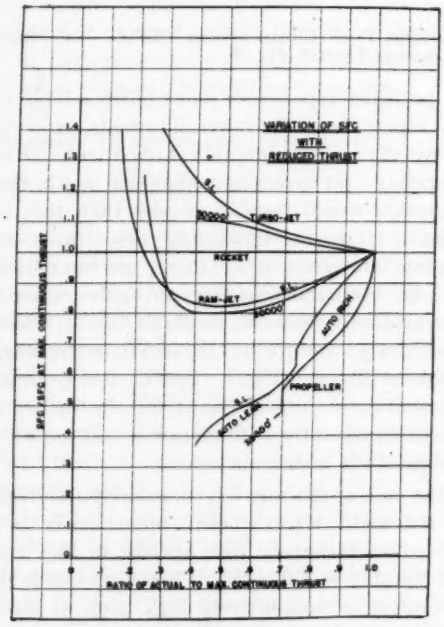

FIG. 4.

Obviously, the best range performer is the propeller, which, at low thrusts, may be operated on a lean mixture. Here the variables, engine r.p.m., manifold pressure, degree of supercharging, fuel mixture setting, and engine operating temperatures must all be carefully controlled in order to obtain maximum economy. Nevertheless, a reduction in S.F.C. of the order of 50 per cent from that at maximum continuous power represents a decided saving. Based on both Figs. 3 and 4, the propeller has no serious competitor for maximum range or endurance at moderately low air speeds.

Unlike the propeller, the turbojet evidences a loss in economy when operating at lower than maximum output, representing about a 10 per cent increase in S.F.C. for cruising conditions. Cruising S.F.C. is better at high altitudes than at low levels in all cases with the exception of the rocket.

An appreciable improvement in economy of the ram-jet at cruising speeds is shown tending to offset its disadvantage when compared to the turbojet at high speed. Maximum thrust and the corresponding S.F.C. are necessarily established as those produced at the maximum speed of the airplane.

The rocket, as always, appears as the only power plant whose characteristics are independent of its application. In this respect, however, the individual rocket motor units are operated at their maximum efficiency conditions dictated by design. In other words, a selected number and size of individual rocket motors are chosen so that thrust available exists in steps according to the motors selected during operation.

Having analyzed the airplane range characteristics, the following table comparing the S.F.C.'s for conditions of maximum range is obtained:

S.F.C. at Economical Cruising Conditions

	Sea Level			20,000 Ft.		
Power Plant	Actual	Relative	Air Speed	Actual	Relative	Air Speed
Propeller	0.28	1.0	175	0.32	1.0	225
Turbojet	2.18	7.8	325	1.66	5.1	365
Ram-jet	4.70	16.8	535	4.43	13.7	500
Rocket	18.75	67.0	415	18.75	58.0	425

The influence of part thrust S.F.C. variation from Fig. 4 is clearly seen. For instance, the opposite cruising trends shown for the turbojet and the propeller increase their relative specific fuel consumptions from 2 or 3 to 1 at maximum continuous thrust to 5 to 8 to 1 at optimum cruising thrust.

Here again, the fact that an enormous sacrifice in economy accompanies premium performance, that is high cruising speeds, is emphasized. Ridiculous comparative S.F.C.'s and cruising speeds for the rocket seem to eliminate this power plant from any consideration involving economical operation.

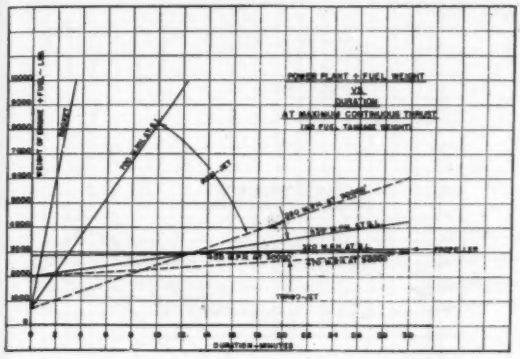

FIG. 5.

(9) *Power Plant Plus Fuel Weight (Fig. 5)*

Fig. 5 is a plot of power-plant weight plus fuel weight, excluding fuel tanks, taken at maximum continuous rating versus duration. Weights of power plant are assumed as follows:

	Propeller	Turbojet	Ram-Jet	Rocket
Motor + controls and plumbing	1,900	2,000	550	450
Cooling system + coolants	450	0	0	0
Propeller	500	0	0	0
Turbine and pumps	0	0	150	225
Total, lbs.	2,850	2,000	700	675

For the rocket motor the power plant plus fuel weight is startling, being 10,000 lbs. for less that 4 min. duration, with no weight allowance for fuel tankage. However, when the vastly superior thrust rating is considered the picture improves somewhat.

Investigations have revealed clearly the fact that for any given airplane and gross weight, the minimum pounds of fuel expended per 1,000 ft. of altitude gained in climbing always occurs at the maximum available thrust. This phenomenon is valid irrespective of compressibility drag increases. Consequently, an extremely high thrust rocket compared to the other power plants has been chosen because it is practical to do so in this case where the power-plant specific weight is small. The tremendous amount of energy available in an extremely short period of time provides dazzling performance for a decidedly limited duration. Even under maximum range operating conditions at vastly reduced thrust the high S.F.C. still obtaining irrevocably limits range and endurance. The only possible recourse would be some means of launching or commencing rocket flight at high altitudes where exceptionally high air speeds will offset the high rate of fuel consumption. Thus, rocket-powered flight in the present instance is considerably limited in range.

Next comes the ram-jet, in which case the fuel consumption depends directly upon speed and altitude. Assuming a maximum speed of 700 m.p.h. at sea level and 550 m.p.h. at 30,000 ft., it is apparent that at low altitudes a substantial, though not large, improvement over the rocket obtains. At altitude, the fuel consumption is not a great deal more than the propeller or turbojet-propelled airplanes. In this case 10,000 lbs. of power plant plus fuel results in a practical average duration of 30 min. Generally, it may be concluded from the figure that the ram-jet is suitable for relatively high maximum speeds at medium to low altitudes for relatively short duration.

By virtue of a lower power-plant weight the turbojet excels over the propeller up to 15 min. at sea level and 30 min. at 30,000 ft., after which the propeller takes over. Considering the decided advantage of speed for the former, it may be generalized that for excellent high-speed performance at all altitudes up to 40,000 ft., the turbojet endurance at maximum continuous thrust is a good half-hour. To compare with the rocket and ram-jet a 10,000 lb. power plant would show an average duration of some 135 min., or $2^1/_4$ hours.

The propeller and internal-combustion engine is by far the best power plant for long endurance at maximum continuous power but at a considerable sacrifice in speed. Extrapolating an average curve to a 10,000-lb. power plant results in an endurance of about 12 hours. Note that the ram-jet and turbojet show an increased economy at altitude as does the propeller, but the latter is the only one to show an improvement in high speed at altitude.

(10) *Power Plant Plus Fuel Volume (Fig. 6)*

In addition to power-plant weight its size is also a critical factor in the design of the aircraft. Fig. 6 shows the volume of power plant plus fuel corresponding to the weights shown in Fig. 5. Power-plant volumes are the volumes occupied by the units if wrapped with cloth. In other words, power plants having an odd shape will result in still more space unusable for other airplane components. Power-plant volumes in cubic feet are estimated as follows, representing the minimum space not available for other airplane components:

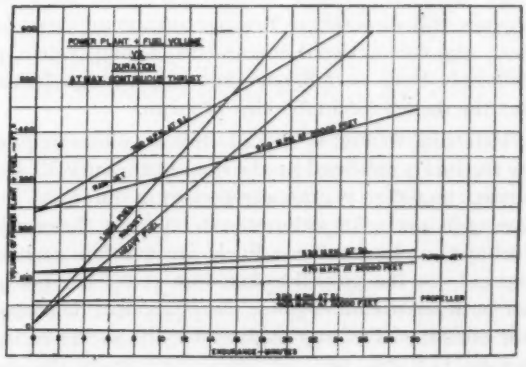

FIG. 6.

	Propeller	Turbojet	Ram-Jet	Rocket
Engine, blower and gear box	33	95	235	9
Air ducting	14	25	0	0
Turbine and pumps	0	0	5	5
Oil and coolant systems	13	0	0	0
Total	60 ft.³	120 ft.³	240 ft.³	14 ft.³
Equivalent frontal diameter	38 in.	52 in.	50 in.	18 in.
Frontal area	5.5 ft.²	14.8 ft.²	13.6 ft.²	1.8 ft.²

In comparing the engine volumes, the power plants in order of preference are the rocket, propeller, turbojet, and ram-jet. Fortunately, although the last-named has a considerable volume, its weight and installation considerations are such that it is practical to convert the aft fuselage, which always is relatively vacant because of balance considerations, into the power plant proper. Tending to offset this effect is the fact that the large mass airflows consumed dictate large duct inlet scoops. The simplicity of mechanisms alleviates installation problems considerably.

Next in bulky space requirements is the turbojet, nearly one-quarter of the volume of which is compressor entrance air supply ducting in an average installation. This feature requires a relatively large nacelle or, because of the weight and diameter, dictates the fuselage size and arrangement in a single-engined airplane.

Although the internal-combustion engine is small, the space requirements are nearly doubled by carburetor, oil cooler, and Prestone radiator air scoops and ducting. Fortunately, the main component parts, the engine, oil coolers, and Prestone coolers, may be disposed about the airplane structure to best advantage.

The rocket motor is by far the smallest and simplest from the design standpoint. Air intake ducts are always a problem, and at high flight speeds considerable research is necessary before satisfactory solutions will become available. In the case of the rocket, no air is taken aboard for the power plant, thus eliminating this problem. Note that the total rocket motor volume equals only the air ducting required for the reciprocating engine and that the power plant consists of two simple components that may be located at the designer's discretion.

In the frontal area comparison both air-stream engines will dictate the fuselage maximum cross section; the conventional engine and cooling system will definitely have an influence upon this design feature, but the rocket eliminates this problem.

Referring to Fig. 6, the additional volume required by the fuel is indicated by the slope of the curves. Here again, the rocket is critically limited in duration. Following in increasing order of preference are the ram-jet, turbojet, and propeller. Fuels are gasoline at 6 lbs. per gal. for the propeller, kerosene at 6.7 lbs. per gal. for both air-stream engines, and equivalent densities of the combined fuel and oxidizer for the rocket of from 8.4 to 11.2 lbs. per gal. depending upon the fuels chosen.

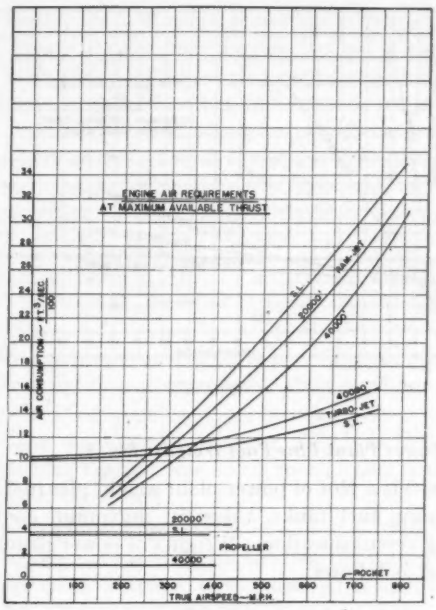

FIG. 7.

(11) *Engine Air Requirements* (*Fig. 7*)

In designing air intake ducts the relative problems are indicated by the engine air requirements shown in the figure for maximum thrust conditions, which would represent take-off, climb, and high-speed operation.

Since the ram-jet curves approximate a straight line through the origin, the scoop entrance velocity will be a relatively constant percentage of airplane speed. Volume of airflow is extremely large, indicating difficult problems to be solved.

The turbojet evidences only a slight increase in air consumption with air speed, indicating that the optimum entrance duct efficiency for a fixed entry will depend upon the conditions selected in the design. Again, large airflows must be handled. In the case of both air-stream engines the ram drag due to taking this air aboard has been subtracted from gross jet thrust to arrive at the maximum thrust available as shown in Fig. 1.

Cooling air requirements for the propeller type represent about 80 per cent of the total shown. Constant air volume requirements dictate scoop design for particular conditions, generally for maximum speed.

In the case of the rocket no air is required.

PART B—AIRPLANE DESIGNS

Since the characteristics of the four power plants are extremely diversified, it is difficult to determine which type is most suitable for a given application until each is translated into an airplane design study and the respective performances are evaluated. As the majority of the power plants potentially represent premium performance aircraft at a sacrifice in pay load, it is

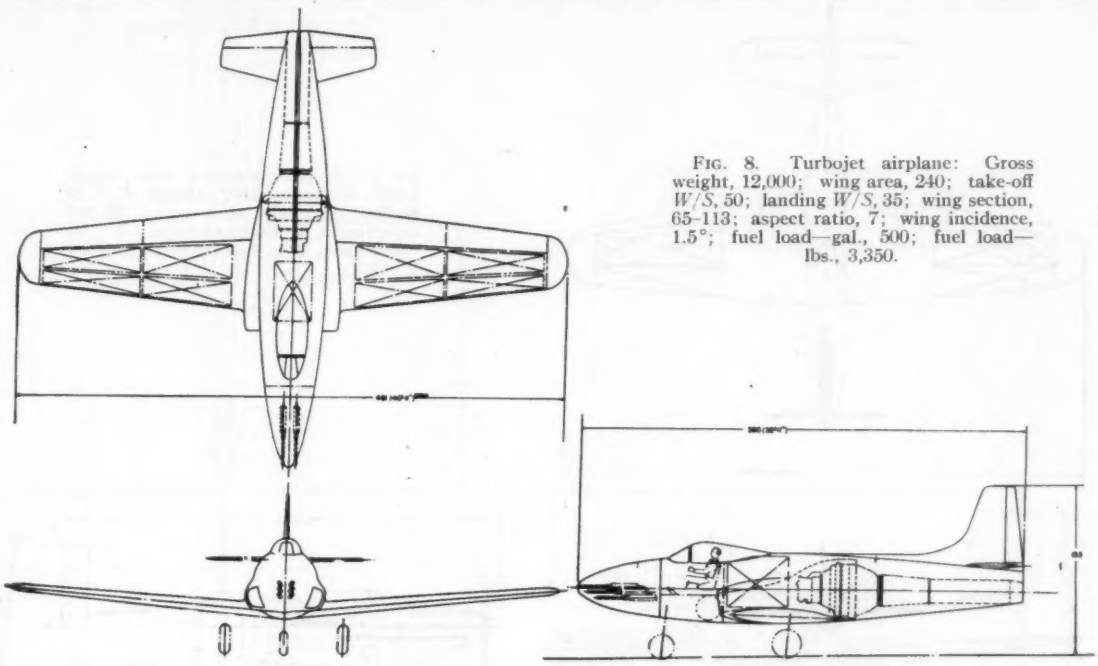

FIG. 8. Turbojet airplane: Gross weight, 12,000; wing area, 240; take-off W/S, 50; landing W/S, 35; wing section, 65–113; aspect ratio, 7; wing incidence, 1.5°; fuel load—gal., 500; fuel load—lbs., 3,350.

reasonable to use a fighter or interceptor-type airplane as a basis for comparison. This represents the type of military application where performance is decidedly at a premium and economy and practicability are sacrificed as a matter of self-preservation. Arbitrarily, for expediency in the comparison, these aircraft will be considered as single-place, single-engined aircraft having conventional wing and tail arrangements, conventional pilot accommodations, and internal fuel only.

Figs. 8–11 show the general arrangements and physical characteristics of the airplanes and Table 1 lists the weight breakdowns. Less armament is carried by the two airplanes whose range and duration of combat are obviously restricted. Unit wing weight depends greatly upon thickness, and structure in general is affected by the operational speed ranges, which affect the design air loads. Landing-gear weight is primarily influenced by the gross weight at landing condition.

A practical limit to the internal fuel capacity appears to be about 200 gal. of high-octane gasoline in self-sealing fuel tanks for this size of propeller-driven fighter. Laminar flow wings of 15 per cent thickness are employed. A nominal wing loading of the order of 35 to 40 lbs. per sq.ft. represents a present-day compromise between performance on the one hand, and maneuverability and serviceability with respect to tactical airfield considerations on the other. Armament load is 1,100 lbs.

Because of the disadvantageous fuel consumption characteristics of the turbojet and also the considerably increased high-speed regime of operation, this type of airplane is forced to higher wing loadings, in this case of 50 lbs. per sq.ft., resulting in a greater difference between take-off and landing wing loadings. Wing thickness of 13 per cent compromises internal fuel capacity with low drag characteristics. In this case, also, leakproof fuel tanks for kerosene are a necessity. Fuel here represents about 31 per cent of the take-off gross weight compared to 16 per cent in the case of the propeller, resulting in landing wing loadings of 35 and 33 ft. lbs. per sq.ft., respectively. The same 1,100-lb. provision is allowed for armament.

TABLE 1
Component Weights

	Propeller	Turbojet	Ram-Jet	Rocket
Wing	1,230	1,550	1,100	1,100
Tail	170	200	260	260
Fuselage	660	1,100	700	970
Landing gear	600	680	400	450
Power plant				
Motor	1,660	1,850	550	400
Accessories	1,150	130		50
Controls	40	20	10	10
Fuel system	600	840	1,050	550
Turbine and pumps	0	0	140	210
Fixed equipment				
Armament	1,100	1,100	700	700
Controls	140	230	200	200
All other	460	700	290	200
Weight empty, lbs.	7,800	8,400	5,400	5,100
Pilot	200	200	200	200
Fuel oil and coolant	1,500	3,400	4,400	8,200
Gross weight, lbs.	9,500	12,000	10,000	13,500

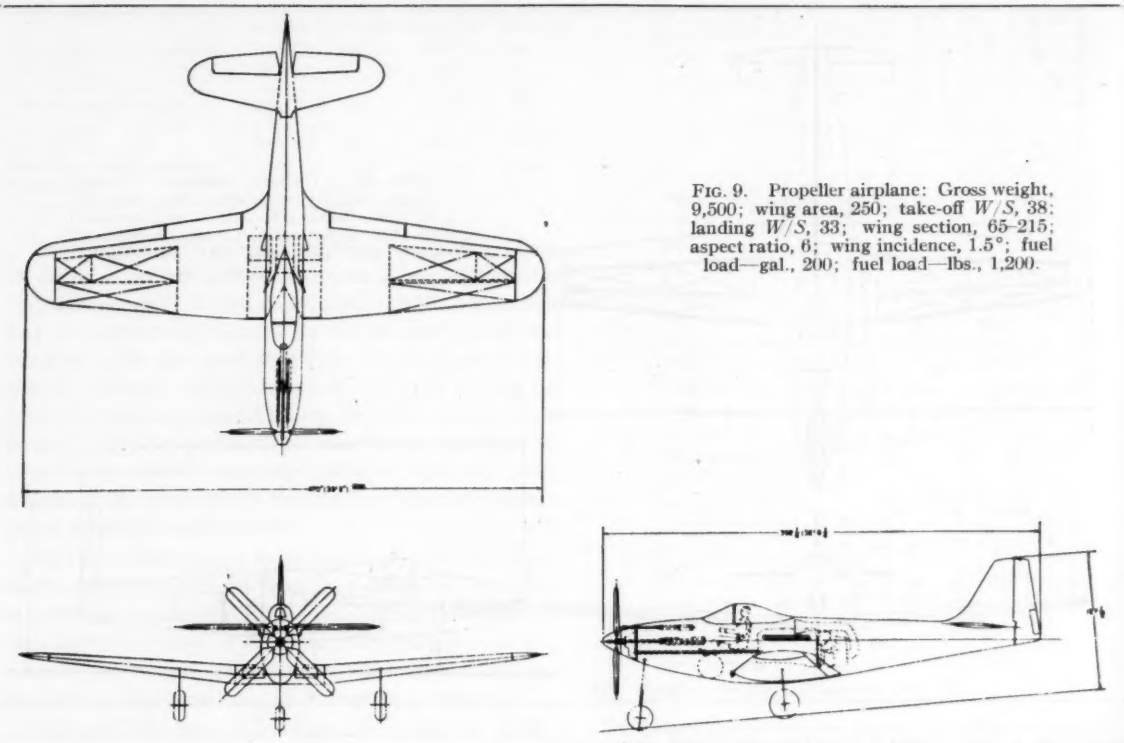

FIG. 9. Propeller airplane: Gross weight, 9,500; wing area, 250; take-off W/S, 38; landing W/S, 33; wing section, 65–215; aspect ratio, 6; wing incidence, 1.5°; fuel load—gal., 200; fuel load—lbs., 1,200.

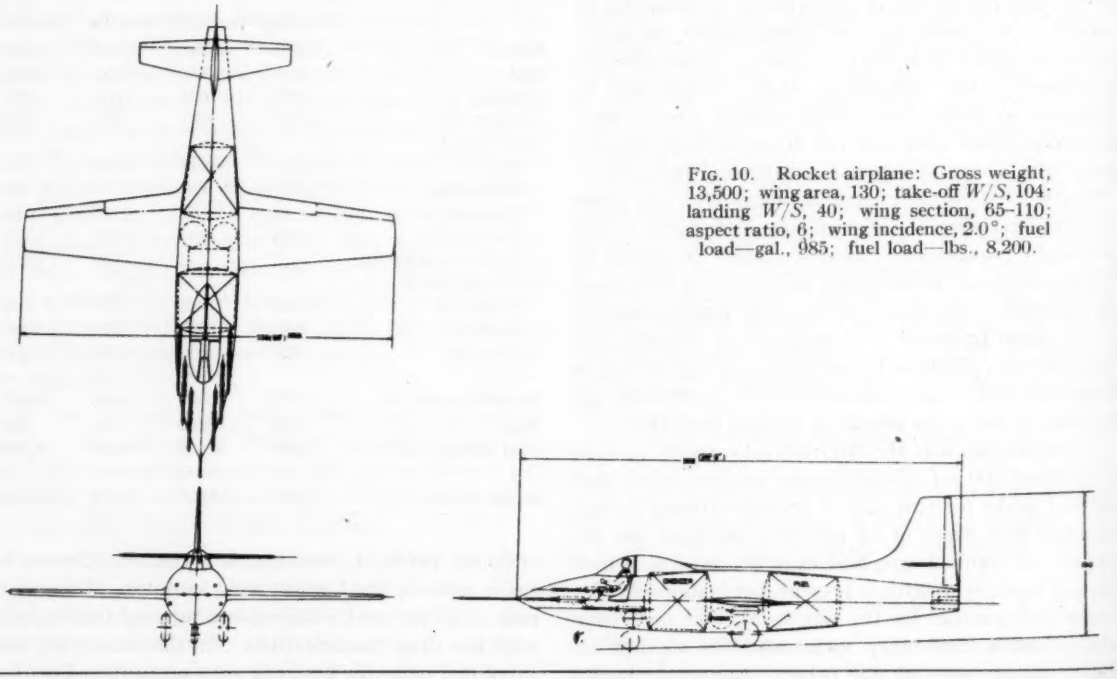

FIG. 10. Rocket airplane: Gross weight, 13,500; wing area, 130; take-off W/S, 104; landing W/S, 40; wing section, 65–110; aspect ratio, 6; wing incidence, 2.0°; fuel load—gal., 985; fuel load—lbs., 8,200.

In the design of the ram-jet airplane, the combustion chamber cross-sectional area dictates the fuselage size. Because of high fuel consumption 44 per cent of the launching gross weight represents fuel carried in both the fuselage and wing. Kerosene is assumed as fuel carried in self-sealing tanks. Since the flight duration and range are limited, this airplane is adaptable only to defensive strategy, and, if self-sealing tanks are elimi-

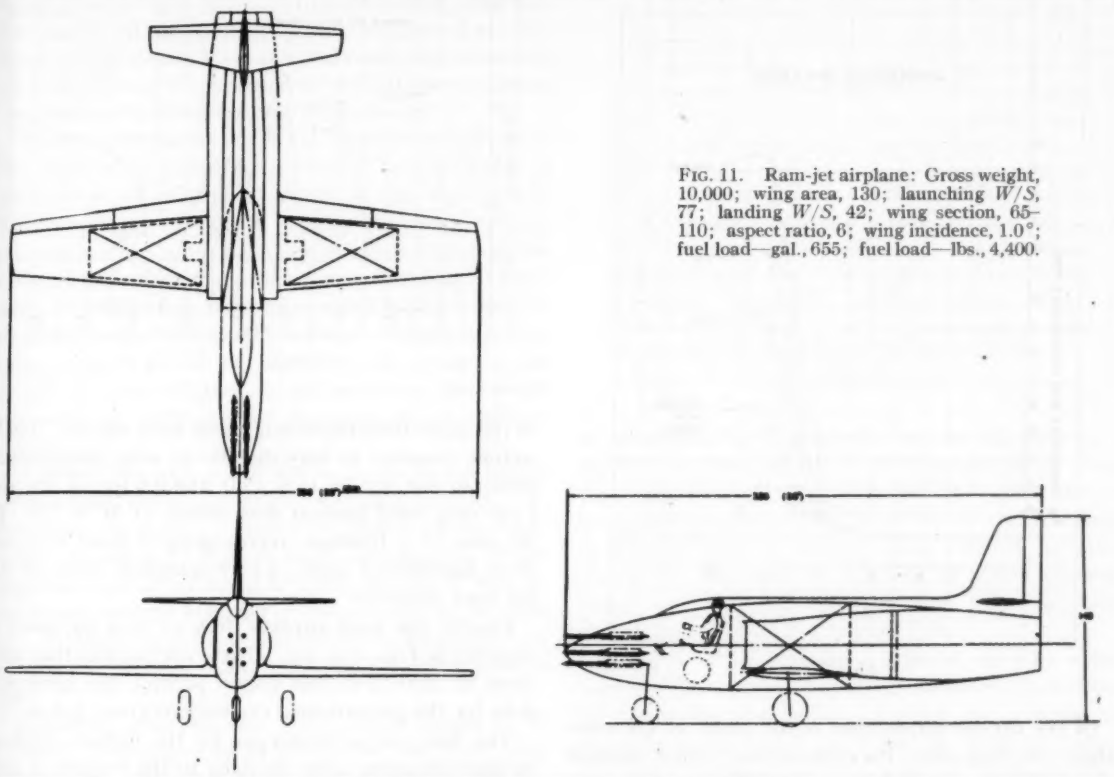

FIG. 11. Ram-jet airplane: Gross weight, 10,000; wing area, 130; launching W/S, 77; landing W/S, 42; wing section, 65–110; aspect ratio, 6; wing incidence, 1.0°; fuel load—gal., 655; fuel load—lbs., 4,400.

nated, a consequent improvement will be afforded by the addition of some 10 per cent in fuel. Some compromise wing loadings must be chosen. In this case 77 lbs. per sq.ft. for take-off represents a relatively low wing loading for this type of airplane but is assumed to allow for auxiliary means of take-off and flight up to 350 m.p.h., at which point the ram-jet power plant is started for the first time, take-off obviously not being possible with the ram-jet alone. The resultant landing wing loading of 42 lbs. per sq.ft. is quite reasonable.

High performance dictates reduction in wing thickness to 10 per cent.

As is obvious from the phenomenal fuel consumption, the rocket-motor-powered airplane must carry an abnormal amount of fuel, in this case 8,200 lbs., or 61 per cent of the take-off gross weight. Wing loading is dictated primarily by the landing condition and has been held at 40 lbs. per sq.ft., resulting in 104 lbs. per sq.ft. for take-off, which seems entirely feasible. Since superperformance is obvious, aerodynamic considerations dictate the entire arrangement. A practicable wing thickness of 10 per cent for the wing and 8 per cent for the tail are chosen. As in the case of the ram-jet, 700 lbs. of armament are installed. Tanks are not self-sealing owing to the nature of the fuels, the extremely short duration, and the exceptional performance. All fuel is carried in the fuselage.

PART C—PERFORMANCE COMPARISONS

(1) *Calculation of Airplane Drag*

Drag estimates for all four airplanes are based upon an identical analysis wherein the wetted areas of the component parts are assigned drag coefficients depending upon fineness ratios, Reynolds Numbers, and Mach Numbers. In this manner, the drag coefficients of the component parts are obtained and adjusted for lift coefficient or angle of attack. The cleanliness factors, C_f = the parasite drag coefficient based upon total wetted area at $C_L = 0$ and $RN = 8 \times 10^6$, and the parasite drag coefficients, based upon wing area, are given in the following table:

	W.A.	C_f	S	C_D
Propeller	931	0.0038	250	0.014
Turbojet	881	0.0034	240	0.013
Ram-jet	672	0.0035	130	0.019
Rocket	645	0.0034	130	0.017

Both the turbojet and the rocket exhibit extremely good aerodynamic cleanliness, being about an 11 per cent improvement over the propeller airplane. Drag coefficients based on wing area are shown in which high wing loadings, because of the relatively large fuselages, result in high parasite drag coefficients. The airplane drag coefficient for the propeller should be increased to 0.015 to allow for cooling drag at high speeds.

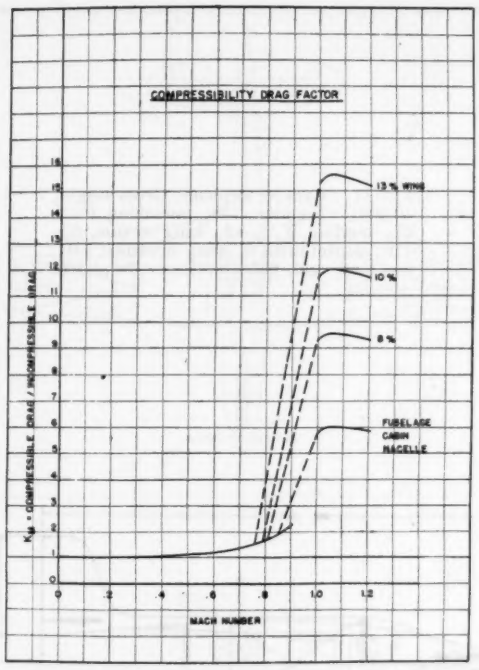

FIG. 12.

Of the utmost importance is the effect of compressibility on drag above the critical speed, which depends upon body shape and altitude. Ballistic data have been useless to the airplane designer because of the complete neglect of aerodynamic characteristics as such, the blunt projectile trailing edge shapes, and generally the extremely high Mach Number regimes of projectile flight.

Reference 2 provides the basis for the compressibility drag multiplication factor used for wings. This factor is multiplied directly times the airplane drag calculated on the above basis neglecting shock wave effects. These factors, assumed to vary directly as wing thickness as shown in Fig. 12, are 15.6, 12.0, and 9.6 for 13, 10, and 8 per cent thick laminar flow airfoils at $M = 1.0$. In the case of a fuselage, representing a more compact three-dimensional body, a corresponding value of 6.0 has been assumed.

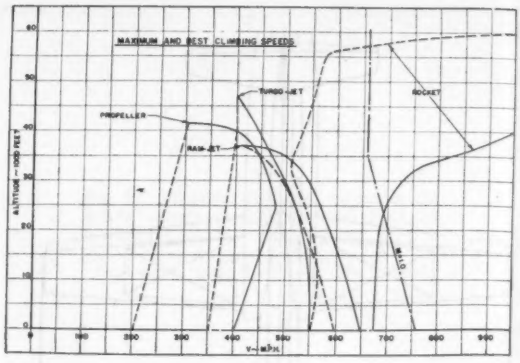

FIG. 14.

Finally, the total airplane drag vs. true air speed is depicted in Figs. 13a–13c. These curves, together with those in Part A of this paper, provide the necessary data for the performance evaluations given below.

The drag curves shown are for the highest airplane weights obtaining after climbing to the respective altitudes. Gross weight variation has been taken into account wherein performance is affected.

(2) *Maximum Speeds and Best Climbing Speeds* (*Fig. 14*)

Maximum speed of the propeller airplane is 480 m.p.h. at 25,000 ft., indicating that the practical high speed limit for this type of propulsion will not greatly exceed 500 m.p.h. At all altitudes up to 40,000 ft. a

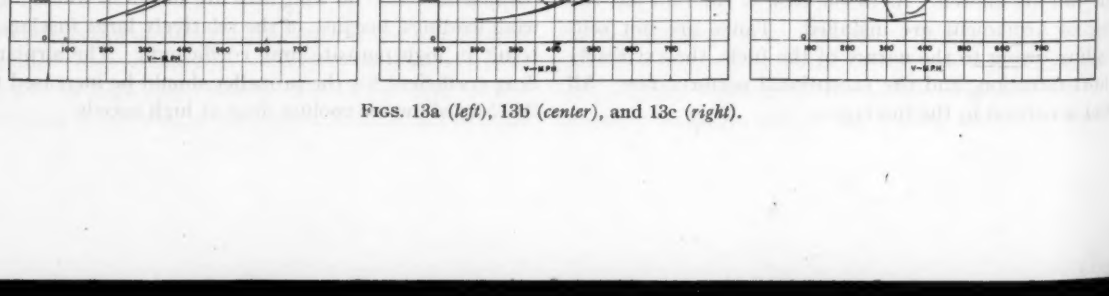

FIGS. 13a (*left*), 13b (*center*), and 13c (*right*).

speed greater than 400 m.p.h. is attainable, although 400 m.p.h. at sea level seems slow for ground strafing work. Best climbing air speed is relatively low, being 50 to 55 per cent of maximum level flight speed between sea level and critical altitude, respectively.

Next in high speed comes the turbojet, which excels the propeller at all altitudes, being 37 per cent faster at sea level and 8 per cent at 25,000 ft., the top speed of 550 m.p.h. representing a decided advantage. Maximum speed for this airplane occurs at sea level only because of the influence of Mach Number on drag. Otherwise, a considerable increase in speed with altitude up to 20,000 to 30,000 ft. would be found. Although at altitudes between 25,000 and 40,000 ft. the speeds are not greatly in excess of those for the propeller, this margin will improve with further development of turbojet engines.

A Mach Number = 1.0 line is shown in the figure, representing the magic barrier to speed performance, being the condition of maximum airplane drag coefficient. In order to achieve sonic velocity, the thrust required at sea level would be 1,000 per cent of that for the speed actually attained or 650 per cent in the case of a 30,000 ft. altitude. Sonic velocities with this type of airplane, therefore, appear impossible at the present time.

Regarding speed for best climb, which occurs at 65 per cent of maximum speed at sea level and 75 per cent at 20,000 ft., a considerable tactical advantage over the propeller airplane is realized. A greater distance covered during climb, since rates of climb for both are comparable, also offers a considerable advantage in being able to protect a given target from a base relatively far distant. An appreciable performance margin also obtains above 40,000 ft. because of the higher ceiling of the turbojet airplane.

Turning to the ram-jet airplane, it is astonishing to note that its speed for best climb considerably exceeds the turbojet's maximum speeds at all altitudes up to 33,000 ft., but that its ceiling is quite low. Maximum speed, 650 m.p.h., occurs at sea level, and the Mach Number limitation on speed is obvious in the figure. Climbing speeds are about 90 per cent of the maximum speeds.

Although the ram-jet engine is hypothetical, and is undoubtedly optimistic, it is interesting to note that 270 per cent of the actual thrust at 650 m.p.h. at sea level is required to reach a Mach Number of 1.0. Because of the fact that thrust increases greatly with speed, this represents an engine of 190 per cent greater power. Because of the impracticability of such high air speeds at high air densities, sonic speeds may be regarded with considerable pessimism in this case also. Nevertheless, from the standpoint of maximum speed alone, the ram-jet excels the turbojet by as good a margin as the latter excels over the propeller.

The rocket airplane excels in speeds at all altitudes by a wide margin. At sea level the ram-jet is capable

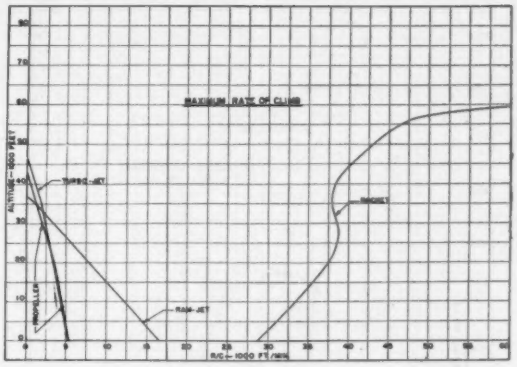

FIG. 15.

of competing for high speed, and at altitudes up to 30,000 ft. it also is similar in speed for best climb. Since the rocket thrust remains constant, the rocket airplane is capable of increasing its Mach Number with increase in altitude until it reaches sonic velocity at about 24,000 ft. Thereafter maximum air speed increases rapidly with altitude, the maximum limitation being imposed purely by the available fuel.

Speed for best climb is of interest, showing a best climbing speed at approximately constant Mach Number up to the tropopause. Beyond this altitude the lower drag resulting from lower air densities enables the best climbing speed to increase until at about 57,000 ft. Mach Number 1.0 is reached. Beyond this altitude, of course, performance is dictated entirely by the available fuel consideration.

(3) *Rates of Climb and Ceilings* (*Fig. 15*)

Maximum rates of climb for both the propeller and turbojet airplanes are similar. The latter, however, climbs at a much higher air speed, giving it a considerable advantage in combat in that it therefore can determine the conditions of engagement in combat or terminate it at will. The absolute ceiling of 47,000 ft., compared with 41,500 ft., also adds to this advantage. Climb and speed calculations for the propeller airplane are practically independent of the small fuel consumption, while in the case of the other three airplanes gross weight has necessarily been reduced according to the rate of fuel consumption. It should be noted that the larger fuel load in per cent of gross weight for the turbojet will result in appreciable improvement in climb performance during tactical operation.

Again, the excellence of low-altitude performance is noted for the ram-jet airplane. Since its thrust falls off with air density, its ceiling is found to be low. The extremely high climbing speeds should be taken into consideration in tactical operations.

The rocket airplane shows amazing rates of climb at all altitudes, varying from 28,500 ft. per min. at sea level to 66,500 ft. per min. at 60,000 ft., where it runs out of fuel. This airplane will coast to about 75,000 ft.

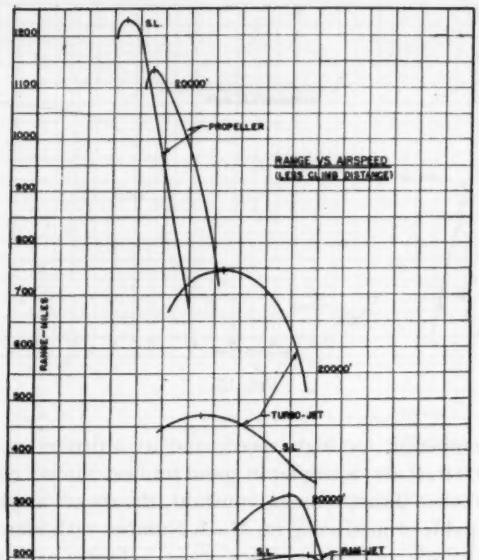

FIG. 16.

Rate of climb reduces considerably at 35,000 ft., because of the reduced speed for best climb, resulting in less thrust horsepower available at constant thrust. As climbing speeds approach and exceed $M = 1.0$, these powers become extremely large. For instance, 57,000 ft. and 660 m.p.h. in climb represents 16,000 thrust horsepower. Climb performance has been integrated and weight variation accounted for, including that required for linear acceleration along the flight path.

Time to climb and absolute ceiling may be compared in the following table, where the rocket ceiling is given as that altitude at which fuel is exhausted.

	Time to Climb to: (Min.)			Absolute
	20,000 Ft.	30,000 Ft.	40,000 Ft.	Ceiling
Propeller	4.9	9.0	19.0	43,000
Turbojet	4.7	8.3	14.3	47,000
Ram-jet	1.6	3.3	...	37,000
Rocket	0.6	0.9	1.1	60,000+

(4) *Range (Figs. 16 and 17)*

In determining range and climb performance the amount of fuel consumed in climb is important, except in the case of the propeller. The following table compares the fuel consumptions in climb.

Sea Level	Propeller		Turbojet		Ram-Jet		Rocket	
to	Lbs.	%	Lbs.	%	Lbs.	%	Lbs.	%
10,000	135	11.2	220	6.7	860	19.5	2,950	36.0
20,000	185	15.2	350	10.4	1,200	27.2	3,700	45.3
30,000	240	19.7	480	14.4	1,600	36.0	4,360	53.1
40,000	290	24.1	620	18.7	...	...	5,190	63.2
50,000	...	...	...	...	...	...	5,950	72.5
60,000	...	...	...	...	...	...	7,650	92.1

As seen from the table, the gross weight change for the propeller is small and for practical purposes may be neglected. Fuel expenditure for the ram-jet is not comparable with the others in that take-off and acceleration to 350 m.p.h. is accomplished by auxiliary means, for which no allowance has been made. Both the ram-jet and rocket are extremely uneconomical. The rocket necessarily suffers in climbing to higher altitudes where it becomes most efficient, while the ram-jet is essentially a low-altitude airplane. Although the turbojet burns more fuel in climb than the propeller, a greater percentage of fuel remains after the climb, owing merely to the fact that fuel is a much larger percentage of the gross weight.

Referring to Fig. 16, the range versus air speed at sea level and at 20,000 ft. is shown, which does not include the distance traveled in climb. Although the propeller has greatly superior maximum range, it obtains at an extremely low air speed, (200 m.p.h.), and a limited range of speeds. At 20,000 ft. and the same air speed, (350 m.p.h.), the propeller and turbojet are equal in range.

Maximum range for the turbojet, although considerably less than for the propeller, occurs at 150 m.p.h. faster air speed, or a 45 per cent reduction in time for equivalent range. Speed for best range increases with altitude in both cases. An outstanding characteristic of the turbojet is its relative insensitivity to air speed insofar as range is concerned, the only power plant variable being engine r.p.m. In the case of the propeller, as previously mentioned, a number of variables must be carefully controlled within close limits to attain optimum range.

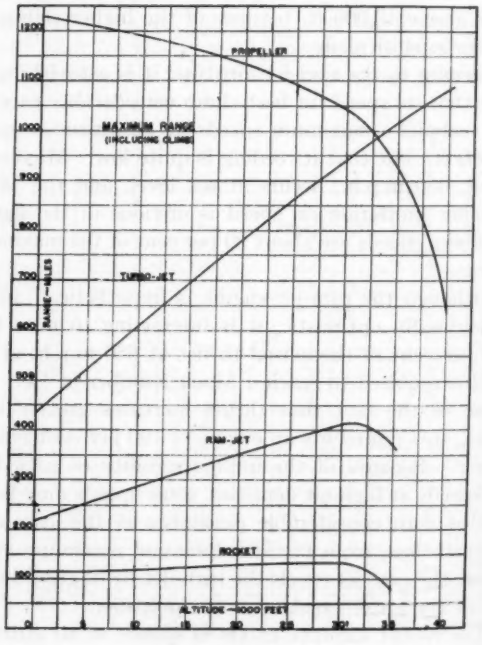

FIG. 17.

The ram-jet suffers still greater in range, but maximum range occurs at extremely high air speeds, above 500 m.p.h. In this case only, speed for economical operation decreases with altitude.

Range characteristics for the rocket indicate a wide speed range, 350 to 500 m.p.h., with an exceedingly limited range, about 100 miles.

Fig. 17 shows the variation in maximum range with altitude, including the distance traveled during climb. The relative maximum ranges and the altitudes at which they occur, up to 40,000 ft., are compared:

	Range		
	Actual	Relative	Altitude
Propeller	1,220	9.4	Sea level
Turbojet	1,080	8.3	40,000
Ram-jet	420	3.2	30,000
Rocket	130	1.0	30,000

Whereas the propeller has the greatest range, it occurs at sea level. At altitudes above 35,000 ft., range for the turbojet is superior. Both air stream engines and the rocket show maximum range increases with altitude of from 18 per cent to 250 per cent, contrary to the propeller.

Conclusions

(1) *Propeller Airplane*

(a) A practical maximum speed limitation not much in excess of 500 m.p.h. is apparent. Maximum speeds obtain in the 20,000 to 30,000-ft. range.

(b) Because of superior range, the propeller type of propulsion cannot be supplanted at the present time. Maximum range is relatively insensitive to altitude up to engine critical altitude.

(c) Greater pay loads possible in addition to range make commercial application and long-range bombers most attractive.

(d) Cruising and climbing speeds are slow.

(e) Operation above 40,000 ft. appears impractical except possibly in the case of power plants incorporating the gas turbine.

(f) Maximum rate of climb occurs at sea level.

(g) Further improvements, adaptations, and variations will be widely developed in terms of compound and gas-turbine engines and various combinations of them.

(2) *Turbojet Airplane*

(a) High maximum speeds where relatively short range is required make this airplane mandatory for military application. Maximum speed occurs at sea level.

(b) Again, for short-range premium operation in commercial fields this power plant is attractive. Range improves markedly with altitude, and economical cruising speeds are relatively high.

(c) Relatively high operating altitudes, at least up to 50,000 ft., are feasible. At high altitudes respectable range is obtained.

(d) Maximum speed of the order of 550 to 600 m.p.h. and above at sea level is ideally suited for air-to-ground military operation.

(e) Maximum rate of climb occurs at sea level.

(f) Speeds for maximum rate of climb are reasonably high.

(3) *Ram-Jet Airplane*

(a) Maximum speed, of the order of 650 m.p.h., occurs at sea level.

(b) Climbing speeds are exceptionally high, being within 5 to 10 per cent of maximum level-flight speeds.

(c) Range is extremely limited, representing some 50 per cent of that for the turbojet, and also increases considerably with altitude.

(d) Maximum rate-of-climb at sea level is exceptionally high, but falls off rapidly with increase in altitude, resulting in a rather low ceiling, below 40,000 ft.

(e) Auxiliary take-off means are required.

(f) Performance characteristics indicate that the ideal application would be in the field of low-altitude, flat trajectory missiles against such tragets as battleships and aircraft carriers in particular. Air launching would probably be more practical than surface launching.

(4) *Rocket Airplane*

(a) This is the only man-carrying airplane capable of flight at supersonic speeds, which distinguishes this type of propulsion from the others considered.

(b) Range is extremely limited and increases slightly with altitude.

(c) As in the case of maximum speed, so also does rate-of-climb increase phenomenally with altitude.

(d) Ceiling, speed, and climb performance are limited only by the amount of fuel it is possible to carry.

(e) Performance characteristics indicate ideal application to missiles following a trajectory. Peak altitudes greatly exceeding the capability of any other man-made mechanisms are possible. Missile ranges can be vastly extended.

(f) Highly specialized applications in terms of research airplanes and interceptors are evident. A research airplane could be used to conduct tests in level flight for application to high-speed and diving problems encountered on other types of airplanes. Target-seeking interceptor missiles powered by rocket motors should be most effective.

References

[1] von Kármán, Th., *Comparative Study of Jet Propulsion Systems as Applied to Missiles and Transonic Aircraft*, Jet Propulsion Laboratory Memorandum JPL-2, California Institute of Technology, March 28, 1944.

[2] Gilruth, R. R., and Wetmore, J. W., *Preliminary Tests of Several Airfoil Models in the Transonic Speed Range*, N.A.C.A. A.C.R., May, 1945.

Numerical Transformation Procedures for Shear-Flow Calculation

STANLEY U. BENSCOTER*

Bureau of Aeronautics, Navy Department

ABSTRACT

Several methods of calculation of shear flows in multicellular members are explained and illustrated. These numerical methods may be used in place of the usual process of solving a system of linear algebraic equations. The processes will have a special appeal to those structural engineers who are familiar with moment distribution because of the similarity in the method of performing the computations. A transformation procedure may be learned and applied by a designer without any knowledge of the equations that govern the solution. The physical significance of the numerical constants involved in the shear-flow problem are emphasized in order to assist the reader in remembering the processes. A mathematical proof of the validity of the procedures is given in the Appendix.

NOMENCLATURE

A = cell area
d = transformation factor
G = shearing modulus of elasticity
J = torsion constant
L = length of wall segment
q = shear flow
t = wall thickness
T = torque
r = L/t (aspect ratio)
τ = shearing stress

INTRODUCTION

THE SHEARING STRESSES in a multicellular beam subjected to pure torsion are generally computed by solving a system of linear algebraic equations which are equal in number to the number of cells. The numerical transformation process, which is herein illustrated, provides the designer with a convenient tool, which is easily remembered, for determining the shearing stresses without setting up the equations or even realizing that a system of equations is being solved.

The possibility of employing such a numerical process has been previously noted and illustrated by Baron.[1] The object of this paper is to simplify the method of writing the computations and to note the simple physical significance that can be attached to the various quantities that enter into the calculation.

SINGLE-CELL FORMULAS

Formulas that are applicable to a single cell serve as the basis of the transformation procedure and should be memorized, just as formulas for fixed-end moments and stiffness values for a single span are memorized and used as a basis in the moment distribution process of analysis of continuous beams.

A single cell is shown in Fig. 1 with the associated stress surface that is a graphical representation of St. Venant's stress function.[2] The shearing stress, τ, for each segment is equal to the slope of the stress surface over that segment. Thus,

$$\tau = q/t \tag{1}$$

where t is the thickness of the segment and is assumed to be constant over the length of the segment. The quantity q, which is equal to the product $t\tau$, is generally called the shear flow in cellular members.

From St. Venant's solution of a prismatic member in torsion, with sections free to warp, it is known that the stresses on a cross section produce a resultant torque that is equal in magnitude to twice the volume beneath the stress surface.[3] Hence, the torque, T, at a given cross section is related to the shear flow by the formula

$$T = 2Aq \tag{2}$$

where A is the cell area (inclosed by the centerlines of the wall segments).

A relationship between the shear flow and the rate of twist may also be derived. Before writing this formula it is convenient to introduce the ratio $r = L/t$ for a particular wall segment of the cell. This quantity

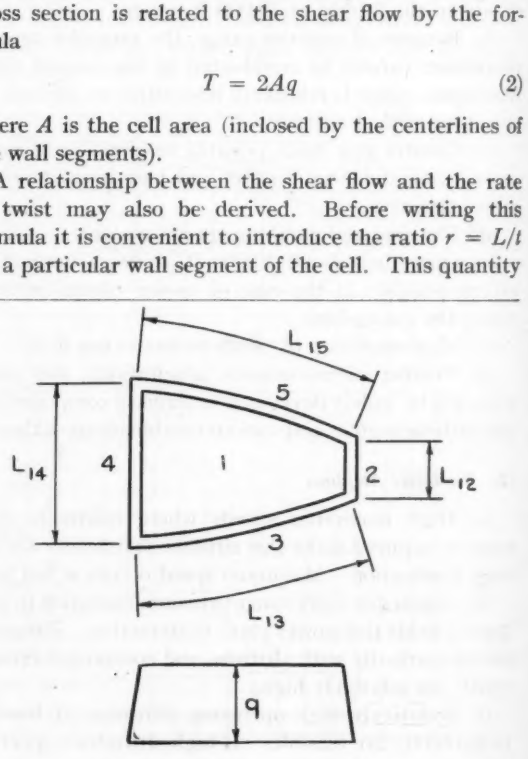

FIG. 1. Single-cell stress surface.

Received September 14, 1945.

* Aeronautical Engineer.

is conveniently remembered as the aspect ratio of a straight segment. The sum of the aspect ratios of all of the wall segments of a cell may be indicated as Σr. The formula for q is given by

$$q = 2AG\theta/\Sigma r \tag{3}$$

This formula is developed in various textbooks[4] by considering a unit slice of a beam and employing the principle of conservation of energy.

The analyses to be described are carried out for a unit rate of twist defined to be such that $G\theta = 1$. In this case the above formula becomes

$$q = 2A/\Sigma r \tag{4}$$

when $G\theta = 1$.

Multicellular Member

When a member in torsion consists of several thin-walled cells, the stress surface forms several steps, or plateaus, corresponding to the number of cells as shown in Fig. 2. The stress-analysis problem consists of determining the shear flows, or stress surface ordinates, q_1, q_2, and q_3, for a three-cell member. As in the case of a single cell, the applied torque is equal to twice the volume beneath the stress surface. Thus, from Fig. 2,

$$T = 2(A_1q_1 + A_2q_2 + A_3q_3) \tag{5a}$$

$$= 2\Sigma Aq \tag{5b}$$

A system of linear equations governing the shear flows may be established (see Appendix). The system may be solved and the resulting shear flows substituted into Eq. (5) to obtain the applied torque for $G\theta = 1$. The shear flows due to any other torque may then be obtained by direct proportion. In the process of solution to be illustrated, the shear flows are obtained from a numerical transformation calculation. This calculation replaces the process of setting up and solving a system of linear equations.

The torsion constant, J, of a section of a beam is defined by expressing the relationship between torque and rate of twist.

$$T = GJ\theta \tag{6}$$

From this definition it is seen that in the case of a unit rate of twist ($G\theta = 1$) the total torque applied to the section will be equal in magnitude to the torsion constant. Consequently, the torsion constant for a multicellular beam may be conveniently obtained by computing the torque from Eq. (5) for shear flows associated with a unit rate of twist.

Two physical properties of the cross section of a member enter into the determination of the shear flows. The first property is the aspect ratio, r, for the various wall segments. The second property is the area, A, of each cell. The shear flows are calculated for a torque that produces a unit rate of twist ($G\theta = 1$). An initial estimate of the shear flow in each cell is first calculated by assuming each cell to be isolated and acted upon by a torque producing a unit rate of twist. This initial estimate may be indicated by q' and is calculated as for a single cell.

$$q' = 2A/\Sigma r \tag{7}$$

The numerical procedure transforms the initial estimates, q', into the final values, q.

In order to carry out the transformation procedure, it is necessary to determine the transformation factors. Two such factors are associated with each internal wall segment or web. A transformation factor is defined as the ratio of the r value of a segment to the sum of the r values of an adjacent cell. The factors are computed only for internal segments. Since there are two cells adjacent to each internal segment, two factors may be computed for each internal segment. The transformation factors for the first internal web between cell No. 1 and cell No. 2 may be expressed as

$$d_{12} = r_{12}/\Sigma_1 r, \quad d_{21} = r_{21}/\Sigma_2 r \tag{8}$$

where $\Sigma_1 r$ and $\Sigma_2 r$ are the sums of the r values for the first and second cells, respectively.

An example of numerical transformation is shown in Fig. 3 for a member of four cells. The area of each cell is shown enclosed by a rectangle. An r value is shown adjacent to each segment. The numerical values of the length and thickness of each segment are not shown. Immediately below the diagram the values of Σr for each cell are shown. On the next line the transformation factors are shown. Before the calculation is begun, the transformation factors must be transposed as indicated by the arrows.

Below the center of each cell a vertical line is drawn, and the initial estimate of shear flow is written on either side of the line. Each initial estimate is multiplied by the transformation factors just above it, and the resulting values are carried over to the adjacent cells. This calculation resembles the carry-over step of a moment distribution solution of a continuous beam. The quantities that are carried over to adjacent cells are corrections to be added to the initial estimates. The total correction for an internal cell consists of two numbers, one of which may be written on either side of the vertical line. The two corrections are added

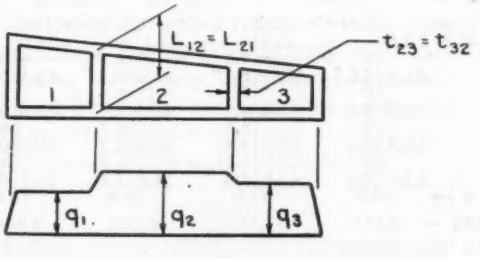

FIG. 2. Multicell stress surface.

mentally and multiplied by the transformation factors in the second step of the calculations. The transformation procedure is repeated until the corrections become negligible. The final value of the shear flow for a given cell is obtained by adding all of the corrections on both sides of the vertical line to the initial estimate.

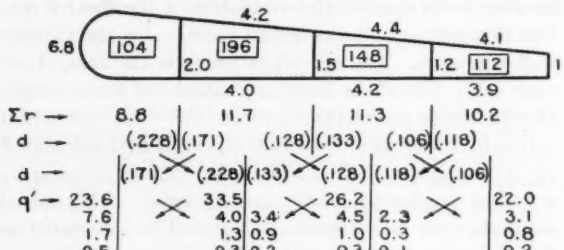

FIG. 3. Shear-flow transformation by successive corrections.

In the example of Fig. 3 the initial estimate of shear flow in the first cell is 23.6 lbs. per in. and the final value is 33.5 lbs. per in. The torque carried by each cell may be determined by calculating the quantity $2Aq$ for the cell in agreement with Eq. (5). The sum of such quantities gives the total torque acting on the section and also the numerical value of the torsion constant. The shear flow in an internal web may be calculated as the difference between the shear flows of the adjacent cells. Thus the shear flow in the first web of the section of Fig. 3 is 10.3 lbs. per in.

The computations of Fig. 3 show that a torque of 40,150 in.lbs. would produce a shear flow of 33.5 lbs. per in. in the first cell. The shear flow produced by any other torque may be obtained by direct proportion. It should be noted that the transformation factors are dependent only upon relative r values and do not require a knowledge of the true numerical values. Thus the shear flows developed by a given torque may be calculated when only relative r values are known. This fact should find practical usefulness in the preliminary stage of design when the cell areas are known but when the skin, or wall, thicknesses have not yet been determined. The r values of Fig. 3 may be regarded as relative values obtained by dividing the true values by a constant k. In such a case the torsion constant as computed would have to be divided by k to obtain the true value. Thus it is seen that a determination of the torsion constant requires a knowledge of the true r values.

A second method of computation, which may be developed from a slightly different physical point of view, is illustrated in Fig. 4. Instead of transforming shear flows, the cell areas are transformed. The area A_1 is transformed into $\bar{A}_1$. The transformed area of each cell is used in the formula for shear flow for a single cell to obtain the true shear flow. Thus the value of $\bar{A}_1$ is substituted into Eq. (4) to obtain q_1. The transformation factors are computed in the same manner as before, but they are not transposed. The transformation procedure is carried out in the same manner as before. The transformed areas will always be larger than the true areas. When the transformed areas have been computed, the shear flows may be determined as shown in Fig. 4. From these the total torque, or torsion constant, may be computed to be as shown. The slight difference in J from Figs. 3 and 4 is due to using a slide rule. The process of area transformation by successive corrections may be shown to correspond closely to the relaxation process developed by Southwell[5] for solving a system of linear equations.

ITERATION

Another method of calculation may be employed which involves the principle of iteration. This process is illustrated in Fig. 5. The transformation factors and initial estimates are determined as in Fig. 3. One cycle of computations is performed to give a pair of correction values for each cell. These corrections are added to the initial estimates to obtain a new set of estimates. The new estimates will be closer to the final

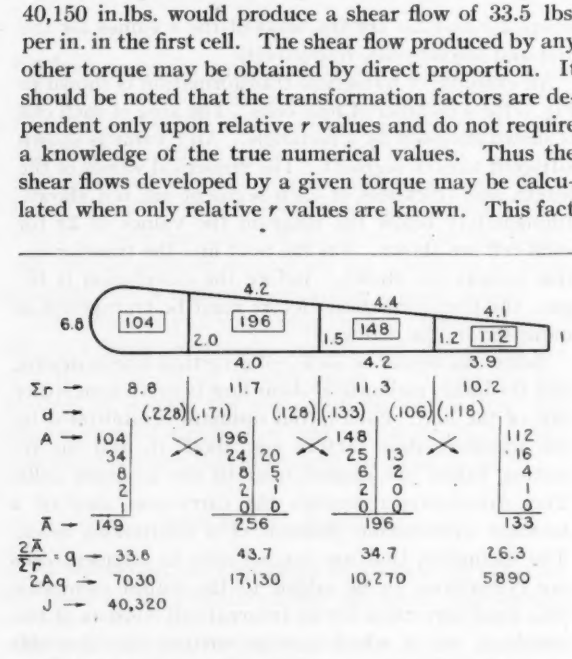

FIG. 4. Area transformation by successive corrections.

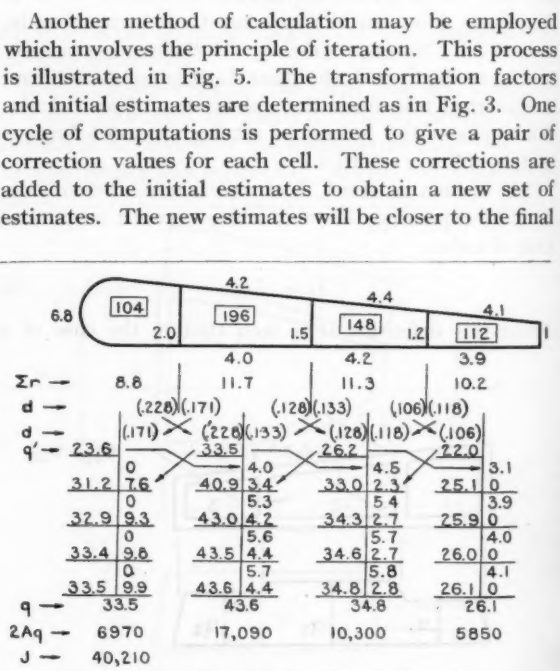

FIG. 5. Shear-flow transformation by iteration.

values than the initial estimates. Additional cycles are performed to obtain a series of shear-flow values which continues to improve and approach a limit. The corrections that are computed in each cycle must be added to the *initial* estimates in order to obtain the improved shear-flow value. The successive estimates are written on the left side of the vertical lines in Fig. 5, while the corrections for each cycle are written on the right side of the lines. A horizontal line is drawn to indicate the completion of each cycle. The transformation of areas may also be performed by iteration but will not be illustrated.

The process of successive corrections is somewhat faster than iteration and easier to learn and remember. The compensating features of the process of iteration are that it is slightly more accurate and that it is self-correcting. An error that is made in the calculations will be gradually eliminated. A solution that is obtained by successive corrections must be checked in some manner, since it may contain an error. This suggests the use of a combined procedure. The solution may be first obtained by successive corrections and then checked by performing a single cycle of iteration. The process of successive corrections, carried out to slide-rule accuracy, will usually contain an error of one or two in the third significant figure, and this small error will be eliminated by a cycle of iteration.

The possibility of writing the computations in the convenient form that has been illustrated arises because the linear system of equations which governs the shear flows has a continuant matrix. The convergence of the process is dependent upon the fact that the transformation factors are, by definition, less than unity. The more important question is whether or not the process converges at a practicable rate so that it can compete with a straightforward solution of the equations. If all of the segments have the same r value, the transformation factors for an interior web are equal to 0.25. It may be shown that factors of this magnitude provide the same rate of convergence as occurs in moment distribution, which is known from experience to converge at a practicable rate. A particular convenience of the transformation procedures is noted in the fact that all numbers that enter into the calculation are positive so that no consideration of signs is required.

A Two-Cell Member

The two-cell member occurs frequently as a wing structure and can be given a simplified treatment that is worthy of note. If the true cell areas are increased by dividing by a factor D to obtain modified areas, the final solution may be obtained from one, and only one, cycle of computations. The factor D is given by

$$D = 1 - d_{12}d_{21} \tag{9}$$

This modification factor corresponds mathematically to the end rotation constant of moment distribution, which is used to determine a modified stiffness for a beam with the opposite end simply supported. The factor D may be used either in a shear-flow transformation or an area transformation process. A transformation of areas is illustrated in Fig. 6. The modified area is operated on by only one transformation cycle to obtain the transformed areas. The shear flows and torsion constant are computed as usual. In a shear-flow transformation the modified areas would be used in calculating the initial estimates.

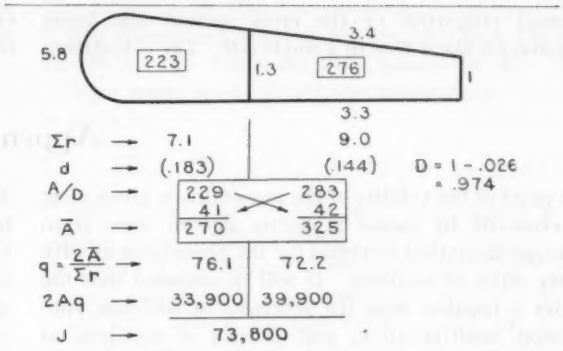

Fig. 6. Two-cell member.

Additional Applications

Two applications of the calculation method should be mentioned, although they will not be illustrated. In a case of pure bending, with a shear force acting through the shear center, the average value of the rate of twist over the section is zero. However, it has been shown by Goodier[6] that the individual cells have rates of twist which are linearly distributed and readily calculated. In place of the assumption that $G\theta = 1$ for all cells, the value of θ for each cell must be computed and used in the numerator of Eq. (3) to determine the initial estimates of shear flow.

It has been shown by von Kármán and Christensen[7] that, in a case of nonlinear torsion, the secondary shearing stresses consist of two parts. The first part is statically determinate, while the second part consists of cellular shear flows that are governed by a system of linear equations. Since this system of equations has the same matrix of coefficients as the system that governs the primary shear flows, the present method of calculation is also applicable to the determination of secondary stresses.

Conclusions

Several numerical transformation procedures have been illustrated for the calculation of shear flows in multicellular members. These procedures include both successive correction and iteration methods. It is shown that only relative values of the aspect ratios of the wall segments need be known to calculate the shear flows. The procedure depends upon the values of

physical properties of the cross section and basic formulas for shear flow in a single cell. The calculation cycles are performed in a manner similar to the carry-over step of moment distribution.

Appendix

A proof of the validity of the procedures is given most conveniently by means of matrix algebra, since complete mathematical formulas for the procedures involve power series of matrices. It will be assumed that the reader is familiar with the processes of addition, subtraction, multiplication, and division of matrices, as well as the significance of the identity matrix and the reciprocal of a matrix.

Considering a member of three cells, for illustration purposes, the equations that govern the shear flows are[8]

$$(\Sigma_1 r)q_1 - r_{12}q_2 = 2A_1G\theta \tag{10a}$$
$$-r_{21}q_1 + (\Sigma_2 r)q_2 - r_{23}q_3 = 2A_2G\theta \tag{10b}$$
$$-r_{32}q_2 + (\Sigma_3 r)q_3 = 2A_3G\theta \tag{10c}$$

The coefficient $\Sigma_1 r$ is the sum of the aspect ratios of all of the wall segments of the first cell and, similarly, for the other diagonal coefficients. The quantity r_{12} is the aspect ratio of the web between the first and second cells and, similarly, for the other nondiagonal coefficients. Dividing through the equations by the diagonal coefficients and substituting $G\theta = 1$ gives

$$q_1 - d_{12}q_2 = q_1' \tag{11a}$$
$$-d_{21}q_1 + q_2 - d_{23}q_3 = q_2' \tag{11b}$$
$$-d_{32}q_2 + q_3 = q_3' \tag{11c}$$

In these equations q' and d have been introduced as defined by Eqs. (7) and (8).

Eqs. (11) may be written in expanded matrix form as follows:

$$\begin{bmatrix} 1 & -d_{12} & 0 \\ -d_{21} & 1 & -d_{23} \\ 0 & -d_{32} & 1 \end{bmatrix} \begin{bmatrix} q_1 \\ q_2 \\ q_3 \end{bmatrix} = \begin{bmatrix} q_1' \\ q_2' \\ q_3' \end{bmatrix} \tag{12}$$

In contracted form this matrix equation may be written as

$$\{[I] - [T]\}[q] = [q'] \tag{13}$$

The matrix $[T]$ of transformation factors has been introduced and is seen to be

$$[T] = \begin{bmatrix} 0 & d_{12} & 0 \\ d_{21} & 0 & d_{23} \\ 0 & d_{32} & 0 \end{bmatrix} \tag{14}$$

The reciprocal of the binomial $[I] - [T]$ is given by

$$\{[I] - [T]\}^{-1} = [I] + [T] + [T]^2 + [T]^3 + \ldots . \tag{15}$$

The proof of this equation is obtained by multiplying both sides by the binomial $[I] - [T]$.

Multiplying through Eq. (13) by the reciprocal of the binomial coefficient gives the solution in the form:

$$[q] = \{[I] + [T] + [T]^2 + [T]^3 + \ldots . .\}[q'] \tag{16}$$

The terms of this series may be shown to correspond to the cycles of a shear-flow transformation process. If only the first term of the series is used, the solution for $[q]$ will be the initial estimates $[q']$. If two terms of the series are used, a better solution will be obtained as follows:

$$[q] = [q'] + [T][q'] \tag{17}$$

The second term on the right-hand side is a column vector of corrections to be added to the initial estimates. This term may be written in expanded form for a four-cell member.

$$[T][q'] = \begin{bmatrix} 0 & d_{12} & 0 & 0 \\ d_{21} & 0 & d_{23} & 0 \\ 0 & d_{32} & 0 & d_{34} \\ 0 & 0 & d_{43} & 0 \end{bmatrix} \begin{bmatrix} q_1' \\ q_2' \\ q_3' \\ q_4' \end{bmatrix} = \begin{bmatrix} d_{12}q_2' \\ d_{21}q_1' + d_{23}q_3' \\ d_{32}q_2' + d_{34}q_4' \\ d_{43}q_3' \end{bmatrix} \tag{18}$$

The components of this column vector are seen to correspond to the corrections obtained by the first cycle of the calculations shown in Fig. 3. In general, the multiplication of a column vector of numbers by the transformation matrix $[T]$ corresponds to operating on that set of numbers with one cycle of the numerical transformation procedure.

If the solution is assumed to be given by three terms of the series, it will have the form

$$[q] = [q'] + [T][q'] + [T]^2[q'] \tag{19}$$

The last term of this solution is seen to be obtained by multiplying the previous term by $[T]$. Consequently, the second set of corrections is obtained by operating on the first set of corrections with one cycle of the transformation procedure. By considering additional terms of the series, it is found that each term corresponds to an additional cycle of the transformation procedure. Thus the calculation process is seen to yield the solution of the system of equations which governs the shear flows.

The iteration procedure for shear-flow transformation may now be explained. Considering Eq. (13), the second term on the left side may be transposed to give

$$[q] = [q'] + [T][q] \tag{20}$$

If any reasonable approximate solution is substituted for $[q]$ on the right-hand side and multiplied by $[T]$, a set of corrections will be obtained which may be added to the initial estimates to obtain a better set of estimates. Using $[q']$ as an approximate solution gives

$$[q] = \{[I] + [T]\}[q'] \tag{21}$$

If this approximate solution is substituted into the right-hand side of Eq. (20), an improved solution is given by

$$[q] = \{[I] + [T] + [T]^2\}[q'] \tag{22}$$

From this result it becomes apparent that the iteration process could be repeated indefinitely to obtain a formula for the solution involving a power series of matrices in exact agreement with Eq. (16). The individual steps of the above-described matrix iteration process may be shown to be in exact agreement with the cycles of the numerical procedure shown in Fig. 5. This results directly from the previously established fact that multiplying a column vector of numbers (which in this case form an approximate solution) by the matrix $[T]$ corresponds to operating on that set of numbers with a cycle of the transformation procedure.

The validity of the procedures for cell-area transformation may be proved in a similar manner. If the transformed area is known, the shear flow may be computed from the formula for a single cell.

$$q_i = 2\bar{A}_i/\Sigma_i r, \quad (G\theta = 1) \tag{23}$$

If this formula is substituted into Eqs. (10), they take the form,

$$\bar{A}_1 - d_{21}\bar{A}_2 = A_1 \tag{24a}$$
$$-d_{12}\bar{A}_1 + \bar{A}_2 - d_{32}\bar{A}_3 = A_2 \tag{24b}$$
$$-d_{23}\bar{A}_2 + \bar{A}_3 = A_3 \tag{24c}$$

In expanded matrix form these equations become

$$\begin{bmatrix} 1 & -d_{21} & 0 \\ -d_{12} & 1 & -d_{32} \\ 0 & -d_{23} & 1 \end{bmatrix} \begin{bmatrix} \bar{A}_1 \\ \bar{A}_2 \\ \bar{A}_3 \end{bmatrix} = \begin{bmatrix} A_1 \\ A_2 \\ A_3 \end{bmatrix} \tag{25}$$

In contracted form this matrix equation becomes

$$\{[I] - [T]'\}[\bar{A}] = [A] \tag{26}$$

The prime on the transformation matrix indicates that it is in transposed form, as may be seen from the subscripts of the transformation factors in Eq. (25). Using a power series of matrices as before, the solution is given by

$$[\bar{A}] = \{[I] + [T]' + [T]'^2 + [T]'^3 + \ldots\}[A] \tag{27}$$

If each of the terms of this series is examined in expanded form, it will be found that they correspond to the cycles of the numerical procedure shown in Fig. 4. The appearance of the transformation matrix in transposed form in this solution explains why the transformation factors did not have to be transposed before beginning the calculations in Fig. 4 as was done in Fig. 3. The validity of the process of area transformation by iteration may be proved in exactly the same manner as previously given for shear-flow transformation and, hence, is omitted.

References

[1] Baron, F. M., *Torsion of Multiconnected Thin-Walled Cylinders*, Journal of Applied Mechanics, Vol. 9, No. 2, June, 1942, pp. A-72–A-74.

[2] Timoshenko, S., *Theory of Elasticity*, p. 270; McGraw-Hill Book Company, Inc., New York, 1934.

[3] Ibid., p. 232.

[4] Timoshenko, S., *Strength of Materials*, Part II, p. 278; D Van Nostrand Company, Inc., New York, 1941.

[5] Southwell, R. V., *Relaxation Methods in Engineering Science;* Oxford University Press, London, 1940.

[6] Goodier, J. N., *A Theorem on the Shearing Stress in Beams with Applications to Multicellular Sections*, Journal of the Aeronautical Sciences, Vol. 11, No. 3, pp. 272–280, July, 1944.

[7] von Kármán, Th., and Christensen, N. B., *Methods of Analysis for Torsion with Variable Twist*, Journal of the Aeronautical Sciences, Vol. 11, No. 2, pp. 110–124, April, 1944.

[8] Timoshenko, S., *Theory of Elasticity*, p. 273; McGraw-Hill Book Company, Inc., New York, 1934.

SUGGESTIONS FOR CONTRIBUTORS TO THE PUBLICATIONS *of the* INSTITUTE *of the* AERONAUTICAL SCIENCES

The Institute of the Aeronautical Sciences invites both members and nonmembers from any country to submit papers for publication in the JOURNAL OF THE AERONAUTICAL SCIENCES and the AERONAUTICAL ENGINEERING REVIEW. The Institute, following the practice of other societies, does not pay for contributions.

The following directions for the preparation of papers, if followed by authors, will save correspondence, avoid the return of papers for changes, minimize the work of preparation for the printer, and save the expense due to the charges made for "author's corrections."

MANUSCRIPTS: Papers must be written in English, in original typewriting on one side only of white paper sheets, consecutively numbered and be double or triple spaced with wide margins. Manuscripts should be prepared with great care so that they will be typographically accurate. Paragraphing should be given special attention. Papers should be written in the third person, reference to the writer being made as "the author." Avoid the use of the words "I," "we," and "you." Blueprint copies of papers are unacceptable as it is impossible to mark directions to the printer on them. Correcting, changing, or adding to papers after they are in type is costly. It is, therefore, imperative that papers submitted be in final form. Typographical errors may be corrected on proofs, but if authors wish to add material, they may do so at their own expense. In mailing, drawings may be rolled, but manuscripts should be sent flat. Send by first class mail (register, if you wish, for your own protection) to the Editorial Office, Institute of the Aeronautical Sciences, 2 East 64th Street, New York 21, N.Y. All manuscripts will be examined by the Editorial Committee and by the Editor. Authors will be advised as promptly as possible whether the paper is acceptable for publication.

TITLES: The title of the paper should be brief. The name and initials of the author should be written as he prefers. The use of the full name of an author is advocated because of the frequent duplication of initials and surnames which sometimes makes it difficult to establish the identity of the author. This is particularly important for large annual indexing and abstracting services. All titles and degrees or honors are omitted. The name of the organization with which the author is associated should be placed after his name on a separate line. The date on which the paper is received will be inserted by the Editor.

SUMMARIES OR ABSTRACTS: An abstract to be printed at the beginning should accompany each article. It should be adequate as an *index* and as a *summary*. It should contain a statement of major conclusions reached, since summaries in many cases constitute the only source of information used in compiling scientific reference indexes. Abstracts printed in other journals, especially foreign, in most cases, consist of summaries from printed papers. The summary should explain as adequately as possible the major conclusions to a nonspecialist in the subject. The summary should contain from 100 to 300 words, depending on the length of the paper.

SUBHEADINGS: Subheadings should be inserted by the author at frequent intervals. The work of editorial preparation will be simplified by the author providing many subheadings. Because of the breaking of columns and the insertion of illustrations, some of the subheadings may have to be omitted.

SHORTENING OF PAPERS: Some papers, at the end, fill in only a portion of a page. This leaves much wasted blank space as succeeding articles are started at the top of a page. Authors should indicate by notation on the left-hand side of the page what matter may be omitted when "runovers" occur. This request is important as the Journal cannot afford in the future, as it has in its earlier issues, to have blank half pages or more at the end of papers.

MATTER USUALLY DELETED: Acknowledgments of assistance in preparation of paper, except by collaborators. Photographs or illustrations of little technical interest and not showing advances in general practice. Too detailed tabular matter (general results of such tables may be included in the text). Lengthy descriptions of materials or processes or of preliminary experiments or theories that preceded final results; salient features only are of interest.

REFERENCES AND FOOTNOTES: References should appear as footnotes only, numbered consecutively, grouped together at the end of the manuscript. The arrangement should be as follows: (for books)—[1] Durand, W. F., *Aerodynamic Theory*, 1st Ed., Vol. 1, p. 23; Julius Springer, Berlin, 1934. (For magazines)—

[1] Englund, C. R., Crawford, A. B., and Mumford, W. W., *Some Results of a Study of Ultra-Short-Wave Transmission Phenomena*, Proc. I. R. E., Vol. 20, No. 12, pp. 481 and 482, March, 1933. Please give author, title, edition, volume, page, publisher, and date of publication as indicated. Omission of one required fact causes much extra editorial work and possible inaccuracies. All references should be grouped at the end of the article.

ILLUSTRATIONS: Illustrations should accompany manuscripts and each should always be referred to in the text, preferably by number. Drawings or graphs should not be larger than 12 × 16 inches, and must be made with jet black India Ink on white paper or tracing cloth, the latter being preferred. *Do not use typewriter for lettering.* The smallest lettering on 8 × 10 inch figures should be no less than 1/4 inch high. Cross-section paper (white with black lines) may be used, but should not have more than 4 lines per inch. If finer ruled paper is used, the major division lines should be drawn in with black ink, omitting the finer divisions. In the case of finely ruled paper, only blue-lined paper can be accepted. *Tracing paper and blueprints* are not acceptable. Lettering and all markings must be large enough to be readable after reduction. Mail rolled or flat, never folded. Drawings that cannot be reproduced (including pencil drawings) will be returned to the author for redrawing, thus delaying publication of the paper. Photographs should be distinct and show clear black and white contrasts. They must be on glossy white paper. Avoid round and oval photographs.

CAPTIONS AND LEGENDS: Legends or captions must accompany each drawing or photograph submitted. If written on the drawing or photograph, they should be placed below and well outside the part to be reproduced. It is better to place them on separate sheets of paper pasted to the back of the drawings or photographs. Each table should have a caption such as Table 1, Table 2, Table 3, etc. Captions should be complete in themselves so as to make the data intelligible to the reader without reference to the text. A duplicate list of captions for figures should be included as the last page of the manuscript. Use "Fig. 1" (not Figure 1), Figs. 3 and 4, etc., in both the text and the numbering of illustrations. In the text, "Eq. (1)," or "Eqs. (1) and (2)" are preferable to "Equation (1)." In captions and legends, except for "Fig." and "Eq.," and in table headings, write all words in full; do not abbreviate. Avoid placing explanatory written matter in the drawings; it should be in the text.

MATHEMATICAL WORK: Only the simplest formulas should be typewritten; all others should be carefully written in pen and ink, the writing to be large enough so that ample room is provided to mark mathematical matter for the printer. A considerable space for marking should be allowed above and below all equations. All complicated equations should be repeated on separate sheets with plenty of space left for marking. The solidus should be used for simple fractions appearing within the text. Make all expressions clear to the typesetter. Greek letters used in formulas should be clearly designated by name on the margin of the manuscript. All symbols should be clearly written and carefully checked. The difference between capital and lower-case letters should be clearly distinguished and care taken to avoid confusion between zero (0) and the letter (o), between the numeral (one) and the letter (ell) and the prime (′), between alpha and a, kappa and k, u and mu, v and nu, n and eta. All subscripts and exponents should be clearly marked and dots and bars over letters or mathematical expressions should be avoided. Avoid complicated exponents and subscripts. When it is necessary to repeat a complicated expression, it should be represented by some convenient symbol.

NOMENCLATURE AND ABBREVIATIONS: The National Advisory Committee for Aeronautics Nomenclature should be used in preference to any others. Standard abbreviations should be used, and it should be noted that most abbreviations are lower case such as m.p.h., b.m.e.p., i.hp., b.hp., hp., . . . etc.

INSTITUTE of the AERONAUTICAL SCIENCES

President
ARTHUR E. RAYMOND

Vice-Presidents
P. R. BASSETT
J. H. KINDELBERGER
JOHN C. LESLIE
BURDETTE S. WRIGHT

Director
S. PAUL JOHNSTON

Executive Vice-President
BENNETT H. HORCHLER

Past-Presidents
J. C. HUNSAKER
CHARLES L. LAWRANCE
DONALD W. DOUGLAS
GLENN L. MARTIN
CLARK B. MILLIKAN
T. P. WRIGHT
GEORGE W. LEWIS
JAMES H. DOOLITTLE
FRANK W. CALDWELL
HALL L. HIBBARD
HUGH L. DRYDEN
R. H. FLEET
CHARLES H. COLVIN

Assistant to the President
GEORGE R. FORMAN

Secretary
ROBERT R. DEXTER

Treasurer
C. S. JONES

Controller
JOSEPH J. MAITAN

COUNCIL

LESTER D. GARDNER, *Chairman*

E. E. ALDRIN
PETER ALTMAN
REX B. BEISEL
LAWRENCE D. BELL
GEORGE W. BRADY
W. A. M. BURDEN
CHARLES H. COLVIN
JAMES H. DOOLITTLE
WILLIAM K. EBEL
SHERMAN M. FAIRCHILD
DONALD W. FINLAY
CHARLES FROESCH
LEROY R. GRUMMAN
R. PAUL HARRINGTON
W. WALLACE KELLETT
OTTO E. KIRCHNER
JEROME LEDERER
ROBERT J. MINSHALL
EARL D. OSBORN
ELMER A. SPERRY, JR.
ERNEST G. STOUT
FRED E. WEICK

ADVISORY COMMITTEE

W. M. ALLEN
WALTER BEECH
ERNEST R. BREECH
RALPH S. DAMON
DONALD W. DOUGLAS
R. H. FLEET
JACK FRYE
ROBERT E. GROSS
R. M. HAZEN
H. MANSFIELD HORNER
J. C. HUNSAKER
CROIL HUNTER
TH. VON KÁRMÁN
I. M. LADDON
P. W. LITCHFIELD
F. W. MAGIN
ALFRED MARCHEV
GLENN L. MARTIN
THOMAS A. MORGAN
R. C. MUIR
JOHN K. NORTHROP
W. A. PATTERSON
E. T. PRICE
F. W. REICHELDERFER
LAURANCE S. ROCKEFELLER
FRED H. ROHR
T. CLAUDE RYAN
GUY W. VAUGHAN
EDWARD P. WARNER

HONORARY MEMBERS

JOHN C. ADAMS
GRIFFITH BREWER
W. A. M. BURDEN
E. U. CONDON
L. C. CRAIGIE
IRA C. EAKER
HARRY F. GUGGENHEIM
HENRY G. HOUGHTON
GEORGE C. KENNEY
CURTIS E. LE MAY
GEORGE B. PEGRAM
E. M. POWERS
J. LAURENCE PRITCHARD
ARTHUR W. RADFORD
F. W. REICHELDERFER
L. B. RICHARDSON
H. B. SALLADA
CARL SPAATZ
L. C. STEVENS
NATHAN F. TWINING

HONORARY FELLOWS

H. H. ARNOLD
DONALD W. DOUGLAS
HUGH L. DRYDEN
W. F. DURAND
SIR RICHARD FAIREY
SIR ROY FEDDEN
J. C. HUNSAKER
SIR MELVILL JONES
GEORGE W. LEWIS
GLENN L. MARTIN
GEORGE J. MEAD
SIR FREDERICK HANDLEY PAGE
D. R. PYE
IGOR I. SIKORSKY
G. I. TAYLOR
TH. VON KÁRMÁN
EDWARD P. WARNER
ORVILLE WRIGHT
T. P. WRIGHT

BENEFACTORS

E. E. ALDRIN
HART O. BERG (Deceased)
W. A. M. BURDEN
E. L. CORD
DONALD W. DOUGLAS
SHERMAN M. FAIRCHILD
SIR RICHARD FAIREY
R. H. FLEET
FLORENCE GUGGENHEIM (Deceased)
C. D. HANSCOM
JOHN P. V. HEINMULLER
ALEXANDER KLEMIN
PAUL KOLLSMAN
BELLA C. LANDAUER
WILLIAM LANDAUER
GROVER LOENING
EDMUND C. LYNCH (Deceased)
F. W. MAGIN
GLENN L. MARTIN
GEORGE J. MEAD
S. A. REED (Deceased)
LAURANCE S. ROCKEFELLER
EDWARD P. WARNER

AMERICAN FELLOWS

JOHN D. AKERMAN
E. E. ALDRIN
HARRY G. ARMSTRONG
KARL ARNSTEIN
J. L. ATWOOD
PAUL S. BAKER
RALPH S. BARNABY
P. R. BASSETT
WELLWOOD E. BEALL
REX B. BEISEL
G. M. BELLANCA
DON R. BERLIN
HENRY A. BERLINER
WILLIAM BOLLAY
B. C. BOULTON
GEORGE W. BRADY
LYMAN J. BRIGGS
W. G. BROMBACHER
CHARLES P. BURGESS
FRANK W. CALDWELL
KENNETH CAMPBELL
CHARLES H. CHATFIELD
ALLAN CHILTON
V. E. CLARK
FRANKLIN R. COLLBOHM
CHARLES H. COLVIN
KARL T. COMPTON
JOHN W. CROWLEY, JR.
RALPH S. DAMON
LUIS DE FLOREZ
SMITH J. DE FRANCE
J. P. DEN HARTOG
WALTER S. DIEHL
JAMES H. DOOLITTLE
C. S. DRAPER
IVAN H. DRIGGS
WILLIAM K. EBEL
C. L. EGTVEDT
FREDERIC FLADER
CHARLES FROESCH
JACK FRYE
GARLAND FULTON
LESTER D. GARDNER
RICHARD C. GAZLEY
MICHAEL E. GLUHAREFF
MELVIN N. GOUGH
LEROY R. GRUMMAN
HAROLD R. HARRIS
R. M. HAZEN
ALBERT F. HEGENBERGER
EDWARD H. HEINEMANN
S. D. HERON
HALL L. HIBBARD
L. S. HOBBS
PAUL E. HOVGAARD
WILLIAM HOVGAARD
ROBERT INSLEY
EASTMAN N. JACOBS
CLARENCE L. JOHNSON
ALEXANDER KARTVELI
PAUL H. KEMMER
J. H. KINDELBERGER
OTTO E. KIRCHNER
ARTHUR L. KLEIN
ALEXANDER KLEMIN
W. B. KLEMPERER
PAUL KOLLSMAN
OTTO C. KOPPEN
B. V. KORVIN-KROUKOVSKY
S. M. KRAUS
I. M. LADDON
E. S. LAND
CHARLES L. LAWRANCE
JOHN G. LEE
JOHN C. LESLIE
CHARLES A. LINDBERGH
WILLIAM LITTLEWOOD
GROVER LOENING
W. RANDOLPH LOVELACE, II
EUGENE E. LUNDQUIST
R. D. MACCART
JOHN R. MARKHAM
ERLE MARTIN
WM. H. MCAVOY
C. J. MCCARTHY
CLARK B. MILLIKAN
ROBERT J. MINSHALL
SANFORD A. MOSS
JOSEPH S. NEWELL
ALFRED S. NILES
JOHN K. NORTHROP
ARTHUR NUTT
SHATSWELL OBER
ROBERT R. OSBORN
W. BAILEY OSWALD
GEORGE A. PAGE, JR.
F. W. PAWLOWSKI
F. W. PENNOYER, JR.
A. A. PRIESTER
ARTHUR E. RAYMOND
F. W. REICHELDERFER
ELLIOTT G. REID
H. J. E. REID
H. C. RICHARDSON
LEONARD E. ROOT
C. E. ROSENDAHL
WILLIAM T. SCHWENDLER
JAMES M. SHORMAKER
MAC SHORT
IGOR ALEXIS SIKORSKY
SELDEN B. SPANGLER
ELMER A. SPERRY, JR.
JOHN STACK
WILLIAM B. STOUT
HARRY A. SUTTON
C. FAYETTE TAYLOR
EDWARD S. TAYLOR
PHILIP B. TAYLOR
TH. THEODORSEN
T. E. TILLINGHAST
S. TIMOSHENKO
L. B. TUCKERMAN
RALPH H. UPSON
J. G. VINCENT
RICHARD VON MISES
FRANK L. WATTENDORF
P. V. H. WEEMS
FRED E. WEICK
R. D. WEYERBACHER
JOHN B. WHEATLEY
ANDREW V. WILLGOOS
DONALD H. WOOD
ROBERT J. WOODS
JOHN E. YOUNGER
ALBERT F. ZAHM
STEPHEN J. ZAND

An Appreciation
To Corporate Members of the Institute of the Aeronautical Sciences

Listed below are the leading aeronautical and industrial companies that make possible the publication of the *Journal of the Aeronautical Sciences*.

They enable the Institute to publish scientific and technical papers in the *Journal* and to devote its pages exclusively to editorial material

Dues from individual members which would normally be used to publish this scientific and engineering monthly are thus released for additional services to the profession and industry.

The *Aeronautical Engineering Review* and the *Aeronautical Engineering Catalog*, together with the *Journal*, provide a comprehensive technical information service for the benefit of the aircraft and related industries.

Academy of Aeronautics, Inc.
Casey Jones School of Aeronautics
Aero Insurance Underwriters
Aerojet Engineering Corporation
Aeroquip Corporation
Agawam Aircraft Products, Inc.
Airborne Instruments Laboratory, Inc.
Airchox Company Division, Joyce Aviation, Inc.
Aircraft Radio Corporation
Aireon Manufacturing Corporation
AiResearch Manufacturing Company
AiResearch Manufacturing Company of Arizona, Inc.
Airex Manufacturing Company, Inc.
Allis-Chalmers Manufacturing Company
Allison Division, General Motors Corporation
Aluminum Company of America
American Airlines System
American Overseas Airlines, Inc.
American Bosch Corporation
American Phenolic Corporation
Associated Aviation Underwriters
Associated Foundries & Manufacturers, Inc.
Atlas Supply Company
Baker Steel & Tube Company
Beech Aircraft Corporation
Bell Aircraft Corporation
Bendix Aviation Corporation
Bendix Products Division
Bendix Radio Corporation
Eclipse-Pioneer Division
Export Division
Friez Instrument Division
Pacific Division
Scintilla Magneto Company
The BG Corporation
Boeing Aircraft Company
Boeing School of Aeronautics
Breeze Corporations, Inc.
Essex Tool & Die Company
Federal Laboratories, Inc.
Cal-Aero Technical Institute, A Division of Grand Central Airport Company
Carrier Corporation
Cessna Aircraft Company
Chandler-Evans Corporation
Chase National Bank of the City of New York
The Cleveland Graphite Bronze Company
The Cleveland Pneumatic Tool Company
Automotive-Aircraft Division
Clifford Manufacturing Company
Consolidated Vultee Aircraft Corporation
Nashville Division
Stinson Aircraft Division
Continental Motors Corporation
Cox and Stevens Aircraft Corporation
Culver Aircraft Corporation
Curtiss-Wright Corporation
Airplane Division
Development Division
Propeller Division
Wright Aeronautical Corporation
Doak Aircraft Company, Inc.
Douglas Aircraft Company, Inc.
El Segundo Plant
Long Beach Plant
The Dow Chemical Company
Dzus Fastener Company, Inc.
Eastern Air Lines, Inc.
Eaton Manufacturing Company
Thomas A. Edison, Incorporated, Instrument Division
Edo Aircraft Corporation
The Electric Auto-Lite Company
Electrol Incorporated
Engineering and Research Corporation
Ethyl Corporation
The Fafnir Bearing Company
Fairchild Camera & Instrument Corporation
Fairchild Aerial Surveys, Inc.
Fairchild Engine and Airplane Corporation
Duramold Division
Fairchild Aircraft Division
Ranger Aircraft Engines Division
Federal Telephone and Radio Corporation

Firestone Aircraft Company
Fletcher Aviation Corporation
G & A Aircraft, Inc.
General Aircraft Equipment, Inc.
General Aviation Equipment Company, Inc.
General Electric Company
General Instrument Corporation
General Motors Corporation
  AC Spark Plug Division
  Aeroproducts Division
  Buick Motor Division
  Cadillac Motor Car Division
  Chevrolet Motor Division
  Delco Products Division
  Delco-Remy Division
  Eastern Aircraft Division
  Fisher Body Division
  Frigidaire Division
  Harrison Radiator Division
  Research Laboratories Division
  Rochester Products Division
The B. F. Goodrich Company
The Goodyear Tire & Rubber Company
The Gray Manufacturing Company
Grumman Aircraft Engineering Corporation
Guiberson Diesel Engine Company
W. & L. E. Gurley
Hanna Engineering Works
Haskelite Manufacturing Corporation
Hawaiian Airlines Limited
The Hilliard Corporation
The International Nickel Company
Irving Air Chute Company, Inc.
Jack & Heintz, Inc.
Johns-Manville Sales Corporation
Kaiser Fleetwings, Inc.
Kellett Aircraft Corporation
Kenyon Instrument Company, Inc.
Walter Kidde & Company, Inc.
Kollsman Instrument Division, Square D Company
Langley Corporation
Lavelle Aircraft Corporation
Lear Incorporated
Liberty Aircraft Products Corporation
Link Aviation Devices, Inc.
The Liquidometer Corporation
Lockheed Aircraft Corporation
Longines-Wittnauer Watch Company, Inc.
Magnaflux Corporation
The Marquette Metal Products Company
The Glenn L. Martin Company
The W. L. Maxson Corporation
Warren McArthur Corporation
McDonnell Aircraft Corporation
Menasco Manufacturing Company
Micromatic Hone Corporation
Minneapolis-Honeywell Regulator Company
Moore Drop Forging Company
National City Bank of New York
National Credit Office, Inc.
The New York Air Brake Company
Norma-Hoffmann Bearings Corporation
North American Aviation, Inc.
  North American Aviation, Inc., of Texas
Northrop Aircraft, Inc.
Northwest Airlines, Inc.
Owens-Corning Fiberglas Corporation
Pan American World Airways System
The Parker Appliance Company
Pennsylvania-Central Airlines Corporation
Pesco Products Company Division, Borg-Warner Corporation
Phillips Petroleum Company
Pioneer Parachute Company, Inc.
The Pure Oil Company
Republic Aviation Corporation
J. P. Riddle Company
A. V. Roe Canada Limited
John A. Roebling's Sons Company
Rohr Aircraft Corporation
Roosevelt Field, Inc.
The Ryan Aeronautical Company
Sciaky Brothers
Scott Aviation Corporation
Shell Oil Company, Inc.
Simmonds Aerocessories, Inc.
Skydyne, Inc.
Socony-Vacuum Oil Company
Solar Aircraft Company
Sperry Gyroscope Company, Inc.
Square D Company
Standard Oil Company of California
Standard Oil Company (Indiana)
Standard Oil Company of New Jersey
Swedlow Aeroplastics Corporation
The Texas Company
Thompson Products, Inc.
Tinnerman Products, Inc.
Titeflex, Inc.
Transcontinental & Western Air, Inc.
Triplett & Barton, Inc.
Union Carbide and Carbon Corporation
  Bakelite Corporation
  Haynes Stellite Company
  Linde Air Products Company
  National Carbon Company
United Aircraft Corporation
  Chance Vought Aircraft Division
  Hamilton Standard Propellers Division
  Pratt & Whitney Aircraft Division
  Pratt & Whitney Aircraft Corporation of Missouri
  Sikorsky Aircraft Division
United Air Lines, Inc.
United States Aviation Underwriters, Inc.
United States Rubber Company
  Dominion Rubber Company, Ltd.
The Variety Aircraft Corporation
Vickers, Inc.
Vidal Corporation
The Waco Aircraft Company
Warner Aircraft Corporation
The Weatherhead Company
Western Air Lines, Inc.
Westinghouse Electric Corporation
Weston Electrical Instrument Corporation
Wyman-Gordon Company
Young Radiator Company

EDITORIAL COMMITTEE

HUGH L. DRYDEN, *Chairman*

Aerodynamics

William Bollay
Kenneth S. M. Davidson
Walter S. Diehl
Hugh L. Dryden
R. Paul Harrington
P. E. Hemke
Eastman N. Jacobs
Alexander Klemin
W. B. Klemperer
Otto C. Koppen
A. M. Kuethe
John G. Lee
John R. Markham
Clark B. Millikan
Shatswell Ober
W. Bailey Oswald
Manfred Rauscher
Elliott G. Reid
H. J. E. Reid
Benjamin F. Ruffner
G. B. Schubauer
W. R. Sears
Abe Silverstein
R. H. Smith
Th. Theodorsen
M. J. Thompson
Th. von Kármán
Richard von Mises
K. D. Wood

Air Transport

Ralph S. Damon
Charles Froesch
Melvin N. Gough
J. A. Herlihy
William Littlewood
A. A. Priester
Paul E. Richter
N. F. Scudder
T P. Wright

Aircraft Design

Karl Arnstein
W. E. Beall
Rex B. Beisel
B. C. Boulton
C. P. Burgess
C. H. Chatfield
J. W. Crowley, Jr.
W. K. Ebel
Leroy R. Grumman
Hall L. Hibbard
C. L. Johnson
A. L. Klein
I. M. Laddon
John G. Lee
C. J. McCarthy
William H. Miller
R. H. Prewitt
A. E. Raymond
Igor I. Sikorsky
Th. Troller
R. H. Upson
Fred E. Weick
Robert J. Woods

Radio

C. S. Draper
Lloyd Espenschied
C. G. Fick
Lewis M. Hull
Haraden Pratt
F. X. Rettenmeyer

Physiologic Problems

H. G. Armstrong
Louis H. Bauer
David B. Dill
Eugene Du Bois
W. Randolph Lovelace, II
Ross A. McFarland
A. D. Tuttle

Power Plants and Propellers

M. A. Biot
George W. Brady
Frank W. Caldwell
Ivan H. Driggs
Louis H. Enos
David Gregg
L. S. Hobbs
Albert R. Jacobs
E. E. Johnson
H. M. McCoy
W. C. Nelson
Arthur Nutt
Shatswell Ober
Hans Reissner
David R. Shoults
C. Fayette Taylor
E. S. Taylor
Th. Theodorsen
A. V. Willgoos
D. H. Wood

Structures and Materials

M. A. Biot
W. B. Bleakney
E. W. Conlon
George W. DeBell
J. P. Den Hartog
L. H. Donnell
L. G. Dunn
E. C. Hartmann
N. J. Hoff
W. B. Klemperer
H. L. Langhaar
E. E. Lundquist
C. F. Nagel, Jr.
J. S. Newell
Alfred S. Niles
W. Ramberg
E. Reissner
F. R. Shanley
H. W. Sibert
C. R. Strang
S. Timoshenko
H. S. Tsien
George Tweney
E. E. Weibel
J. E. Younger

Meteorology

C. F. Brooks
D. M. Little
E. J. Minser
Sverre Petterssen
F. W. Reichelderfer
A. F. Spilhaus
P. V. H. Weems
H. C. Willett

Fuels and Oils

D. P. Barnard
A. L. Beall
Luis de Florez
J. H. Doolittle
Graham Edgar
R. T. Goodwin
S. D. Heron
A. M. Rothrock

Instruments

P. R. Bassett
W. G. Brombacher
Charles H. Colvin
C. S. Draper
Lucien L. Friez
Walter McKay
W. A. Reichel
C. F. Savage
A. F. Spilhaus
S. J. Zand

I.A.S. REPRESENTATIVES TO OTHER ORGANIZATIONS

Aircraft Industries Association of America, Inc.—CHARLES MARCUS
American Association for the Advancement of Science—J. C. HUNSAKER
American Society of Mechanical Engineers—JOHN E. YOUNGER
American Standards Association—P. R. BASSETT
Engineering Society of Detroit—DONALD C. HUNT, GEORGE TWENEY
Greater New York Safety Council—WILLIAM LITTLEWOOD
Daniel Guggenheim Medal Board of Award—CHARLES H. COLVIN, RALPH S. DAMON, LESTER D. GARDNER
Institute of Radio Engineers—L. M. HULL
Manufacturers Aircraft Association—J. T. HARTSON
National Aeronautic Association—WILLIAM R. ENYART
National Fire Protection Association—E. E. ALDRIN
National Research Council Engineering Division—HUGH L DRYDEN
National Safety Council—JEROME LEDERER
New York Museum of Science and Industry—LESTER D. GARDNER
Society of Automotive Engineers—EDWARD P. WARNER